GERALDO JAMISSE HODELA

IN SILICO IDENTIFICATION OF THE PROTEIN TARGETS OF CHAETOGLOBOSINS AND BENZOTRIAZINES FOR THE SELECTION OF ALTERNATIVE NEMATICIDES TO CONTROL *Meloidogyne incognita*

LAVRAS - MG
2025

GERALDO JAMISSE HODELA

IN SILICO IDENTIFICATION OF THE PROTEIN TARGETS OF CHAETOGLOBOSINS AND BENZOTRIAZINES FOR THE SELECTION OF ALTERNATIVE NEMATICIDES TO CONTROL *Meloidogyne incognita*

Thesis presented to the Federal University of Lavras, as part of the requirements of the Postgraduate Program in Agrochemistry, area of concentration in Chemistry/Biochemistry, to obtain the title of Doctor.

Prof. Dr. Denilson Ferreira de Oliveira
Advisor

Prof. Dr. Willian César Terra
Co-advisor

LAVRAS – MG
2025

Ficha Catalográfica elaborada pelo Sistema de Geração de Ficha Catalográfica da Biblioteca Universitária da UFLA, com dados informados pelo(a) próprio(a) autor(a).

Hodela, Geraldo Jamisse .
In silico identification of the protein targets of chaetoglobosins and benzotriazines for the selection of alternative nematicides to control Meloidogyne incognita / Geraldo Jamisse Hodela. - 2025.
117 p. : il.

Orientador: Denilson Ferreira de Oliveira
Coorientador: Willian César Terra

Tese (Doutorado) - Universidade Federal de Lavras, 2025.
Bibliografia.

1. Chaetoglobosin. 2. Benzoatriazine. 3. Molecular docking. 4. Nematicide. 5. Meloidogyne incognita. I. Oliveira, Denilson Ferreira de. II. Terra, Willian César . III. Universidade Federal de Lavras. IV. Título.

GERALDO JAMISSE HODELA

IN SILICO IDENTIFICATION OF THE PROTEIN TARGETS OF CHAETOGLOBOSINS AND BENZOTRIAZINES FOR THE SELECTION OF ALTERNATIVE NEMATICIDES TO CONTROL *Meloidogyne incognita*

IDENTIFICAÇÃO *IN SILICO* DOS ALVOS PROTEICOS DE CHAETOGLOBOSINAS E BENZOTRIAZINAS PARA A SELEÇÃO DE NEMATICIDAS ALTERNATIVOS PARA O CONTROLE DE *Meloidogyne incognita*

Thesis presented to the Federal University of Lavras, as part of the requirements of the Postgraduate Program in Agrochemistry, area of concentration in Chemistry/Biochemistry, to obtain the title of Doctor.

APPROVED on February 21, 2025

Prof. Dr. Denilson Ferreira de Oliveira	UFLA
Prof. Dr. Willian César Terra	UFLA
Prof. Dr. Geraldo Humberto Silva	UFV
Profa. Dra. Elisângela Jaqueline Magalhães	UFLA
Frof. Dr. Jorge Teodoro De Sousa	UFLA

Prof. Dr. Denilson Ferreira de Oliveira
Advisor

Prof. Dr. Willian César Terra
Co-advisor

LAVRAS - MG
2025

I dedicate this to my father (in memory) and my mother, Luísa Tingane, for their love.

I dedicate.

THANKS

I would like to thank:

The Federal University of Lavras, especially the Chemistry Department, for the opportunity.

To my advisor, Prof. Dr. Denílson Ferreira de Oliveira and my co-advisor Prof. Dr. Willian César Terra for their teachings during the research.

To all the professors of the Postgraduate Program in Agrochemistry, for their teachings during the training.

To Tarlei Luz de Paula, for teaching me the techniques and handling of the equipment in the nematology laboratory.

To all my colleagues in the nematology and natural products labs for their help during the research.

To Artinéia Widnesse Saguate, Barnabé Chachel, Horácio Bambo Pacule, Vitor Pereira de Sousa and the Reis Family, for their friendship during the training.

To my entire family, who supported me throughout the teaching and learning process.

This study was financed in part by the Coordenação de Aperfeiçoamento de Pessoal de Nível Superior – Brasil (CAPES) – Finance Code 001 and the Conselho Nacional de Desenvolvimento Científico e Tecnológico (CNPq) or Fundação de Amparo à Pesquisa de Minas Gerais (FAPEMIG).

Thank you very much!

GENERAL ABSTRACT

Phytonematodes of the genus *Meloidogyne* are parasites responsible for reducing agricultural production worldwide. Among the methods for controlling these parasites is chemical management, which can lead to contamination of humans and the environment with highly toxic substances. Therefore, new methods and products for controlling these nematodes, with less impact on humans and the environment, are in demand by society in general. As a result, several organic substances active against nematodes have been identified. However, the production of these substances on a commercial scale is not always feasible, which makes it necessary to use them as a basis for the development of new, affordable nematicides. To this end, computational chemistry is a very promising tool. Therefore, in order to contribute to the development of new nematicides for the control of *Meloidogyne* spp., this work aimed to identify *in silico* the protein targets of chaetoglobosins A and B, and benzotriazines A6 and A8, in the aforementioned nematodes, so that they can serve as models for the future generation of more efficient chemical structures as nematicides. In addition, the nematicidal activities of the inhibitors of the targets of each group of substances were also investigated *in vitro* and *in vivo*. The results of the *in silico* study show that the affinities of chaetoglobosins A and B for the sodium-dependent serotonin transporter protein (SERT) are similar to the affinities calculated for inhibitors of this protein; and that the affinities of benzoatriazines A6 and A8 for mitogen-activated protein kinase 14 (MAPK14) are also similar to the values calculated for inhibitors of this protein. Among the SERT inhibitors, paroxetine was selected, which showed a lethal concentration for 50% (LC_{50}) of *Meloidogyne incognita* second stage juveniles (J2) equal to 351.26 µg/mL. Under the same conditions, the positive control (fluensulfone) showed an LC_{50} of 39.31 µg/mL. Paroxetine also reduced the pathogenicity of *M. incognita* under greenhouse conditions. Among the MAPK14 inhibitors, the most promising was TCS ERK 11e, which showed moderate nematicidal activity against J2 of *M. incognita in vitro*. Therefore, the future study of SERT and MAPK14 inhibitors is potentially useful for the development of new nematicides to control *M. incognita*.

Keywords: chaetoglobosin; benzoatriazine; molecular docking; mitogen-activated protein kinase 14 (MAPK14); sodium-dependent serotonin transport protein (SERT); nematicide, *Meloidogyne incognita.*

RESUMO GERAL

Fitonematoides do gênero *Meloidogyn*e são parasitas responsáveis pela redução da produção agrícola em todo mundo. Dentre os métodos para o controle de tais parasitas se destaca o manejo químico, que pode ocasionar a contaminação do homem e do ambiente com substâncias de elevada toxicidade. Portanto, novos métodos e produtos para o controle de tais nematoides, com menores impactos sobre o homem e ambiente, são demandados pela sociedade em geral. Em decorrência, várias substâncias orgânicas ativas contra nematoides têm sido identificadas. Entretanto, a produção dessas substâncias em escala comercial nem sempre é exequível, o que torna necessário o uso de tais substâncias como base para o desenvolvimento de novos nematicidas de custo acessível. Para tanto, a química computacional é uma ferramenta muito promissora. Logo, com vistas a contribuir para o desenvolvimento de novos nematicidas para o controle de *Meloidogyne* spp., este trabalho objetivou identificar *in silico* os alvos proteicos das chaetoglobosinas A e B, e das benzotriazinas A6 e A8, nos referidos nematoides, para que sirvam de modelos para a geração futura de estruturas químicas mais eficientes como nematicidas. Além disso, também se investigou *in vitro* e *in vivo* as atividades nematicidas dos inibidores dos alvos de cada grupo de substâncias. Os resultados do estudo *in silico* mostram que as afinidades das chaetoglobosinas A e B pela proteína transportadora de serotonina dependente de sódio (SERT) são similares às afinidades calculadas para os inibidores de tal proteína; e que as afinidades das benzoatriazinas A6 e A8 pela proteína quinase ativada por mitógeno 14 (MAPK14) também são similares aos valores calculados para os inibidores dessa proteína. Dentre os inibidores da SERT, selecionou-se a paroxetina, que apresentou concentração letal para 50% (CL_{50}) dos juvenis do segundo estádio (J2) de *Meloidogyne incognita* igual a 351,26 µg/mL. Nas mesmas condições, o controle positivo (fluensulfona) apresentou CL_{50} de 39,31 µg/mL. A paroxetina também reduziu a patogenicidade de *M. incognita* em casa de vegetação. Dentre os inibidores da MAPK14, o que se mostrou mais promissor foi o TCS ERK 11e, que apresentou atividade nematicida moderada contra J2 de *M. incognita in vitro*. Portanto, o estudo futuro de inibidores da SERT e MAPK14 se mostra potencialmente útil para o desenvolvimento de novos nematicidas com vistas ao controle de *M. incognita*.

Palavras–Chave: chaetoglobosina; benzoatriazina; *docking* molecular; proteína quinase ativada por mitógeno 14 (MAPK14); proteína transportadora de serotonina dependente de sódio (SERT); nematicida; *Meloidogyne incognita*.

INDICADORES DE IMPACTO

Os nematoides parasitas de plantas (NPPs) são responsáveis por grandes perdas agrícolas em nível Mundial. O principal método de controle de NPPs se baseia no emprego de nematicidas químicos que são tóxicos para o homem e o ambiente. Consequentemente, existe uma elevada demanda por novos nematicidas, de baixa toxicidade para organismos não alvos e mais eficientes que aqueles atualmente disponíveis. Diante deste problema, a realização desta pesquisa foi uma oportunidade ímpar para contribuir com o desenvolvimento de novos nematicidas, para solucionar problemas de grande importância social, tecnológica, econômica e cultural, tanto no Brasil quanto em Moçambique. Além disto, durante a realização da pesquisa foi possível estar em contacto com vários pesquisadores, de diferentes grupos de pesquisas, o que será de valia para ampliação de conhecimentos, bem como para afirmar parcerias futuras com vistas a dar continuidade ao trabalho ou desenvolver novos projetos de importância agrícola para o Brasil e Moçambique.

IMPACT INDICATORS

Plant parasitic nematodes (PPNs) are responsible for major agricultural losses worldwide. The main method of controlling PPNs is based on the use of chemical nematicides that are toxic to humans and the environment. Consequently, there is a high demand for new nematicides that are low in toxicity to non-target organisms and more efficient than those currently available. Given this problem, this research was a unique opportunity to contribute to the development of new nematicides to solve problems of great social, technological, economic and cultural importance, both in Brazil and in Mozambique. In addition, during the research it was possible to be in contact with several researchers from different research groups, which will be valuable for expanding knowledge, as well as for establishing future partnerships with a view to continuing the work or developing new projects of agricultural importance for Brazil and Mozambique.

SUMMARY

FIRST PART

1 GENERAL INTRODUCTION

Plant-parasitic nematodes (PPNs) are responsible for worldwide losses of around 12-14% of agricultural production, which corresponds to approximately US$127 billion in annual harvests (Kim *et al*., 2021). In eastern and southern Africa, annual agricultural losses vary between 7 and 50% (Talwana *et al.,* 2016). Among PPNs it is worth mentioning root-knot nematodes (*Meloidogyne* spp.) that cause the greatest losses, which are estimated at US$75 billion per year (Li *at al*., 2015). Specifically, in Brazil, we can cite as an example the losses in coffee production, which are estimated at around 20% (Lordello,1986). For tomato crops, losses can be estimated at 85% (Ferraz; Churata-Masca, 1983), while cotton crop losses are in the 10-20% range (Machado, 2021).

Currently, more than 100 species of the *Meloidogyne* genus have been reported (Yeon *et al*., 2019). They are more abundant in regions with a tropical climate, where their reproduction can occur in greater number of host plants, making it difficult to eradicate these phytoparasites once they have established themselves in the field. Among the most common species worldwide are: *Meloidogyne incognita* (Kofoid & White) Chitwood, *Meloidogyne javanica* (Treub) Chitwood, *Meloidogyne arenaria* (Neal) Chitwood, and *Meloidogyne hapla* Chitwood (Chen; Li; Song, 2020). In the specific case of Brazil, the species that cause the greatest damage include *M. incognita*, *M. javanica*, and *Meloidogyne enterolobii* Yang & Eisenback, the first two being the most common (Campos *et al*., 2016).

The *M. incognita* species is one of the most widespread phytopathogens in the world, causing major losses in agricultural production worldwide, and is found in various crops and regions of Brazil. In Mozambique, it is most common in the provinces of Gaza and Inhambane, where it causes major losses to farmers in general (Kisitu *et al*., 2017). Plants attacked by this phytonematode can show dwarfism, yellowing of the leaves and the formation of galls on the roots, which hinders the absorption of water and nutrients (Ajith *et al*., 2020).

There are several possibilities described for the control of *Meloidogyne* spp. For example: crop rotation, the use of organisms antagonistic to nematodes, solarisation and the use of resistant cultivars (Bi; Gao; Yu, 2018). However, due to various shortcomings observed for such forms of control, the main method currently in use is based on the application of chemical nematicides that, in addition to increasing production costs, generally have various undesirable effects on the environment and humans (Bano *et al*., 2020). For example, poisoning with aldicarb [*O*-(*N*-methylcarbamoyl) oxime of 2-methyl-2-(methylthio) propanal] or carbofuran (2,2-dimethyl-2,3-dihydro-1-benzofuran-7-yl methylcarbamate) causes irreversible inhibition

of acetylcholinesterase (Baron, 1994; Moore *et al*., 2010). Consequently, several of these nematicides have been withdrawn from the market, creating a growing demand for new products, less aggressive to humans and the environment, for the efficient control of PPNs (Kaur *et al*., 2021). To satisfy this demand, one of the possibilities concerns the use of substances of natural or synthetic origin, since some of these substances have nematicidal action against nematodes (Campos *et al*., 2016) and are less toxic to human and the environment than several older nematicides. Among the various substances of natural origin with nematicidal action, it is worth highlighting chaetoglobosins A and B (Figure 1) (Khan *et al*., 2019). There have also been several studies on chemical structures of synthetic origin, such as the benzotriazines A6 and A8 (Chen *et al*., 2019) (Figure 1).

Figure 1- Chemical structures of chaetoglobosins and benzotriazines with nematicidal activities

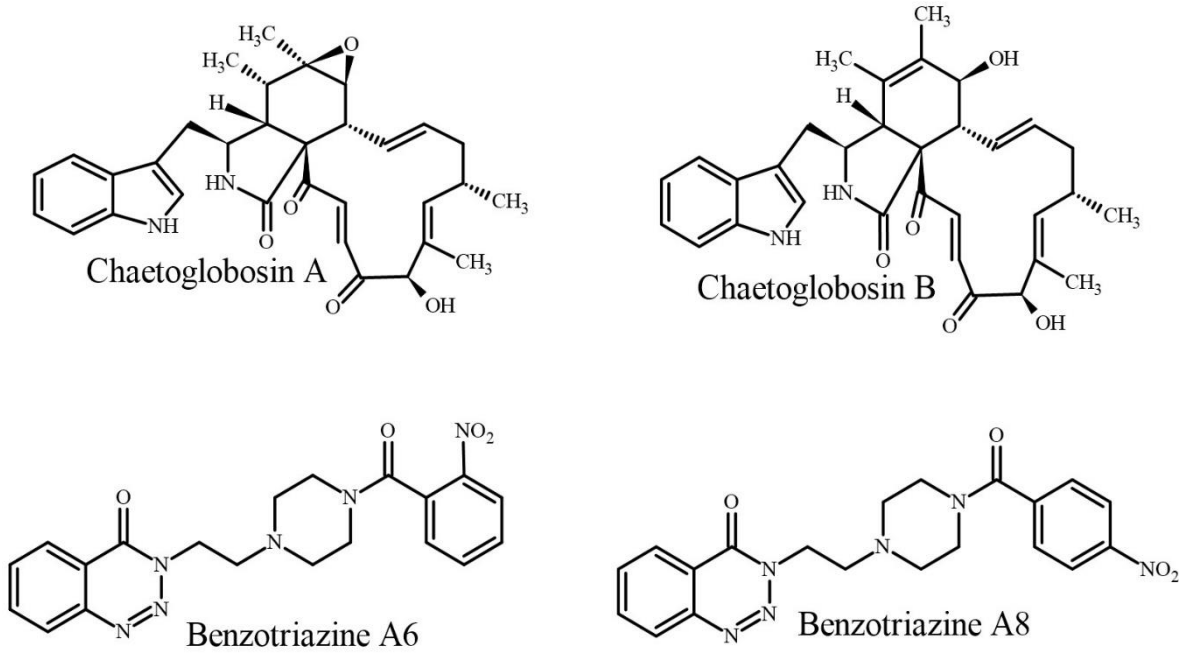

Source: From the author (2024).

In the specific case of chaetoglobosins A and B (Figure 1), isolated from *Chaetomium globosum* YSC5, an *in vitro* study carried out by Khan *et al*. (2019) revealed that the lethal concentrations for 50% (LC_{50}) *M. javanica* second-stage juveniles (J2) were equal to 88.4 and 107.07 µg/mL, respectively. Under the same conditions, the positive control, fosthiazate, had an LC_{50} of 73.7 µg/mL. In an *in vivo* experiment, the same authors showed that chaetoglobosin B reduced the number of galls per plant by 61.5%, the number of egg masses per plant by

72.4%, and the number of eggs per egg mass by 35.4%. As for chaetoglobosin A, it reduced the number of galls per plant by 59.0 %, the number of egg masses per plant by 71.1%, and the number of eggs per egg mass by 30.1%. The positive control (fosthiazate), under the same conditions, reduced the number of galls, number of egg masses, and number of eggs per egg mass by 72.5%, 84.3%, and 42.0%, respectively. In their work with the benzotriazines A6 and A8 (Figure 1), Chen *et al*. (2019) observed *in vitro* mortalities of *M. incognita* J2 equal to 71.1% and 70.0%, respectively, when the substances were studied at a concentration of 20 µg/mL.

The commercial production of substances with complex chemical structures, such as chaetoglobosins A and B and benzotriazines A6 and A8, can be economically unviable. Therefore, it is usually necessary to invest in long-term research to develop a methodology to produce these substances in an economically viable way (Leelananda; Lindert, 2016). One way around this problem could be to use the active substances as a starting point for *in silico* studies to obtain chemical structures that are more viable for commercial use than the substances used as a starting point. To this end, there are various computational methods, including pharmacophore search (Sotomayor; Schulten, 2007) and molecular docking (Huang *et al*., 2016), which can be combined with molecular dynamics simulation (Hernández-Rodríguez et al., 2016; Huang *et al*., 2016). These methods have been used to specifically explore the affinities and interactions between organic substances and their target proteins, as well as to target structural modifications in organic substances in order to maximise their attractive interactions with a specific protein (Hernández-Rodríguez *et al*., 2016).

1.1 Objectives

1.1.2 General objectives

In order to contribute to the development of new nematicides for the control of PPNs, the project aimed to identify the protein targets of chaetoglobosins A and B, and benzotriazines A6 and A8, in *Meloidogyne* spp. as well as to select substances active against *M. incognita*.

1.1.3 Specific objectives

a) To select substances pharmacophorically similar to chaetoglobosins A and B from a database of protein ligands in general.

b) To select, among the proteins whose ligands show greater similarity to chaetoglobosins A and B, those whose amino acid sequences are similar to the amino acid sequences of proteins encoded in the genomes of *Meloidogyne* spp.

c) To carry out molecular docking of chaetoglobosins A and B to the binding sites of the selected proteins, and compare the affinities of the chaetoglobosins for the proteins with those calculated for the inhibitors of these proteins.

d) To evaluate *in vitro* and/or *in vivo* the effects of the inhibitors of the proteins selected in 'c' on *M. incognita*.

e) To select substances that are pharmacophorically similar to benzotriazines A6 and A8 from a database of protein ligands in general.

f) To select, among the proteins whose ligands show the greatest similarity to benzotriazines A6 and A8, those whose amino acid sequences are similar to the amino acid sequences of proteins encoded in the genomes of *Meloidogyne* spp.

g) To carry out molecular docking of benzotriazines A6 and A8 to the binding sites of the selected proteins, and compare the affinities of the benzotriazines for the proteins with those calculated for the inhibitors of these proteins.

h) To evaluate *in vitro* and/or *in vivo* the effects of the inhibitors of the proteins selected in 'g' on *M. incognita*.

2 THEORETICAL FRAMEWORK

2.1 Plant-parasitic nematodes

Plant-parasitic nematodes (PPNs), also known as phytonematoides, are microscopic organisms (Crisford *et al*., 2020) that have an elongated body with a length of 0.2 to 3.0 mm and a width of 50 to 250 μm (Labandeira; Prevec, 2014). They also have hollow styli used for feeding (Bird; Kaloshian, 2003; Jones *et al*., 2013). According to their lifestyles and modes of parasitism, they can be categorised as ectoparasites or endoparasites, or as sedentary or migratory. The PPNs that cause the greatest losses in many cultivars are sedentary endoparasites, including cyst nematodes (*Heterodera* spp. and *Globodera* spp.) and root-knot nematodes (*Meloidogyne* spp.) (Bartlem; Jones; Hammes, 2014; Desmedt *et al*., 2020). Nematodes of the genus *Meloidogyne* are considered polyphagous and have a wide geographical distribution, tending to be more damaging in regions with a tropical and subtropical climate (Ozdemir; Gozel, 2018). PPNs life cycles depend on the species and various other factors such as humidity, soil type and, above all, temperature, the optimum value of which for most species varies between 15-30 °C. In general, most PPNs complete the cycle in three (03) to six (06) weeks,

depending on environmental conditions. Once mature females of the genus *Meloidogyne* are formed, the can lay eggs in gelatinous masses (egg masses), in which the nematode can survive in the soil or in plant residues for months. The first stage juveniles (J1), still in the egg, give rise to the second stage juveniles (J2), which correspond to the infective phase of the nematode. After hatching, J2 move towards the root tips, through which they penetrate the plant and migrate to the differentiation zone. They then establish a feeding site in the vascular parenchyma cells by injecting substances that induce plant cell differentiation. Once the feeding site has been established, the J2 increase in size and undergo successive ecdysis into the third (J3) and fourth stage juveniles (J4). Finally, they move on to the adult male or female stage (Bartlem; Jones; Hammes, 2014; Bird; Kaloshian, 2003; Castagnone-sereno *et al*. 2013) (Figure 2). As a result, the roots become distorted due to the formation of galls, which result in wilting and discolouration of the leaves, as well as stunted growth of the plant (Jones *et al*., 2013). In addition to the direct damage caused by the nematode, it must be taken into account that its parasitism can increase the likelihood of opportunistic infections by other soil pathogens, such as viruses, bacteria and fungi (Wesemael; VIaene; Moens, 2011).

Figure 2- Life cycle of *Meloidogyne* spp

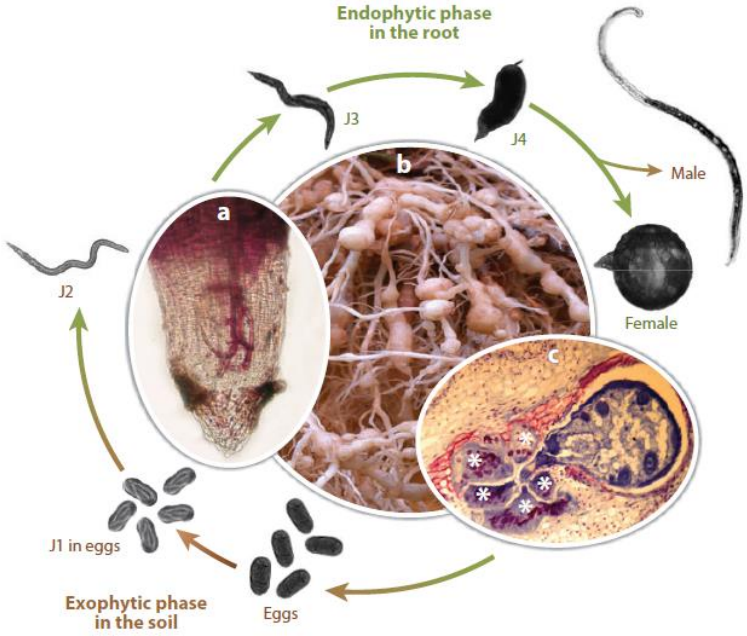

Source: Castagnone-sereno *et al*. (2013).

2.2 Natural products with nematicidal activities

Natural products are substances synthesised by plants, fungi, bacteria, insects and other organisms. Due to the great success of the use of such products in drug discovery in general, they have attracted significant attention in other areas, such as the development of new nematicides. They include isoprene, α-pinene, α-terpinene, β-pinene, camphor etc., as well as other chemical structures with organic functions like: alkene, aldehyde, ketone, alcohol, ester, carboxylic acid etc. (Chen; Li; Song, 2020).

Alcoholic and phenolic compounds, which are widely present in plants and microorganisms, can have a broad spectrum of biological activities (Chen; Li; Song, 2020). Examples include the alcohol geraniol and the phenol eugenol, which can be found in various plant species. Both have inhibitory effects against *Meloidogyne graminicola* Golden & Birchfield, with geraniol causing the greatest nematode mortality (Ajith *et al*., 2020).

Natural aldehydes with nematicidal properties are largely produced by plants (Chen; Li; Song, 2020). This is the case, for example, with (*E*, *E*)-deca-2,4-dienal and (*E*)-dec-2-enal (Figure 3), isolated from *Ailanthus altissima* (Mill) Swingle. These substances showed an LC_{50} for *M. javanica* J2 equal to 11.7 and 20.43 µg/mL, respectively. Under the same conditions, the positive control (fosthiazate) showed an LC_{50} equal to 11.9 µg/mL (Caboni *et al*., 2012). When the aldehyde *trans*-hex-2-enal (Figure 3) was tested *in vitro* directly against the J2 of *Bursaphelenchus xylophilus* Nickle, it was observed that its LC_{50} was equal to 9.87 µg/mL, after 48h of exposure of the nematode to the aldehyde. Under the same conditions, the commercial nematicide abamectin showed an LC_{50} equal to 0.099 µg/mL (Cheng *et al*., 2017).

Figure 3- Chemical structures of aldehydes active against nematodes

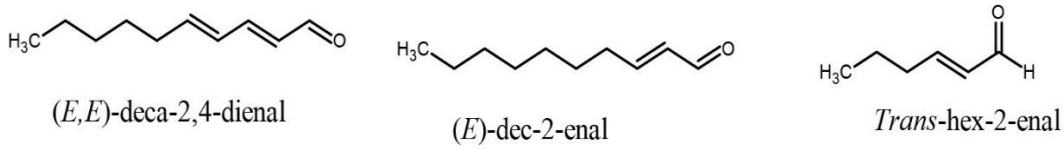

(*E,E*)-deca-2,4-dienal (*E*)-dec-2-enal *Trans*-hex-2-enal

Source: From the author (2024).

With regard to alkaloids, it is possible to cite, for example, those isolated from the plant *Fumaria parviflora* Lam., which produces substances capable of reducing crop damage caused by PPNs. For example, *cis*- and *trans*-protopinium (Figure 4), isolated from the roots of *F. parviflora*, caused 100% mortality of J2 and 95% inhibition of the hatching of J2 of *M. incognita* after 120 h of exposure of the nematode to these substances at a concentration of 200 µg/mL

(Naz *et al*., 2016). There are also the alkaloids isolated from the roots of *Waltheria indica* L. (5′-methoxyalterione A and Walteherione A - Figure 4), which showed LC_{50} values against the J2 of *B. xylophilus* ranging from 2.1 to 3.5 µg/mL. Under the same conditions, the chemical nematicide abamectin showed an LC_{50} equal to 0.09 µg/mL (Jang *et al*., 2019).

Figure 4- Chemical structures of alkaloids active against nematodes

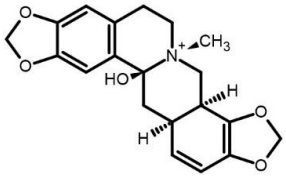

Cis- protopinium

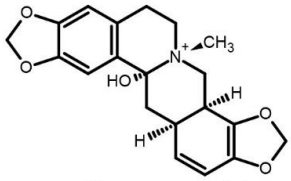

Trans-protopinium

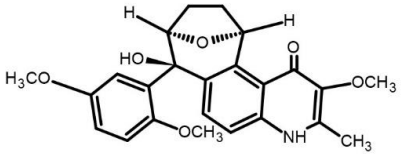

5′-methoxyalterione A

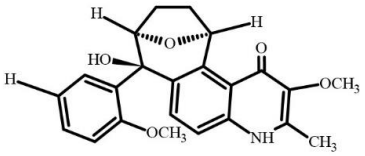

Walteherione A

Source: From the author (2024).

Nematicidal peptides can be found, for example, in microorganisms of the *Fusarium* and *Bacillus* genera, as well as in plants (Chen; Li; Song, 2020), which can be exemplified by the plant species *Picea sitchensis* (Bong) Carr, from which a peptide with strong nematicidal activity against the free-living nematode *Caenorhabditis elegans* Maupas was isolated. After 5 h of exposure of the nematode to the peptide at concentrations ranging from 10 to 200 µg/mL, mortalities of 55.9 to 76.7 % were observed (Liu *et al*., 2011). Rhabdoptide J (Figure 5), a peptide isolated from the culture of the bacterium *Xenorhabdus budapestensis* SN84 Thomas & Poinar, showed an LC_{50} for *M. incognita* J2 equal to 27.8 µg/mL. Under the same conditions, the commercial nematicide abamectin showed an LC_{50} of 9.9 µg/mL (Bi; Gao; Yu, 2018). The peptides leucinostatin U, Q and P (Figure 5), isolated from the fungus *Ijuhya vitelina* Fechat & Fourn, showed nematicidal action against *C. elegans*. The lethal concentrations for 90% (LC_{90}) of the nematode population varied between 5 and 7 µg/mL, while the LC_{90} for the commercial nematicide abamectin was equal to 1 µg/mL (Moussa *et al*., 2020).

Figure 5- Chemical structures of peptides active against nematodes.

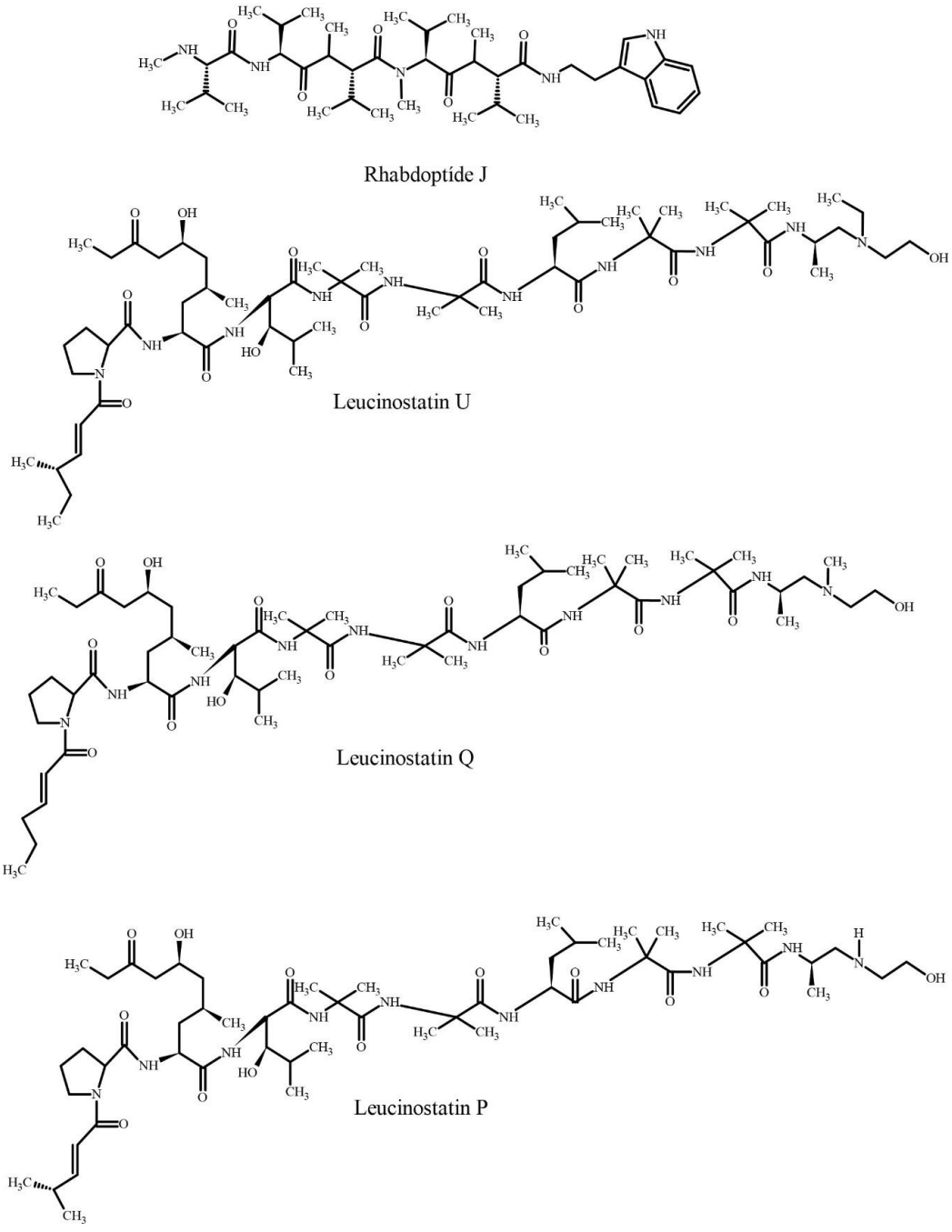

Source: From the author (2024).

In the specific case of carboxylic acids, Faizi *et al*. (2011) observed that the substances showed promising results. For example, when the same authors studied the nematicidal activities of linoleic acid and oleic acid (Figure 6) *in vitro* on the species *Heterodera zeae* Koshy, Swarup & Sethi, they found that 100% of the nematode's J2 were dead after 24 h of exposure

to the acids. Yeon *et al*. (2019), when studying the nematicidal activities of maleic acid (Figure 6) on *M. incognita in vitro*, also observed 100% mortality of *M. incognita* J2 and inhibition of nematode egg hatching by 70.4%. Bogner *et al*. (2017) demonstrated that indole-2-acetic acid (Figure 6), produced by the fungus *Fusarium oxysporum* 162, showed nematicidal activity against J2 of *M. incognita*, with an LC_{50} value of 117.28 µg/mL in *in vitro* tests. Under the same conditions, the chemical nematicides carbofuran and aldicarb showed LC_{50} values of 180.00 and 64.15 µg/mL, respectively.

Figure 6- Chemical structures of carboxylic acids active against nematodes.

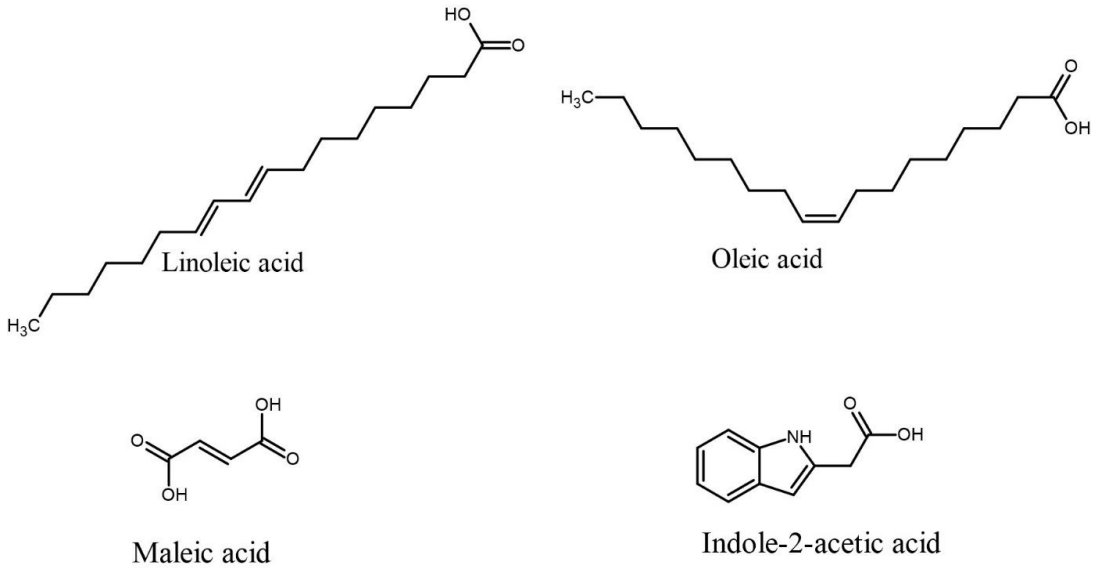

Source: From the author (2024).

Terpenoids have a broad spectrum of biological activities, including nematicidal activity (Chen; Li; Song, 2020). For example, *α*-terpinene, *α*-pinene and nerolidol (Figure 7), in *in vitro* tests, showed nematicidal activity against *M. javanica* J2, with LC_{50} values equal to 36.22, 47.49 and 53.60 µg/mL, respectively, while the commercial nematicide oxamyl showed an LC_{50} equal to 10.94 µg/mL (El-Habashy; Abdel Rasoul; Abdelgaleil, 2020). Gymnoascole acetate (Figure 7), which is a terpenoid isolated from the fungus *Gymnoascus reessii* Baran, induced immobility in 100% of *M. incognita* J2 *in vitro* and inhibited the hatching of J2 of the nematode by 90%, at a concentration of 133 µg/mL, after 7 days of exposure. In an *in vivo* experiment, the same terpenoid reduced the number of galls per plant by 72.2%, the number of J2 in the soil by 85.2% and the number of J2 in the roots by 84.2% (Liu *et al*., 2017).

Figure 7- Chemical structures of terpenes active against nematodes.

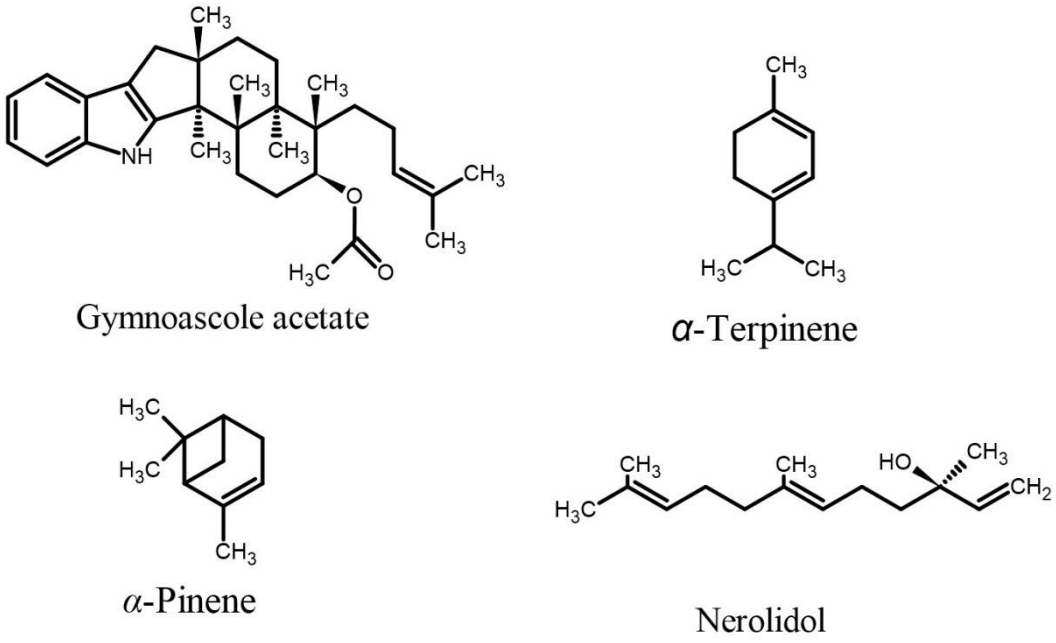

Source: From the author (2024)

2.3 Molecular docking

Computational chemistry can be seen as a tool capable of providing important information for the process of discovering new bioactive molecules, as well as for optimizing existing prototypes. In general, it is made up of various methods used to build, visualize and manipulate diverse chemical structures, through which conformational analyses and calculations of physical properties, molecular modeling, molecular docking, etc. can be carried out, which are useful for interpreting the structure-activity relationship. Its development in recent years is mainly due to advances in computational resources (hardware and software) (Fan; Fu; Zhang, 2019).

Molecular docking is one of the most widely used computational methods in recent years for *in silico* screening, which aims to obtain optimal conformations according to complementarity and pre-organization in order to predict the ideal orientation of the ligand in the binding site of the target protein. This method has been used at various stages of drug discovery and development, at low cost and in a very short time (Gupta, Sharma, Kumar, 2018).

For molocular docking, several databases can be used, including, for example, the NCBI research database (National Center for Biotechnology information;

https://www.ncbi.nlm.nih.gov/), the RCSB Protein Data Bank https://www.rcsb.org/, Berman *et al*., 2000), Ligand Expo database (http://ligand-expo.rcsb.org/index.html, Feng *et al*., 2004), CHEMBL database (European Molecular Biology Laboratory's European Bioinformatics Institute, https://www.ebi.ac.uk/, Mendez *et al*.,2019), among others.

3 GERAL CONSIDERATIONS

The chemical nematicides available for controlling plant-parasitic nematodes (PPNs) are toxic to humans and the environment. In addition, the commercial production of such substances can lead to increased costs for agricultural producers in general. In order to contribute to solving these problems, an *in silco* study was carried out, resulting in the identification of the sodium-dependent serotonin transporter protein (SERT) as the target of chaetoglobosins A and B; and the identification of mitogen-activated protein kinase 14 (MAPK14) as the target of benzotriazines A6 and A8.

With regard to SERT inhibitors, paroxetine showed a lethal concentration for 50% (LC_{50}) of second-stage juveniles (J2) of *Meloidogyne incognita* equal to 351.26 µg/mL. This substance also reduced the pathogenicity of *M. incognita* in the greenhouse. Among the MAPK14 inhibitors, TCS ERK 11e showed moderate nematicidal activity against J2 of *M. incognita in vitro*. Therefore, it is believed that these inhibitors could be useful in the development of new nematicides for the control of *M. incognita* and other PPNs.

REFERENCES

AJITH, M. *et al*. Chemical composition and nematicidal activity of essential oils and their major compounds against *Meloidogyne graminicola* (Rice Root-Knot Nematode). **Journal of Essential Oil Research**, v. 32, n. 6, p. 526-535, 2020.

BANO, Samina *et al*. Nematicidal activity of flavonoids with structure activity relationship (SAR) studies against root knot nematode *Meloidogyne incognita*. **European Journal of Plant Pathology**, v. 157, p. 299-309, 2020.

BARON, Ronald L. A carbamate insecticide: a case study of aldicarb. **Environmental Health Perspectives**, v. 102, n. suppl 11, p. 23-27, 1994.

BARTLEM, Derek G.; JONES, Michael GK; HAMMES, Ulrich Z. Vascularization and nutrient delivery at root-knot nematode feeding sites in host roots. **Journal of experimental botany**, v. 65, n. 7, p. 1789-1798, 2014.

BERMAN, Helen M. *et al*. The protein data bank. **Nucleic acids research**, v. 28, n. 1, p. 235-242, 2000.

BI, Yuhui; GAO, Chunzhi; YU, Zhiguo. Rhabdopeptides from *Xenorhabdus budapestensis* SN84 and their nematicidal activities against *Meloidogyne incognita*. **Journal of agricultural and food chemistry**, v. 66, n. 15, p. 3833-3839, 2018.

BIRD, David McK; KALOSHIAN, Isgouhi. Are roots special Nematodes have their say. **Physiological and Molecular Plant Pathology**, v. 62, n. 2, p. 115-123, 2003.

BOGNER, Catherine W. *et al*. Bioactive secondary metabolites with multiple activities from a fungal endophyte. **Microbial biotechnology**, v. 10, n. 1, p. 175-188, 2017.

CABONI, Pierluigi *et al*. Nematicidal activity of (*E, E*)-2, 4-decadienal and (*E*)-2-decenal from *Ailanthus altissima* against *Meloidogyne javanica*. **Journal of Agricultural and food Chemistry**, v. 60, n. 4, p. 1146-1151, 2012.

CAMPOS, Viviane AC *et al*. Styryllactones from *Cryptocarya aschersoniana* Mez.(Lauraceae Juss.) with activity against *Meloidogyne* spp. and *in silico* interaction with a putative fumarase from *Meloidogyne hapla*. 2016.

CASTAGNONE-SERENO, Philippe *et al*. Diversity and evolution of root-knot nematodes, genus *Meloidogyne*: new insights from the genomic era. **Annual review of phytopathology**, v. 51, n. 1, p. 203-220, 2013.

CHEN, Jixiang; LI, Qing X.; SONG, Baoan. Chemical nematicides: Recent research progress and outlook. **Journal of Agricultural and Food Chemistry**, v. 68, n. 44, p. 12175-12188, 2020.

CHEN, Xiulei *et al.* Synthesis and nematicidal evaluation of 1, 2, 3-benzotriazin-4-one derivatives containing piperazine as linker against *Meloidogyne incognita*. **Chinese Chemical Letters**, v. 30, n. 6, p. 1207-1213, 2019.

CHENG, Le *et al*. Effects of *trans*-2-hexenal on reproduction, growth and behaviour and efficacy against the pinewood nematode, *Bursaphelenchus xylophilus*. **Pest management science**, v. 73, n. 5, p. 888-895, 2017.

CRISFORD, Anna *et al*. Identification and characterisation of serotonin signalling in the potato cyst nematode *Globodera pallida* reveals new targets for crop protection. **PLoS Pathogens**, v. 16, n. 10, p. e1008884, 2020.

DESMEDT, Willem *et al*. A phytochemical perspective on plant defense against nematodes. **Frontiers in plant science**, v. 11, p. 602079, 2020.

EL-HABASHY, Deiaa E.; ABDEL RASOUL, Mona A.; ABDELGALEIL, Samir AM. Nematicidal activity of phytochemicals and their potential use for the control of *Meloidogyne javanica* infected eggplant in the greenhouse. **European Journal of Plant Pathology**, v. 158, p. 381-390, 2020.

FAIZI, Shaheen *et al*. Isolation of nematicidal compounds from Tagetes patula L. yellow flowers: Structure–activity relationship studies against cyst nematode *Heterodera zeae* infective stage larvae. **Journal of Agricultural and Food Chemistry**, v. 59, n. 17, p. 9080-9093, 2011.

FAN, Jiyu; FU, Ailing; ZHANG, Le. Progress in molecular docking. **Quantitative Biology**, v. 7, p. 83-89, 2019.

FENG, Zukang *et al*. Ligand Depot: a data warehouse for ligands bound to macromolecules. **Bioinformatics**, v. 20, n. 13, p. 2153-2155, 2004.

FERRAZ, LCC B.; CHURATA-MASCA, MG C. Comportamento de cultivares de tomateiro (*Lycopersicon esculentum* Mill.) de crescimento determinado em relaçáo ao nemayoide Meloidogyne incognita (Kofoid & White, 1919) Chitwood, 1949. 1983.

GUPTA, Meenakshi; SHARMA, Ruchika; KUMAR, Anoop. Docking techniques in pharmacology: How much promising? **Computational biology and chemistry**, v. 76, p. 210-217, 2018.

HERNÁNDEZ-RODRÍGUEZ, Maricarmen *et al*. Current tools and methods in molecular dynamics (MD) simulations for drug design. **Current medicinal chemistry**, v. 23, n. 34, p. 3909-3924, 2016.

HUANG, Sheng-You *et al*. HybridDock: A hybrid protein–ligand docking protocol integrating protein-and ligand-based approaches. **Journal of Chemical Information and Modeling**, v. 56, n. 6, p. 1078-1087, 2016.

JANG, Ja Yeong *et al*. Control of root-knot nematodes using *Waltheria indica* producing 4-quinolone alkaloids. **Pest management science**, v. 75, n. 8, p. 2264-2270, 2019.

JONES, John T. *et al*. Top 10 plant-parasitic nematodes in molecular plant pathology. **Molecular plant pathology**, v. 14, n. 9, p. 946-961, 2013.

KAUR, Komalpreet *et al.* N-alkyl isatin derivatives: Synthesis, nematicidal evaluation and protein target identifications for their mode of action. **Pesticide Biochemistry and Physiology**, v. 171, p. 104736, 2021.

KHAN, Babar *et al*. Nematicidal metabolites from endophytic fungus *Chaetomium globosum* YSC5. **FEMS microbiology letters**, v. 366, n. 14, p. fnz169, 2019.

KIM, Yoon Jee *et al.* Nematicidal activity of grammicin biosynthesis pathway intermediates in *Xylaria grammica* KCTC 13121BP against *Meloidogyne incognita*. **Molecules**, v. 26, n. 15, p. 4675, 2021.

KISITU, J. *et al*. Intensity and distribution of *Meloidogyne* spp. in cowpea growing areas of Mozambique. 2017.

LABANDEIRA, Conrad C.; PREVEC, Rose. Plant paleopathology and the roles of pathogens and insects. **International Journal of Paleopathology**, v. 4, p. 1-16, 2014.

LEELANANDA, Sumudu P.; LINDERT, Steffen. Computational methods in drug discovery. **Beilstein journal of organic chemistry**, v. 12, n. 1, p. 2694-2718, 2016.

LI, Juan *et al*. Molecular mechanisms of nematode-nematophagous microbe interactions: basis for biological control of plant-parasitic nematodes. **Annual review of phytopathology**, v. 53, n. 1, p. 67-95, 2015.

LIU, Feng *et al.* Structure-based optimization of pyridoxal 5′-phosphate-dependent transaminase enzyme (BioA) inhibitors that target biotin biosynthesis in *Mycobacterium tuberculosis*. **Journal of medicinal chemistry**, v. 60, n. 13, p. 5507-5520, 2017.

LIU, Rui *et al*. Two antimicrobial and nematicidal peptides derived from sequences encoded *Picea sitchensis*. **Journal of Peptide Science**, v. 17, n. 9, p. 627-631, 2011.

LORDELLO, Luiz Gonzaga E. Nematóides das plantas cultivadas. 1986.

MACHADO, Andressa Cristina Zamboni. Problems and solutions to integrated nematode management of root-knot, reniform and lesion nematodes in cotton in Brazil. In: **Integrated Nematode Management: State-of-the-art and visions for the future**. Wallingford UK: CABI, 2021. p. 73-79.

MENDEZ, David *et al*. ChEMBL: towards direct deposition of bioassay data. **Nucleic acids research**, v. 47, n. D1, p. D930-D940, 2019.

MOORE, Dwayne RJ *et al*. Refined aquatic risk assessment for aldicarb in the United States. **Integrated Environmental Assessment and Management: An International Journal**, v. 6, n. 1, p. 102-118, 2010.

MOUSSA, Ashaimaa Y. *et al*. New peptaibiotics and a cyclodepsipeptide from *Ijuhya vitellina*: Isolation, identification, cytotoxic and nematicidal activities. **Antibiotics**, v. 9, n. 3, p. 132, 2020.

NAZ, Ishrat *et al*. *Cis*-and *trans*-protopinium, a novel nematicide, for the eco-friendly management of root-knot nematodes. **Crop Protection**, v. 81, p. 138-144, 2016.

OZDEMIR, Esengul; GOZEL, Ugur. Nematicidal activities of essential oils against *Meloidogyne incognita* on tomato plant. **Fresenius Environmental Bulletin**, v. 27, n. 6, p. 4511-4517, 2018.

SOTOMAYOR, Marcos; SCHULTEN, Klaus. Single-molecule experiments *in vitro* and *in silico.* **Science**, v. 316, n. 5828, p. 1144-1148, 2007.

TALWANA, Herbert *et al*. Agricultural nematology in East and Southern Africa: problems, management strategies and stakeholder linkages. **Pest Management Science**, v. 72, n. 2, p. 226-245, 2016.

WESEMAEL, Wim; VIAENE, Nicole; MOENS, Maurice. Root-knot nematodes (*Meloidogyne* spp.) in Europe. **Nematology**, v. 13, n. 1, p. 3-16, 2011.

YEON, Jehyeong *et al*. Control of root-knot nematodes by a mixture of maleic acid and copper sulfate. **Applied Soil Ecology**, v. 141, p. 61-68, 2019.

PART TWO - ARTICLES

ARTICLE 1

Predicting the Enzymatic Target of Benzotriazines in the Plant-Parasitic Nematode *Meloidogyne incognita* by Virtual Screening, Amino Acid Sequence Analysis, Molecular Docking, and Biological Evaluation

Article Submitted to Journal of Molecular Recognition

Geraldo J. Hodela, Vitor P. Sousa, Rodrigo M. Fráguas, Willian C. Terra, and Denilson F. Oliveira

Geraldo J. Hodela (orcid.org/0000-0002-14832452; jamisse2008@yahoo.com.br), **Rodrigo M. Fráguas (**orcid.org/0009-0002-2241-2834; rodrigofraguas1@hotmail.com) and **Denilson F. Oliveira** (orcid.org/0000-0001-9326-8716; denilson@ufla.br) - *Laboratório de Produtos Naturais, Departamento de Química, Universidade Federal de Lavras, Lavras-MG, Brazil.*

Willian C. Terra (orcid.org/0000-0002-7683-6790; willianterra@ufla.br) and **Vitor P. Sousa (**orcid.org/0009-0005-5470-1480; vitorpeira.s@gmail.com) - *Laboratório de Nematologia, Departamento de Fitopatologia, Universidade Federal de Lavras, Lavras-MG, Brazil*.

Corresponding author:

Denilson F. Oliveira - *Laboratório de Produtos Naturais, Departamento de Química, Universidade Federal de Lavras, Lavras-MG, Brazil; orcid.org/0000-0001-9326-8716; Phone: +55 35 3829 1623*; Email: denilson@ufla.br.

ABSTRACT

Plant-parasitic nematodes (PPNs) cause significant agricultural losses worldwide by parasitizing various plant species. Since commercially available nematicides pose toxicity risks to non-target organisms, this study aimed to use two benzotriazines – previously found to be active against the PPN *Meloidogyne incognita* – as a starting point for selecting target enzymes to develop new nematicides. To this end, the study had two specific objectives: a) to identify, *in silico*, the protein target of benzotriazines in *Meloidogyne* spp.; and b) to investigate, *in vitro*, the nematicidal activity of inhibitors of the identified protein target against *M. incognita*. The *in silico* analysis revealed that benzotriazines exhibited affinities for mitogen-activated protein kinase 14 (MAPK14), comparable to those calculated for MAPK14 inhibitors. The *in vitro* study further demonstrated that commercially available MAPK14 inhibitors reduced nematode mobility by 49.75 – 55.06% when applied at a concentration of 666 µg/mL. These findings indicate that benzotriazines interact with *M. incognita* protein MAPK14, making it a promising target for developing new nematicides.

Keywords: Nematicide, *Meloidogyne incognita*, docking, mitogen-activated protein kinase 14, benzotriazine, plant-parasitic nematode.

1| INTRODUCTION

Plant-parasitic nematodes (PPNs) cause annual agricultural losses of approximately US$157 billion per year worldwide [1]. Among these parasites, root-knot nematodes (*Meloidogyne* spp.) [2] are particularly notable, with *Meloidogyne incognita* (Kofoid & White) Chitwood being the most widespread species [1]. In a study on biotic risk factors affecting global food security, *M. incognita* was ranked as the most invasive plant disease-causing agent [3]. This pathogen has been responsible for significant losses in economically important crops such as tomatoes [4].

On many conventional farms, PPN control has traditionally been conducted using chemical nematicides. However, some of these agrochemicals are highly toxic to non-target organisms, leading to their removal from the market. Offending nematicides include aldicarb [*O*-(*N*-methylcarbamoyl) oxime of 2-methyl-2-(methylthio)propanal], carbofuran (2,2-dimethyl-2,3-dihydro-1-benzofuran-7-yl methylcarbamate), and CH_3Br (methyl bromide) [1, 5].

Despite the introduction of new molecules for PPN control, such as fluensulfone (5-chloro-2-(3,4,4-trifluorobut-3-en-1-ylsulfonyl)-1,3-thiazole) [1, 5], there remains a high demand for new nematicides that are more cost-effective and less harmful to humans and the environment [6]. One promising approach is the study of novel molecules with nematode activity, which could expand the possibilities for developing more efficient products than those commercially available. Among these molecules, benzotriazines A6 and A8 (Figure 1) have shown significant *in vitro* effectiveness, causing mortality rates of *M. incognita* second-stage juveniles (J2) of 71.1% and 70.0%, respectively, at a concentration of 20 µg/mL [7].

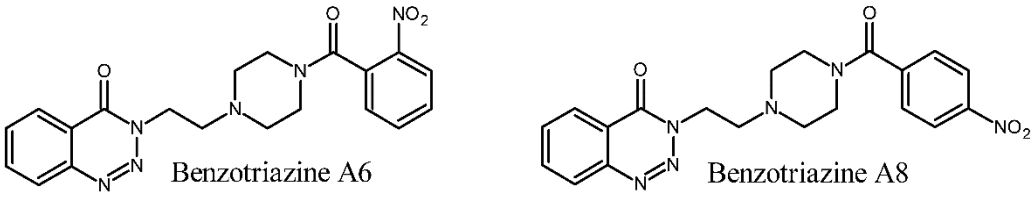

FIGURE 1 | Chemical structures of benzotriazines A6 and A8.

Given the above considerations, the general objective of this study was to identify, *in silico*, the enzymatic target of benzotriazines A6 and A8 in *Meloidogyne* spp. using a simple, low-cost computational methodology. This target could then be utilized in future research to develop efficient enzyme inhibitors aimed at controlling *M. incognita*.

The specific objectives of this study were: a) to select protein ligands that are structurally similar to the benzotriazines A6 and A8; b) to identify, among the proteins complexed to the selected ligands, those with the greatest amino acid sequences similarity to the corresponding proteins produced in *Meloidogyne* spp.; c) to perform molecular docking of benzotriazines A6 and A8 to the binding sites of these proteins to determine which can be inhibited by benzotriazines A6 and A8; and d) to conduct biological tests using inhibitors of the selected proteins against *M. incognita* in order to validate the results obtained *in silico*.

2 | Materials and Methods

2.1 | Preparation of Three-Dimensional Structures of Benzotriazines

Based on the work of Texeira et al. [8], the chemical structures of benzotriazines A6 and A8 (Figure 1) were drawn to calculate their pKa values at pH 7 using the Marvin Sketch 22.11 program (http:\www.chemaxon.com\marv), with default settings applied to all parameters. Both structures were protonated at the amine function and subjected to conformational searches using the Open3Dalign 2.3 [9] computer program.

For this purpose, 1,000 molecular dynamics simulations were performed, each consisting of 1,000 steps of 1 fs, using the Merck Molecular Force Field 94 (MMFF94). The most stable conformations, as well as all conformations within 10 kcal/mol of the most stable, were optimized using the Mopac 2016 program (http://openmopac.net/background.html). The optimization employed the PM7 Hamiltonian and implicitly accounted for the solvent (water) through the COnductor-like Screening MOdel (COSMO). Using the same program, the optimized structures underwent thermodynamic calculations to determine Gibbs free energy values. Finally, Boltzmann distributions were calculated for each conformation of each chemical structure.

2. 2 | Virtual Screening: Protein Ligands Three-Dimensionally Similar to Benzotriazines

For this stage, only those conformations representing 3.33% of the benzotriazine A6 population and 9.09% of the benzotriazine A8 population were used (Supporting Information, Tables S1 and S2 and Figures S1 and S2). The search for three-dimensionally similar structures to the benzotriazines was conducted using the Ligand Expo database (http://ligand-expo.rcsb.org/ld-download.html) [10] and the Lisica 1.0.1 computer program (http://insilab.org/lisica) [11]. Only ligands with a Tanimoto score ≥ 0.4 were selected, provided they were not chemically bound to the protein or randomly complexed on its surface.

2.3 | Amino Acid Sequence Analysis

The amino acid sequences of the proteins complexed with the selected ligands (Section 2.2) were used to search for similar sequences in the genomes of nematodes of the genus *Meloidogyne* (taxid:18290) via NCBI (National Center for Biotechnology Information;https://www.ncbi.nlm.nih.gov/) [12], using the Blastp +2.13.0 computer program (https://blast.ncbi.nlm.nih.gov/Blast.cgi) [13]. Only those proteins with scores above 200 were selected: protein kinase 2 (code: 2DS1) [14] and mitogen-activated kinase 14 (code: 3IW7) [15].

The amino acid sequences of these proteins were then used to search the RCSB Protein Data Bank (https://www.rcsb.org) [16] for proteins with at least 95% sequence similarity.

All protein sequences were aligned using Clustal Omega 1.2.1 [17] via the UGENE 1.32.0 program [18]. Hamming dissimilarities (%) were calculated, including gaps, and sequence similarity was determined as 100 – dissimilarity (Supporting Information, Tables S3 and S4). The protein with the highest similarity to the *Meloidogyne* spp. genome was selected to continue the study.

2.4 | Molecular Docking of Benzotriazines and Inhibitors of Mitogen-activated Protein Kinase 14

Files in PDB (Protein Data Bank) format containing the biological units of mitogen-activated protein kinase 14 (Supporting Information, Table S5) were downloaded from the RCSB Protein Data Bank (https://www.rcsb.org) [16] for alignment with the structure of 3IW7 [15]. The alignment was performed using the LovoAlign 21.027 computer program [19], which was also used to calculate root mean square deviation (RMSD) values for the atomic positions.

Proteins that did not visually align or had RMSD values exceeding 4 Å were discarded. Additionally, proteins with mutations that were not at the ends of their chains, as well as those missing amino acid residues in or near the active site, were excluded from further analysis.

The structures of the inhibitors of mitogen-activated protein kinase 14 (Supporting Information, Table S6) were obtained in SDF (Structure Data File) format from the RCSB Protein Data Bank (https://www.rcsb.org) [16] and subjected to pKa calculations at pH 7 using the Marvin Sketch 22.11 program (http://www.chemaxon.com/marvi). Based on the results of these calculations,

the inhibitors were appropriately protonated and saved in PDB format. They were then converted to PDBQT **(**Protein Data Bank, Partial Charge (Q), & Atom Type (T)) format using MGLTools 1.5.7rcl [20]. Using the same program, the conformations of benzotriazines A6 and A8 (Supporting Information, Tables S1 and S2 and Figures S1 and S2) were also converted to PDBQT format. The three-dimensional structures of the selected biological units (Supporting Information, Table S5), after alignment with the 3IW7 [15] protein, were similarly converted to PDBQT format.

The grid was then centered at 20.17, 0.78, and –22.61 Å (x, y, and z), with dimensions of 19.01, 29.58, and 24.19 Å (x, y, and z), encompassing the entire experimental complexation region of the mitogen-activated protein kinase 14 inhibitors. Using the QuickVina 2.1 program [21], the inhibitors of mitogen-activated protein kinase 14 and the conformations of the benzotriazines A6 and A8 were docked to the target protein. All program parameters were kept at the default settings, except for the exhaustiveness parameter, which was increased to 256.

Next, the overlaps between inhibitors docked with QuickVina [21] and those experimentally complexed with proteins were analyzed using the UCSF Chimera 1.17.3 computer program (https://www.cgl.ucsf.edu/chimera/download.html) [22]. Finally, affinity values obtained from the docking step were subjected to the Shapiro-Wilk test for normality [23] and Bartlett's homoscedasticity test [24], followed by analysis of variance (ANOVA). Mean values were then compared using the Scott-Knott grouping test [25] at a 5% significance level, using the R program version 4.4.0 [26].

2.5 | Immobility of *M. incognita* J2 After Exposure to Mitogen-Activated Protein Kinase 14 Inhibitors

Approximately 5,000 *M. incognita* eggs were placed in pots containing tomato seedlings (*Solanum lycopersicum* L. 'Santa Clara'). After 45 days, the roots were removed, thoroughly washed under running water, and cut into approximately 1 cm pieces. The root fragments were then ground in a blender for 30 seconds in 750 mL of a 0.5% (g/mL) aqueous sodium hypochlorite solution.

The resulting suspension was filtered through two sieves with 200- and 500-mesh pores. The eggs were then rinsed thoroughly with water to remove any residual sodium hypochlorite. Eggs retained on the 500-mesh sieve were collected in a 500 mL beaker and placed in a hatching chamber maintained at a constant temperature of 28 ºC. J2 hatched within the first 24 h were discarded, and only J2 with a maximum of 48 h between hatching and experimental setup were used.

A 20 µL aqueous suspension containing approximately 20 *M. incognita* J2 and 100 µL of a solution of a mitogen-activated protein kinase 14 inhibitor (Figure 2) were placed in 96-well microplates. To prepare these inhibitor solutions, the components were dissolved in an aqueous solution of Tween 80® at a concentration of 0.02 g/mL. The final concentration in the microplate was 666 µg/mL. The microplates were maintained in a BOD at 28 ºC.

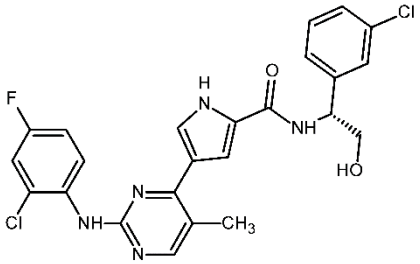

4-[2-[(2-chloro-4-fluorophenyl)amino]-5-methyl-4-pyrimidinyl]-*N*-[(1*S*)-1-(3-chlorophenyl)-2-hydroxyethyl]-1H-pyrrole-2-carboxamide (TCS ERR 11e)

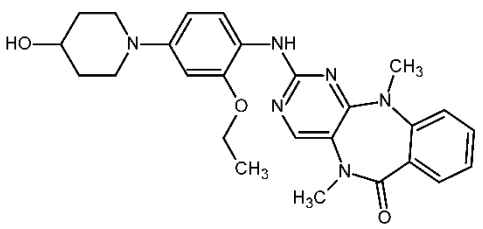

2-[[2-ethoxy-4-(4-hydroxy-1-piperidinyl)phenyl]amino]-5,11-dihydro-5,11-dimethyl-6*H*-pyrimido[4,5-b][1,4]benzodiazepine-6-one (XMD8-92)

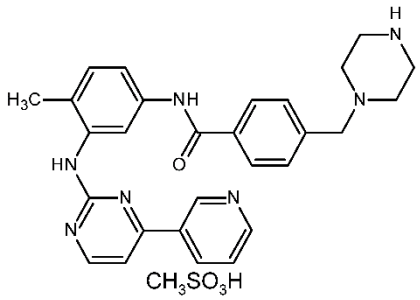

4-[(4-methyl-1-piperazinyl)methyl]-*N*-[4-methyl-3-[[4-(3-pyridinyl)-2-pyrimidinyl]amino]-phenyl]benzamide methanesulfonate (Imatinib mesylate)

FIGURE 2 | Chemical structures of mitogen-activated protein kinase 14 inhibitors: TCS ERK 11e (purity: ≥ 98%; origin: Cayman Chemical Company), XMD8-92 (purity ≥ 99%; origin: Cayman Chemical Company), and imatinib mesylate (purity ≥ 98%; origin: Sigma-Aldrich).

Each treatment was performed in five replicates, using fluensulfone (Nimitz®, ADAMA) at 34 µg/mL (final concentration in the microplate) as a positive control, corresponding to the lethal concentration for 50% (LC_{50}) of nematodes according to literature data [27, 28]. An aqueous solution of Tween 80® at 0.02 g/mL was used as a negative control.

After 72 h, mobile and immobile J2 were counted using a microscope. The data were converted into percentages and subjected to the Shapiro-Wilk normality [23] and Bartlett's homoscedasticity [24] tests. Since normality and homoscedasticity were not observed, the non-parametric Kruskal-Wallis test [29] was performed, revealing that at least one treatment differed significantly

from the others ($p < 0.05$). Subsequently, the Conover test [30] was conducted at a 5% significance level, with Bonferoni's method [31] used to adjust the *p*-values. All statistical analyses were performed using R version 4.4.0 [26]. The experiment was conducted twice.

3 | Results and Discussions

3.1 | Preparation of Three-Dimensional Structures of Benzotriazines

A large number of conformations with identical energy values were observed for both benzotriazines (Supporting Information, Tables S1 and S2 and Figures S1 and S2). This phenomenon occurs due to the possibility of rotation around the C–C single bonds, for which there must be a low energy barrier [32].

Although the energy values remained constant across the different conformations, the RMSD values varied between 1.93 and 3.36 Å for A6, and between 1.67 and 3.31 Å for A8. Consequently, all conformations were considered in the subsequent stages of the study.

3.2 | Virtual Screening: Protein Ligands Three-Dimensionally Similar to Benzotriazines

Protein ligands that are three-dimensionally similar to benzotriazines A6 and A8, were complexed with the following proteins: 2Y57 (acetylcholine receptor), 2NSD (reductase), 2VYA (hydrolase 1), 2Y56 (soluble acetylcholine receptor), 1UK0 (polymerase-1), 2BYS (acetylcholine binding protein), 3QEM (glutamate receptor subunit), 3B3P (nitric oxide synthase), 1IF8 (carbonic anhydrase II), 3IW7 (mitogen-activated protein kinase 14), 2WCP (reductase), 3EIO (soluble form of dipeptidyl peptidase 4), 2Y58 (soluble acetylcholine receptor), 3H0J (acetyl-

CoA carboxylase), 3E68 (nitric oxide synthase), 3SFF (histone deacetylase 8), 1IA4 (dihydrofolate reductase), 3EAI (nitric oxide synthase), 3EKR (heat shock protein HSP 90-alpha), 1UK1 (poly [ADP-ribose] polymerase-1), 1ZZ1 (amidohydrolase-type histone deacetylase), 1RPW (transcription regulator qacR), 3DQT (nitric oxide synthase), 3DQS (nitric oxide synthase, endothelial), 1IF7 (carbonic anhydrase II), 2DS1 (protein kinase 2), and 3ZK3 (heat shock protein HSP 90-alpha) (Supporting Information, Tables S7 and S8). The structural similarity between benzotriazines A6 and A8 and the ligands of these proteins suggests that benzotriazines may inhibit their activity.

3.3 | Amino Acid Sequence Analysis

When the amino acid sequences of the aforementioned proteins were used to search for similar sequences in the genomes of *Meloidogyne* spp., only mitogen-activated protein kinase 14 (3IW7) [15] and protein kinase 2 (2DS1) [14] had scores above 200. Of the two, 3IW7 had the highest score, and its number of amino acid residues was also closer to the number observed for the sequence identified in the nematode genome (Supporting Information, Table S9).

These results were corroborated by calculations performed using UGENE 1.32.0 [18], which determined that 3IW7 [15] exhibited similarity equal to or greater than 80% compared to the amino acid sequence extracted from the *Meloidogyne* spp. genome (Supporting Information, Table S3), whereas 2DS1 [14] showed 65% similarity (Supporting Information, Table S4).

These findings suggest that the most likely target for benzotriazines in *Meloidogyne* spp. is mitogen-activated protein kinase 14. Consequently, further research focused exclusively on this enzyme.

Mitogen-activated protein kinase 14 (MAPK14), also called p38-α [33], belongs to the group of transferases responsible for proliferation, differentiation, and regulation of protein kinase transcription, and cell death [34]. MAPK14 is located in the cytoplasm and, upon activation, translocates to the nucleus of the cell [35]. In nematodes, this protein plays a role in longevity [36], stress resistance [37], embryogenesis, proliferation, and cell death [34]. One possible approach to controlling in *M. incognita* is targeting the *Mi-mpk-1* and *Mi-flp-18* genes, which encode protein kinase nematode reproduction.

In a study using RNA interference (RNAi), a decrease in the relative abundance of *Mi-mpk-1* and *Mi-flp-18* genes was observed in *M. incognita*, leading to a reduction in the number of galls, egg mass, and number of eggs by 32%, 42%, and 22%, respectively [34].

Lim et al. [38], in an *in vitro* study of the nematicidal activity of silver nanoparticles on the free-living nematode *Caenorhabditis elegans* Maupas, observed the induction of oxidative stress, the formation of reactive oxygen species, and decreased reproduction due to MAPK activation. Therefore, substances that act on MAPK have the potential to serve as a basis for developing new products to control PPNs.

3.4 | Molecular Docking of Benzotriazines and Inhibitors of Mitogen-Activated Protein Kinase 14

Although 104 three-dimensional structures of MAPKs were obtained from the RCSB Protein Data Bank (Supporting Information, Table S5), only 23 met the criteria for molecular docking (Supporting Information, Table S10). As shown visually (Supporting Information, Figure S3)

and confirmed by RMSD values (Supporting Information, Table S11), the selected three-dimensional structures exhibited good overlap. Additionally, the active sites demonstrated strong alignment, allowing for the selection of a single grid for all the three-dimensional protein structures (Figure 3).

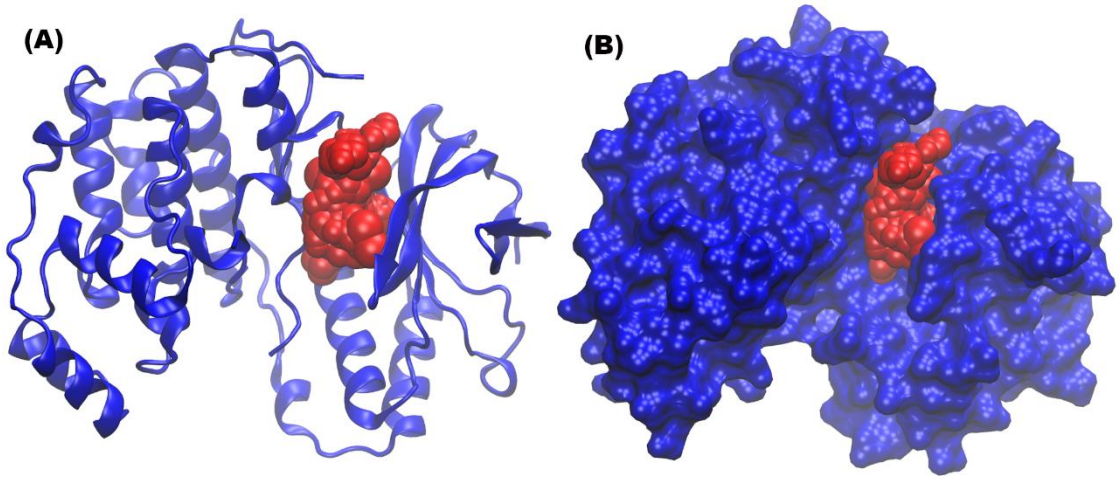

FIGURE 3 | Three-dimensional structure of mitogen-activated protein kinase 14 with ligands (Table S6) experimentally complexed to various structures shown in red: **A)** Representation of the protein in new cartoon; **B)** Representation of the protein in MSMS.

The poses of the docked ligands generated by the computer program closely matched the experimentally complexed ligand structures, suggesting that the docking method accurately reproduced the experimental data. Furthermore, the affinity values calculated for benzotriazines A6 and A8 were statistically equal to the lowest values determined for the enzyme inhibitors (Figure 4).

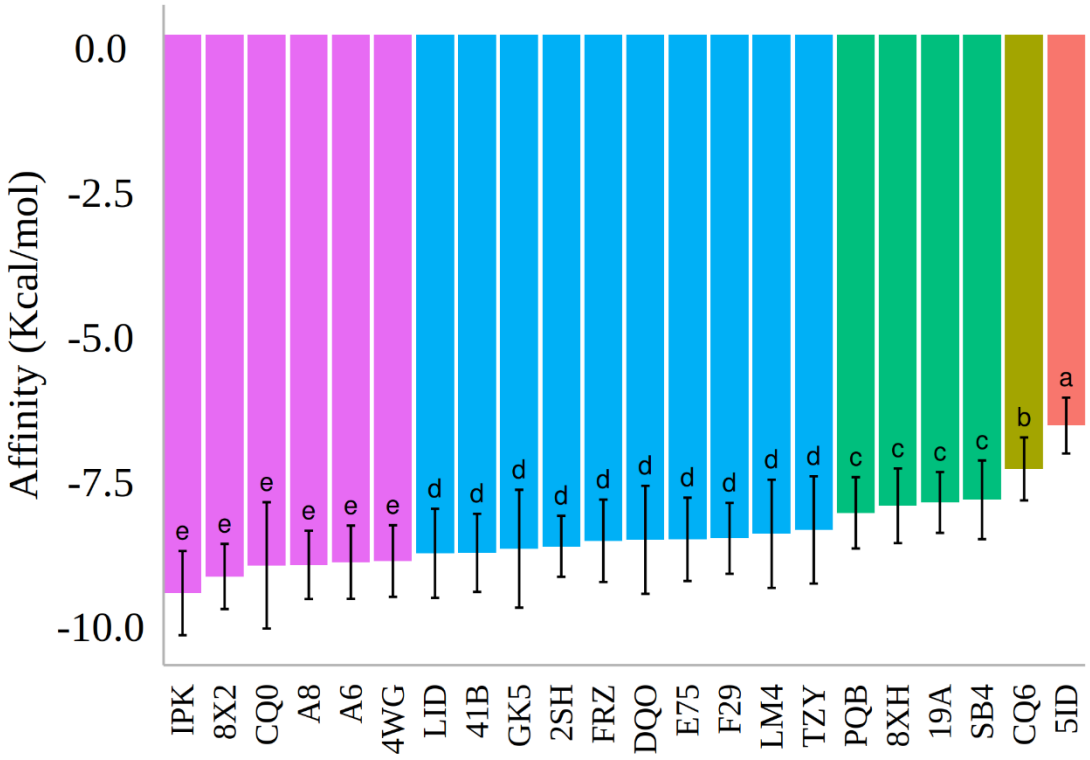

FIGURE 4 | Affinities of benzotriazines A6 and A8, and mitogen-activated protein kinase 14 (MAPK) inhibitors for MAPK: 1-(2,6-dichlorophenyl)-5-(2,4-difluorophenyl)-7-piperazin-1-yl-3,4-dihydrouizolin-2(1*H*)-one (DQO), 5-(2-phenylpyrazol[1,5-a]pyridine-3-mil)-1*H*-pyrozolo[3,4-c]pyridazine-3-amine (FZR); 1-ethyl-5-(2-phenylpyrazol[1,5-a]pyridine-3-yl)-1*H*-pyrazolo[3,4-c]pyridazine-3-amine (F29); 6-[4-(4-fluorophenyl)-1,3-oxazol-5-mil]-3-isopropyl[1,2,4]triazolo[4,3-a]pyridine (TZY); (2*R*,3*R*,4*S*,5*R*)-2-(4-amino-5-iodo-7*H*-pyrrolo[2,3-d]pyrimidin-7-yl)-5-(hydroxemethyl)tetrahydrofuran-3,4-diol (5ID); 5-amino-1-(4-fluorophenyl)-1*H*-pyrazol-4-yl](3-{[(2*R*-2,3diidoxypropyl]oxy}phenyl)methanone (PQB); *N*,*N*-dimethyl-6-(naphthalen-2-yl)-5-(pyridin-4-yl)pyridazin-3-amine (LM4); *trans*-4-{[4-(5-methyl-3-phenyl-1,2-oxazol-4-yl)pyrimidin-2-yl]amino}cyclohexanol (E75); 4-(4-fluorophenyl)-1-(4-piperidinyl)-5-(2-amino-4-pyrimidinyl)-imidazole (SB4); *N*-[(1*S*)-1-(3-chloro-4-fluorophenyl)-2-hydroxyethyl]-2-(tetrahydro-2*H*-pyran-4-ylamino)-5,8-dihydropyrido[3,4-d]pyrimidine-7(6H)-carboxamide (2SH); 5-(2-methyl ethyl)-2-[2-(oxy-4-amino)pyrimidine-4-yl]-6,7-dihydro-1-(*H*)-pyrrolo[3,2-c]pyridin-4-one (8XH); 2-[2-[[4-(4-dimethylpiperazin-1-

yl)phenyl]aminopyrimidine-4-yl]-1,5,6,7-tetrahydropyrrolo[3,2-c]pyridin-4-one (8X2); 8-(2-chlorophenylamino)-2-(2,6-difluorophenylamino)-9-ethyl-9*H*-purine-1,7-diium (LID); 2-({4-[(4-benzylpiperidin-1-yl)carbonyl]benzyl}sulfanyl)-3*H*-imidazo[4,5-c]pyridine (IPK); *N*,*N*-dimethyl-4-(4-phenyl-1*H*-pyrazyl-3-yl)-1*H*-pyrrole-carboxamide (19A); N3-cyclopropyl-N-4-(cyclopropylmethyl)-6-methylbiphenyl-3,4'-dicarboxamide (GK5); 3-(3-*tert*-butyl[1,2,4]triazolo[4,3-a]pyridin-7-yl)-*N*-cyclopropyl-4-methylbenzamide (CQ0); *N*-[(1*S*)-1-(3-chloro-4-fluorophenyl)-2-hydroxyethyl]-2-(tetrahydro-2*H*-pyran-4-ylamino)-5,8-dihydropyrido[3 ,4-d]pyrimidine-7(6*H*)-carboxamide (41B); and 2-{[2-ethoxy-4-(4-hydroxypiperidin-1-yl)phenyl]amino}-5,11-dimethyl-5,11-dihydro-6*H*-pyrimido[4,5-b][1,4]benzodiazepine-6-one (4WG). Columns with the same letters are statistically equal ($p < 0.05$) according to the Scott-Knott test at 5% significance.

Two hydrogen bonds involving the hydroxyl group (OH) and the nitrogen atom (N) of the amide group were observed in each benzotriazine-protein interaction. Specifically, benzotriazine A6 formed a hydrogen bond with the methionine residue (Met140), while benzotriazine A8 interacted with the tyrosine residue (Tyr66) (Figure 5). These findings suggest that benzotriazines A6 and A8 may function as MAPK14 inhibitors.

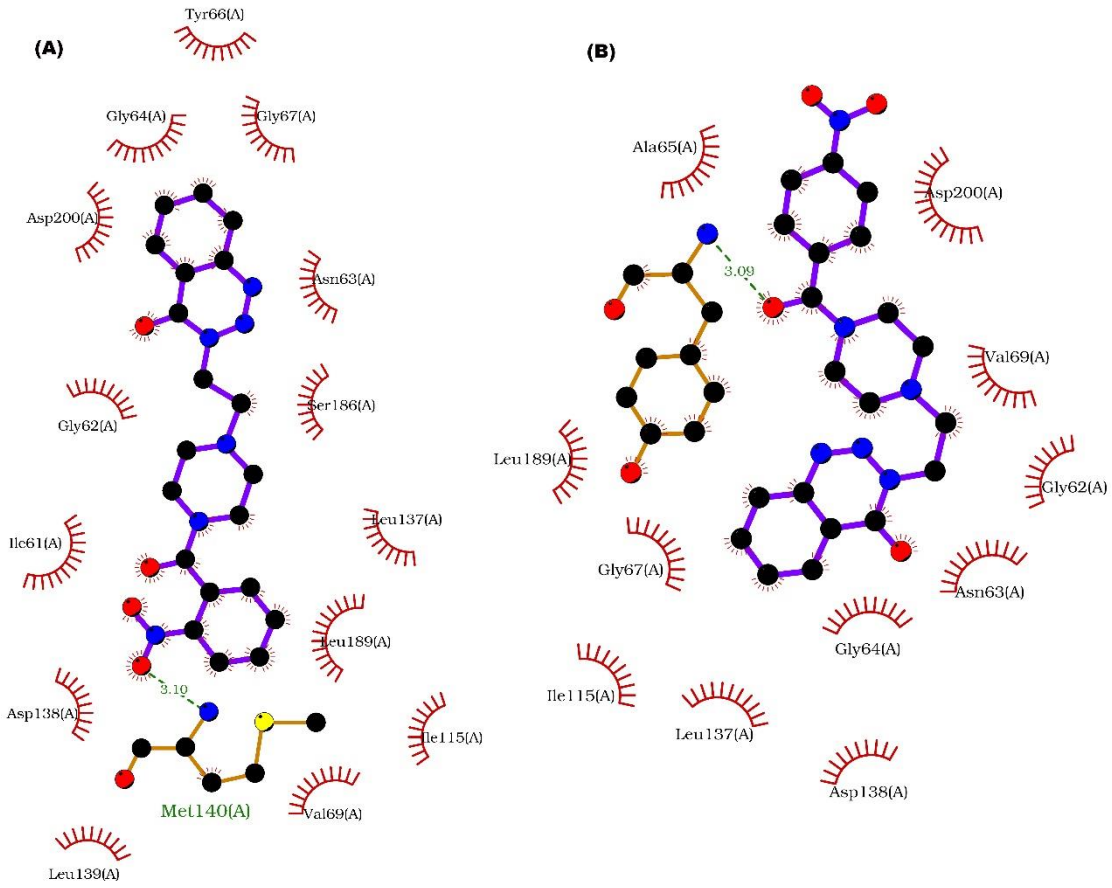

FIGURE 5 | Structure of benzotriazines A6 (A) and A8 (B) interacting with mitogen-activated protein kinase (MAPK) 14. Image generated by LigPlot+ version 2.2.8.

3.5 | Immobility of *M. incognita* J2 After Exposure to Mitogen-Activated Protein Kinase 14 Inhibitors

All the inhibitors studied affected nematode motility compared to the aqueous Tween® 80 solution, which served as the negative control (Figure 6). The best result was obtained for the TCS ERK 11e inhibitor (Figure 2).

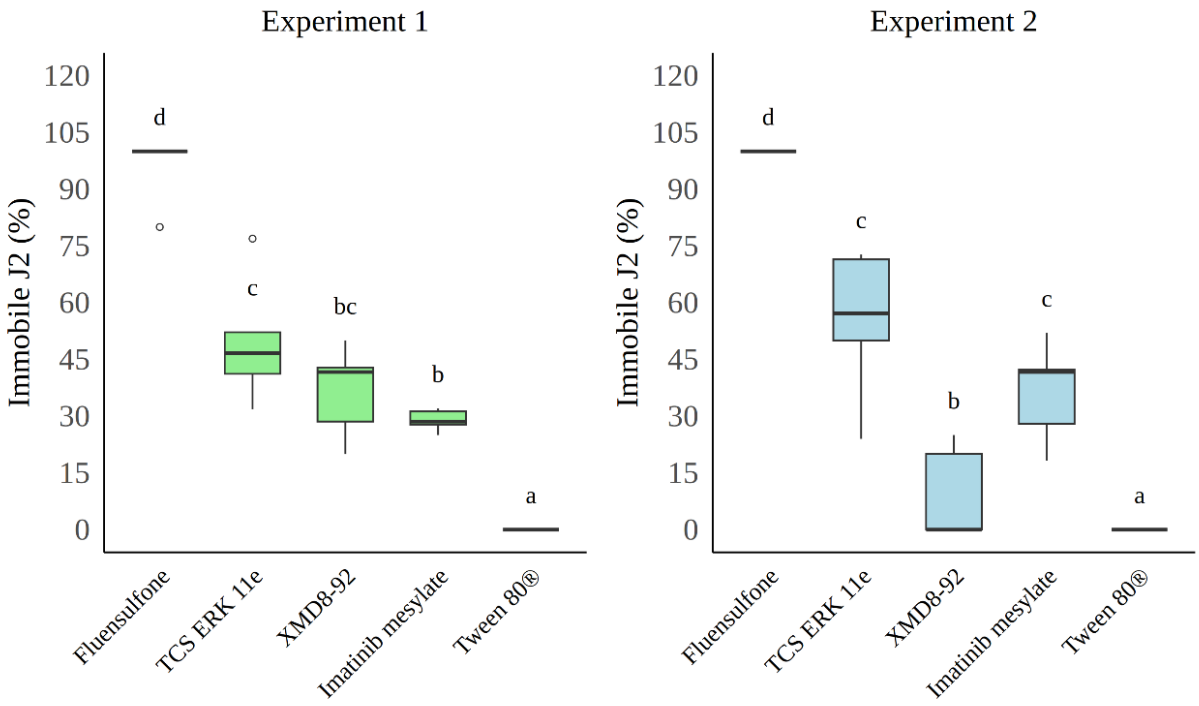

FIGURE 6 | Boxplot of the immobility of second-stage juveniles (J2) of *Meloidogyne incognita* after 72-hour exposure to different inhibitors (XMD8-92, SMIL1027, TCS ERK 11e) of mitogen-activated protein kinase 14. Fluensulfone and Tween® 80 were used as positive and negative controls, respectively. Boxes with the same letter in each experiment do not differ from each other according to the Conover test ($p < 0.05$). Values are presented without transformation.

This is a promising finding, since reduced motility prevents the nematode from reaching the root, penetrating it, and establishing a feeding site. Additionally, this result is unprecedented, as there is no prior report in the literature of tests involving TCS ERK 11e, XMD8-92, and imatinib mesylate against PPNs.

Conclusions

According to the *in silico* study, mitogen-activated protein kinase 14 (MAPK14) is the enzymatic target of benzotriazines A6 and A8 in *Meloidogyne* spp. This finding was further supported by the observation that commercial MAPK14 inhibitors reduced the motility of *M. incognita* J2 *in vitro*, with the strongest effect seen with TCS ERK 11e. Therefore, MAPK14 produced by *Meloidogyne* spp. presents a potential target for the development of new nematicides.

Acknowledgments

Financial support and fellowships were provided by Fundação de Amparo à Pesquisa do Estado de Minas Gerais (FAPEMIG), Coordenação de Aperfeiçoamento de Pessoal de Nível Superior (CAPES), and Conselho Nacional de Desenvolvimento Científico e Tecnológico (CNPq).

Conflict of Interest Statement

The authors declare that they have no known competing financial interests or personal relationships that could have appeared to influence the work reported in this paper.

Authors' Contribution Statement

D.F.O. Writing – original draft, Methodology, Funding acquisition, Formal analysis, Data curation, Conceptualization. **G.J.H.** Writing – original draft, Methodology, Formal analysis, Conceptualization. **V.P.S.** Writing – original draft, Methodology. **R.M.F.** Writing – originalraft, Methodology. **W.C.T.** Writing – original draft, Methodology. All authors have read and approved the final manuscript.

Data Availability Statement

The data supporting the findings of these studies are available from the corresponding author upon reasonable request.

Appendix A. Supporting Information

References

[1] F. Ahamed and G. Nombela, "Root-Galling Disease of Vegetable Plants," *Springer Nature Singapore*, (2023), https://doi.org/10.1007/978-981-99-3892-6.

[2] D. F. Oliveira, V. A. Costa, W. C. Terra, V. P. Campos, P. M. Paula, and S. J. Martins, "Impact of Phenolic Compounds on *Meloidogyne incognita in Vitro* and in Tomato Plants," *Experimental Parasitology* 199 (2019): 17–23, https://doi.org/10.1016/j.exppara.2019.02.009.

[3] D. P. Bebber, T. Holmes, and S. J. Gurr, "The Global Spread of Crop Pests and Pathogens," *Global Ecology and Biogeography* 23, no. 12 (2014): 1398–1407, https://doi.org/10.1111/geb.12214.

[4] J. T. Jones, A. Haegeman, E. G. J. Danchin, et al., "Top 10 Plant-Parasitic Nematodes in Molecular Plant Pathology," *Molecular Plant Pathology* 14, no. 9 (2013): 946–961, https://doi.org/10.1111/mpp.12057.

[5] J. de O. Silva, A. Loffredo, M. R. da Rocha, and J. O. Becker, "Efficacy of New Nematicides for Managing *Meloidogyne incognita* in Tomato Crop," *Journal of Phytopathology* 167, no. 5 (2019): 295–298, https://doi.org/10.1111/jph.12798.

[6] E. Feist, J. Kearn, Y. Gaihre, V. O'Connor, and L. Holden-Dye, "The Distinct Profiles of the Inhibitory Effects of Fluensulfone, Abamectin, Aldicarb and Fluopyram on Globodera Pallida Hatching," *Pesticide Biochemistry and Physiology* 165 (2020): 104541, https://doi.org/10.1016/j.pestbp.2020.02.007.

[7] X. Chen, H. Jia, Z. Li, and X. Xu, "Synthesis and Nematicidal Evaluation of 1,2,3-Benzotriazin-4-one Derivatives Containing Piperazine as Linker Against *Meloidogyne incognita*," *Chinese Chemical Letters* 30, no. 6 (2019): 1207–1213, https://doi.org/10.1016/j.cclet.2019.02.033.

[8] M. G. Teixeira, E. S. Alvarenga, D. T. Lopes, and D. F. Oliveira, "Herbicidal Activity of Isobenzofuranones and *in Silico* Identification of their Enzyme Target," *Pest Management Science* 75, no. 12 (2019): 3331–3339, https://doi.org/10.1002/ps.5456.

[9] P. Tosco, T. Balle, and F. Shiri, "Open3DALIGN: An Open-Source Software Aimed at Unsupervised Ligand Alignment," *Journal of Computer-Aided Molecular Design* 25, no. 8 (2011): 777–783, https://doi.org/10.1007/s10822-011-9462-9.

[10] Z. Feng, L. Chen, H. Maddula, et al., "Ligand Depot: A Data Warehouse for Ligands Bound to Macromolecules," *Bioinformatics* 20, no. 13 (2004): 2153–2155, https://doi.org/10.1093/bioinformatics/bth214.

[11] S. Lešnik, T. Štular, B. Brus, et al., "LiSiCA: A Software for Ligand-Based Virtual Screening and Its Application for the Discovery of Butyrylcholinesterase Inhibitors," *Journal of Chemical Information and Modeling* 55, no. 8 (2015): 1521–1528, https://doi.org/10.1021/acs.jcim.5b00136.

[12] D. L. Wheeler, T. Barrett, D. A. Benson, et al., "Database Resources of the National Center for Biotechnology Information," *Nucleic Acids Research* 35, no. SUPPL. 1 (2007): D5–D12, https://doi.org/10.1093/nar/gkl1031.

[13] S. F. Altschul, T. L. Madden, A. A. Schäffer, et al., "Gapped BLAST and PSI-BLAST: A New Generation of Protein Database Search Programs," *Nucleic Acids Research*, 25, no. 17 (1997): 3389–3402, https://doi.org/10.1093/nar/25.17.3389.

[14] N. Kawanishi, T. Sugimoto, J. Shibata, et al., "Structure-Based Drug Design of a Highly Potent CDK1,2,4,6 Inhibitor with Novel Macrocyclic Quinoxalin-2-one Structure," *Bioorganic & Medicinal Chemistry Letters* 16, no. 19 (2006): 5122–5126, https://doi.org/10.1016/j.bmcl.2006.07.026.

[15] J. R. Simard, C. Grütter, V, Pawar, et al., "High-Throughput Screening to Identify Inhibitors Which Stabilize Inactive Kinase Conformations in p38α," *Journal of the American Chemical Society* 131, no. 51 (2009): 18478–18488, https://doi.org/10.1021/ja907795q.

[16] H. Berman, K. Henrick, H. Nakamura, and J. L. Markley, "The Worldwide Protein Data Bank (wwPDB): Ensuring a Single, Uniform Archive of PDB Data," *Nucleic Acids Research* 35, no. SUPPL. 1 (2007): D301–D303, https://doi.org/10.1093/nar/gkl971.

[17] F. Sievers and D. G. Higgins, "Clustal Omega for Making Accurate Alignments of Many Protein Sequences," *Protein Science* 27, no. 1 (2018): 135–145, https://doi.org/10.1002/pro.3290.

[18] K. Okonechnikov, A. Golosova, M. Fursov, et al., "Unipro UGENE: A Unified Bioinformatics Toolkit," *Bioinfomatics* 28, no. 8 (2012): 1166–1167, https://doi.org/10.1093/bioinformatics/bts091.

[19] L. Martínez, R. Andreani, and J. M. Martínez, "Convergent Algorithms for Protein Structural Alignment," *BMC Bioinformatics* 8 (2007): 306, https://doi.org/10.1186/1471-2105-8-306.

[20] G. M. Morris, R. Huey, W. Lindstrom, et al., "AutoDock4 and AutoDockTools4: Automated Docking with Selective Receptor Flexibility," *Journal of Computational Chemistry* 30, no. 16 (2009): 2785–2791, https://doi.org/10.1002/jcc.21256.

[21] S. D. Handoko, X. Ouyang, C. T. T. Su, C. K. Kwoh, and Y. S. Ong, "QuickVina: Accelerating AutoDock Vina using Gradient-Based Heuristics for Global Optimization," *IEEE/ACM Transactions on Computational Biology and Bioinformatics* 9, no. 5 (2012): 1266–1272, https://doi.org/10.1109/TCBB.2012.82.

[22] E. F. Pettersen, T. D. Goddard, C. C. Huang, et al., "UCSF Chimera - A Visualization System for Exploratory Research and Analysis," *Journal of Computational Chemistry* 25, no. 13 (2004): 1605–1612, https://doi.org/10.1002/jcc.20084.

[23] S. S. Shapiro and M. B. Wilk, "An Analysis of Variance Test for Normality (complete samples)," *Biometrika* 52, no. 3–4 (1965): 591–611, https://doi.org/10.1093/biomet/52.3-4.591.

[24] M. S. Bartlett, “Properties of Sufficiency and Statistical Tests,” *Proceedings of the Royal Society A* 160, no. 901 (1937): 268–282, https://doi.org/10.1098/rspa.1937.0109.

[25] A. J. Scott and M. Knott, “A Cluster Analysis Method for Grouping Means in the Analysis of Variance,” *Biometrics* 30, no. 3 (1974): 507–512, https://doi.org/10.2307/2529204.

[26] R Core Team, “R: A Language and Environment for Statistical Computing,” R Foundation for Statistical, Vienna, Austria (2020), https://www.r-project.org/.

[27] J. A. G. Vanegas, H. B. Pacule, R. M. Capitão, et al., “Methyl Esters of (*E*)-Cinnamic Acid: Activity Against the Plant-Parasitic Nematode *Meloidogyne incognita* and *in Silico* Interaction with Histone Deacetylase,” *Journal of Agricultural and Food Chemistry* 70, no. 22 (2022): 6624–6633, https://doi.org/10.1021/acs.jafc.1c08142.

[28] H. B. Pacule, J. A. G. Vanegas, W. C. Terra, V. P. Campos, and D. F. Oliveira, “(R)-Carvone is a Potential Soil Fumigant Against *Meloidogyne incognita* whose likely Enzymatic Target in the Nematode is Acetylcholinesterase,” *Experimental Parasitology* 241, (2022): 108359, https://doi.org/10.1016/j.exppara.2022.108359.

[29] W. H. Kruskal and W. A. Wallis, “Use of Ranks in One-Criterion Variance Analysis,” *Journal of the American Statistical Association* 47, no. 260 (1952): 583–621, https://doi.org/10.1080/01621459.1952.10483441.

[30] W. J. Conover and R. L. Iman, “Multiple-Comparisons Procedures. Informal Report,” U.S. Department of Energy, Los Alamos National Laboratory, University of California, Los Alamos, NM, (1979), https://doi.org/10.2172/6057803.

[31] C. Bonferroni, “Teoria Statistica Delle Classi e Calcolo Delle Probabilita,” *Pubblicazioni del R Istituto Superiore di Scienze Economiche e Commericiali di Firenze (Libreria Internazionale Seeber, Florence, Italy)*, 8 (1936): pp. 3–62, 1936.

[32] K. B. Wiberg and E. Martin, "Barriers to Rotation Adjacent to Double Bonds," *Journal of the American Chemical Society* 107, no. 18 (1985): 5035–5041, https://doi.org/10.1021/ja00304a002.

[33] J. C. Lee, J. T. Laydon, P. C. McDonell, et al., "A Protein Kinase Involved in the Regulation of Inflammatory Cytokine Biosynthesis," *Nature* 372, no. 6508 (1994): 739–746, https://doi.org/10.1038/372739a0.

[34] L. Dong, J. Xu, S. Chen, X. Li, and Y. Zuo, "*Mi-flp-18* and *Mi-mpk-1* Genes are Potential Targets for *Meloidogyne incognita* Control," *Journal of Parasitology*, 102, no. 2 (2016): 208–213, https://doi.org/10.1645/15-768.

[35] M. J. Robinson and M. H. Cobb, "Mitogen-Activated Protein Kinase Pathways," *Current Opinion in Cell Biology* 9, no. 2 (1997): 180–186, https://doi.org/10.1016/S0955-0674(97)80061-0.

[36] E. Moreno-Arriola, M. El Hafidi, D. Ortega-Cuéllar, and K. Carvajal, "AMP-Activated Protein Kinase Regulates Oxidative Metabolism in *Caenorhabditis elegans* through the NHR-49 and MDT-15 Transcriptional Regulators," *PLoS One* 11, no. 1 (2016): 0148089, https://doi.org/10.1371/journal.pone.0148089.

[37] W. Li, D. Wang, and D. Wang, "Regulation of the Response of *Caenorhabditis elegans* to Simulated Microgravity by p38 Mitogen-Activated Protein Kinase Signaling," *Scientific Reports*, 8, no. 1 (2018): 857, https://doi.org/10.1038/s41598-018-19377-z.

[38] D. Lim, J.-Y. Roh, H.-J. Eom, J.-Y. Choi, J. W. Hyun, and J. Choi, "Oxidative Stress-Related PMK-1 P38 MAPK Activation as a Mechanism for Toxicity of Silver Nanoparticles to Reproduction in the Nematode *Caenorhabditis elegans*," *Environmental Toxicology and Chemistry* 31, no. 3 (2012): 585–592, https://doi.org/10.1002/etc.1

SUPPOTING INFORMATION

Predicting the Enzymatic Target of Benzotriazines in the Plant-Parasitic Nematode *Meloidogyne incognita* by Virtual Screening, Amino Acid Sequence Analysis, Molecular Docking, and Biological Evaluation

Geraldo J. Hodela, Vitor P. Sousa, Rodrigues M. Fráguas, Willian C. Terra and Denilson F. Oliveira

Geraldo J. Hodela (orcid.org/0000-0002-14832452; jamisse2008@yahoo.com.br), **Rodrigues M. Fráguas (**orcid.org/0009-0002-2241- 2834; rodrigofraguas1@hotmail.com) and **Denilson F. Oliveira** (orcid.org/0000-0001-9326-8716; denilson@ufla.br)- *Laboratório de Produtos Naturais, Departamento de Química, Universidade Federal de Lavras, Lavras-MG, Brazil, CEP 37.203-202.*

Willian C. Terra (orcid.org/0000-0002-7683-6790; willianterra@ufla.br) and **Vitor P. Sousa (**orcid.org/0009-0005-5470-1480**;** vitorpeira.s@gmail.com) - *Laboratório de Nematologia, Departamento de Fitopatologia, Universidade Federal de Lavras, CEP 37.203-202, Lavras – MG, Brazil.*

Corresponding author:

Denilson F. Oliveira - *Laboratório de Produtos Naturais, Departamento de Química, Universidade Federal de Lavras, Lavras-MG, Brazil, CEP 37.203-202; orcid.org/0000-0001-9326-8716; Phone: +55 35 3829 1623; Email: denilson@ufla.br*

FIGURES

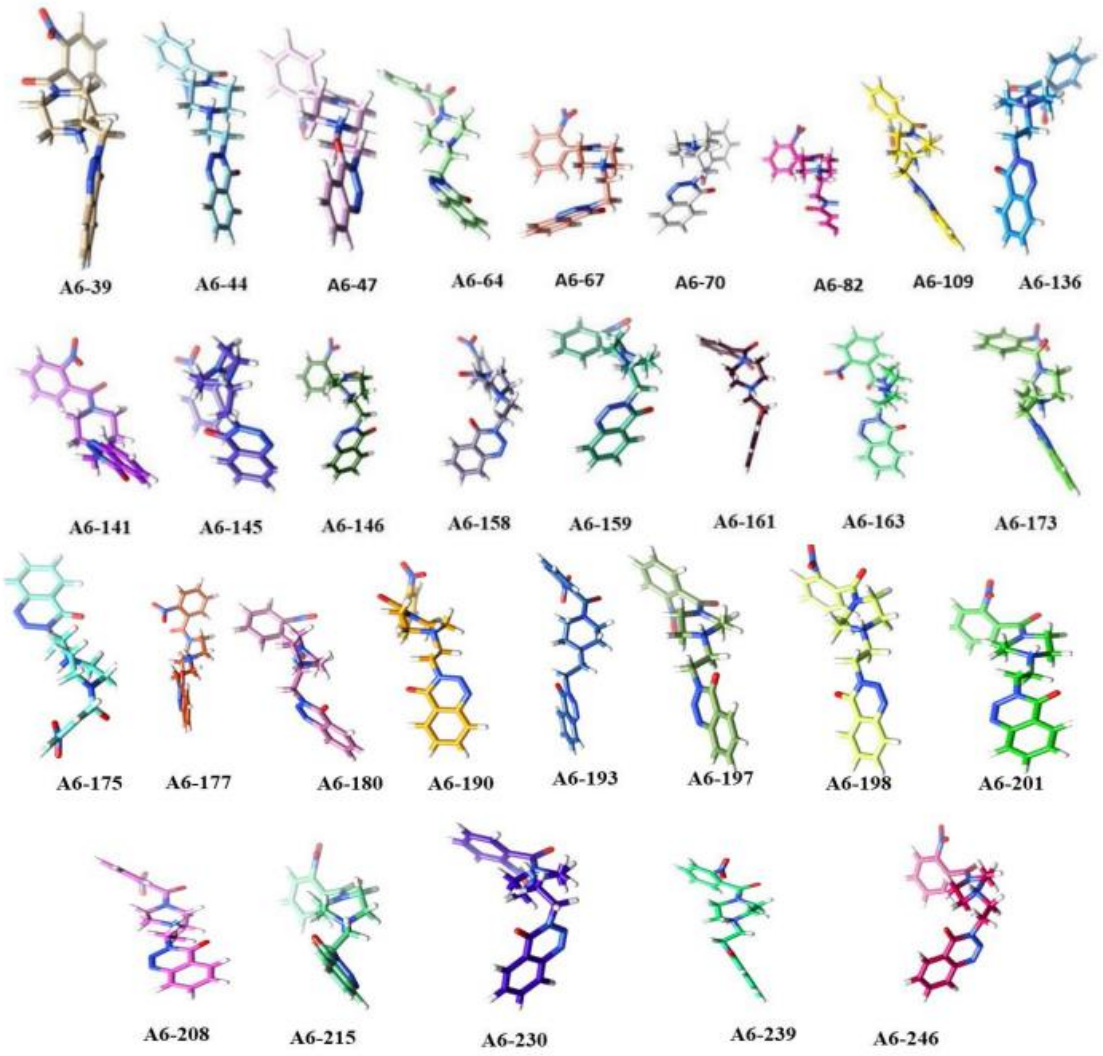

FIGURE S1 | Most stable conformations of benzotriazine A6 (A6-39, A6-44, A6-47, A6-64, A6-67, A6-70, A6-82 , A6-109, A6-136, A6-141, A6-145, A6-146, A6-158, A6-159, A6-161, A6-163, A6-173, A6-175, A6-177, A6-180, A6-190, A6-193, A6-197, A6-198, A6-201, A6-208, A6-215, A6-230, A6-239, and A6-246) according to calculations made with the Mopac2016 programme.

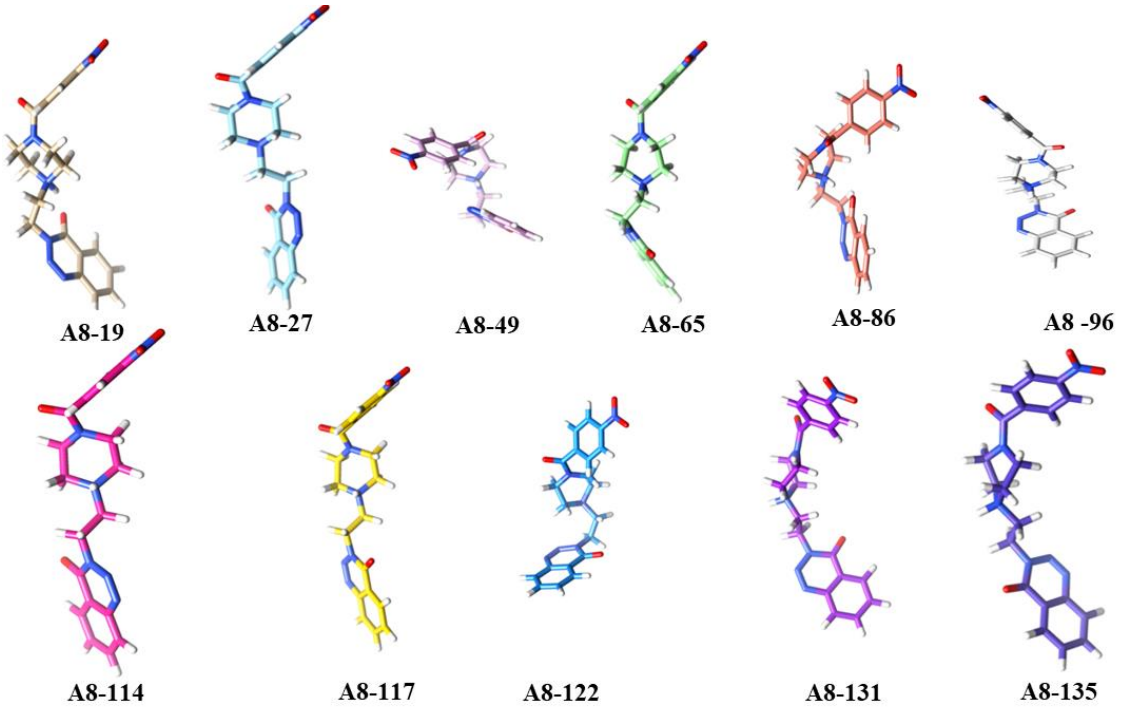

FIGURE | S2. Most stable conformations of benzotriazine A8 (A8-19, A8-27, A8-49, A8-65, A8-86, A8-96, A8-114, A8-117, A8-122, A8-131, and A8-135) according to calculations made with the Mopac2016 programme.

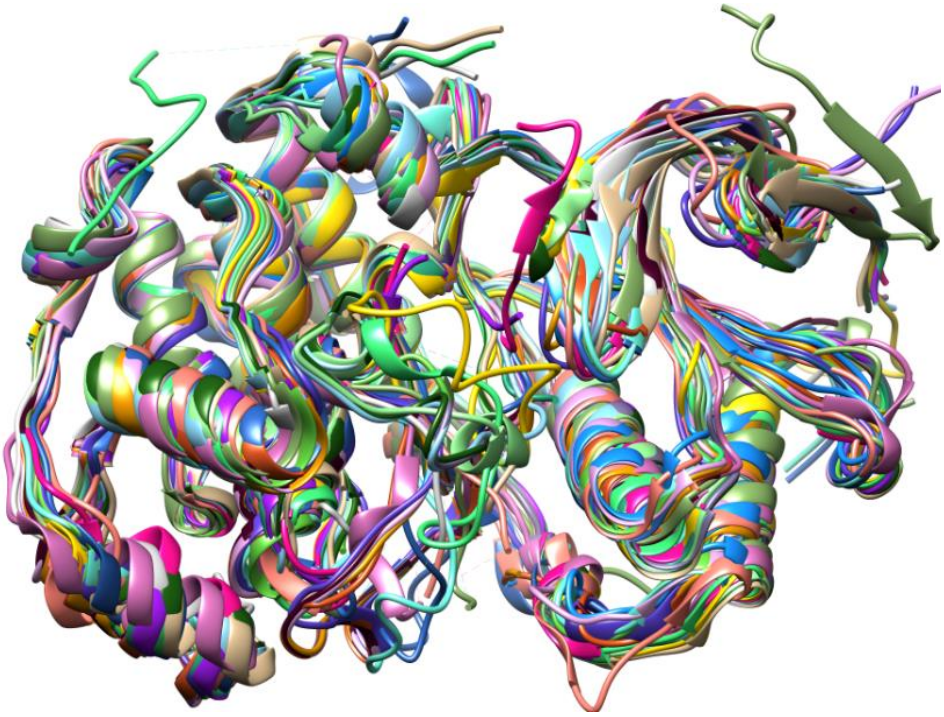

FIGURE S3 | Three-dimensional structures of mitogen-activated proteins kinases 14: 1LEW[1], 1M7Q[2], 1TVO[3] 1ZZL[4] 2B9F[5], 2FYS[6], 2GTM[7], 2YIS[8], 2ZOQ[9], 3D7Z[10], 3S3I[11] ,4F9W[12] 4FUX (https://www.rcsb.org/structure/4FUX), 4LOO[13], 4O6E[14], 4XJO[15], 4ZZM[16], 5BYY[17] , 5NGU[18], 5NHH[18], 5V62[19] e 6DTL[20]. They were three-dimensionaly aligned by the Lovoalign 18.320 program[21]. Image generated by the UCSF Chimera 1.13.1 program[22].

TABLES

TABLE S1 | Most stable conformations of benzotriazine A6, according to calculations made with the Mopac2016 programme.

Conformation	Energy (Kcal/mol)	Boltzmann distribution (%)
39	175.88	3.3
44	175.88	3.3
47	175.88	3.3
64	175.88	3.3
67	175.88	3.3
70	175.88	3.3
82	175.88	3.3
109	175.88	3.3
136	175.88	3.3
141	175.88	3.3
145	175.88	3,3
146	175.88	3.3
158	175.88	3.3
159	175.88	3.3
161	175.88	3.3
163	175.88	3.3
173	175.88	3.3
175	175.88	3.3
177	175.88	3.3
180	175.88	3.3
190	175.88	3.3
193	175.88	3.3
197	175.88	3.3
198	175.88	3.3
201	175.88	3.3
208	175.88	3.3
215	175.88	3.3
230	175.88	3.3
239	175.88	3.3
246	175.88	3.3

TABLE S2 | Most stable conformations of benzotriazine A8, according to calculations made with the Mopac2016 programme.

Conformation	Energy (Kcal/mol)	Boltzmann distribution (%)
19	175.88	9.09
27	175.88	9.09
49	175.88	9.09
65	175.88	9.09
86	175.88	9.09
96	175.88	9.09
114	175.88	9.09
117	175.88	9.09
122	175.88	9.09
131	175.88	9.09
135	175.88	9.09

TABLE S3 | Similarity (%) of amino acid sequences to the mitogen-activated kinase 14 (3IW7), calculated by Ugene 1.32.0[23], which considered the gaps. The calculation was made after alignment with Clustal Omega 1.2.4, through four iterations[24].

Protein code	Amino acid residues	Producing organism	3IW7[a] (*Homo sapiens)*	ABI96897.1[b] (*Meloidogyne incognita*)	KAF7633967.1[j] (*Meloidogyne graminicola*)	KAF7638919.1[j] (*Meloidogyne graminicola*)	KAF7635334.1[j] (*Meloidogyne graminicola*)	KAF7633235.1[j] (*Meloidogyne graminicola*)	CAD56894.1[b] (*Meloidogyne artiellia*)	AMA07359.1[b] (*Meloidogyne enterolobii*)
3IW7[a]	360	*Homo sapiens*	100	80	22	80	67	42	80	80
3D7Z[a]	360	*Homo sapiens*	100	80	23	80	67	42	80	80
1DI9[a]	360	*Homo sapiens*	100	80	23	80	67	42	80	80
2YIS[a]	359	*Homo sapiens*	100	80	23	80	68	42	80	80
3GCU[a]	360	*Homo sapiens*	100	80	23	80	67	42	80	80
3D7Z[a]	360	*Homo sapiens*	100	80	23	80	67	42	80	80
3HEC[a]	348	*Homo sapiens*	99	80	24	80	68	43	80	80
5ETC[a]	363	*Homo sapiens*	99	80	22	80	67	42	80	80
2BAJ[a]	365	*Homo sapiens*	99	80	22	80	67	42	81	80
3NNU[a]	351	*Homo sapiens*	99	80	23	80	68	42	80	80
3OEF[a]	360	*Homo sapiens*	99	80	23	80	67	42	81	80
2FSL[a]	367	*Homo sapiens*	99	80	22	80	67	42	80	80
4LOO[a]	361	*Mus musculus*	99	80	22	80	67	42	80	80
1LEW[a]	360	*Mus musculus*	99	80	23	80	67	42	80	80
2FSO[a]	367	*Homo sapiens*	99	80	22	80	67	42	80	80
3K3J[a]	362	*Homo sapiens*	99	80	22	80	67	42	80	80
2LGC[a]	359	*Homo sapiens*	99	80	23	80	68	42	80	80
3OD6[a]	360	*Homo sapiens*	99	80	23	80	67	42	80	80
3MPT[a]	371	*Homo sapiens*	99	80	22	80	67	41	80	80
3ODZ[a]	360	*Homo sapiens*	99	80	23	80	67	42	80	80
3ZS5[a]	362	*Homo sapiens*	99	80	22	80	67	42	80	80
1M7Q[a]	366	*Homo sapiens*	99	80	22	80	67	42	80	80
3ODY[a]	360	*Homo sapiens*	99	80	23	80	67	42	80	80
2NP[a]	367	*Homo sapiens*	99	80	22	80	67	42	81	80
1OZ1[a]	372	*Homo sapiens*	99	80	22	80	67	41	80	80
2GFS[a]	372	*Homo sapiens*	99	80	22	80	67	41	80	80
3HVC[a]	362	*Homo sapiens*	99	80	22	80	67	42	80	80
1IAN[h]	366	*Homo sapiens*	99	80	22	80	67	42	80	80
3OEF[a]	360	*Homo sapiens*	99	80	23	80	67	42	81	80
4E5A[a]	360	*Homo sapiens*	99	80	23	80	67	42	80	80
3ZS5[a]	362	*Homo sapiens*	99	80	22	80	67	42	80	80
2FST[a]	367	*Homo sapiens*	99	80	22	80	67	42	80	80
3OEF[a]	360	*Homo sapiens*	99	80	23	80	67	42	81	80
4E5A[a]	360	*Homo sapiens*	99	80	23	80	67	42	80	80
5O8V[a]	360	*Homo sapiens*	99	80	23	80	67	42	80	80
3NNX[a]	354	*Homo sapiens*	99	80	23	80	68	42	80	80

Protein code	Amino acid residues	Producing organism	3IW7[a] (*Homo sapiens*)	ABI96897.1[b] (*Meloidogyne incognita*)	KAF7633967.1[j] (*Meloidogyne graminicola*)	KAF7638919.1[j] (*Meloidogyne graminicola*)	KAF7635334.1[j] (*Meloidogyne graminicola*)	KAF7633235.1[j] (*Meloidogyne graminicola*)	CAD56894.1[b] (*Meloidogyne artiellia*)	AMA07359.1[b] (*Meloidogyne enterolobii*)
4E5A[a]	360	*Homo sapiens*	99	80	23	80	67	42	80	80
3K3I[a]	350	*Homo sapiens*	99	80	24	80	68	42	80	80
3S3I[a]	349	*Homo sapiens*	99	80	24	80	68	42	81	80
3OEF[a]	360	*Homo sapiens*	99	80	23	80	67	42	81	80
2LGC[a]	359	*Homo sapiens*	99	80	23	80	68	42	80	80
3ZS5[a]	362	*Homo sapiens*	99	80	22	80	67	42	80	80
2OZA[a]	366	*Mus musculus*	99	80	22	80	67	42	80	80
4LOO[a]	361	*Mus musculus*	99	80	22	80	67	42	80	80
2OZA[a]	366	*Mus musculus*	99	80	22	80	67	42	80	80
5NZZ[a]	360	*Mus musculus*	99	80	22	80	67	42	80	80
1ZZL[a]	366	*Rattus norvegicus*	99	81	23	80	68	42	81	81
6QYX[a]	366	*Homo sapiens*	98	81	22	81	67	42	81	81
3KQ7[i]	380	*Homo sapiens*	98	80	22	80	67	40	80	80
6QYX[a]	366	*Homo sapiens*	98	81	22	81	67	42	81	81
1BMK[h]	379	*Homo sapiens*	98	80	22	80	67	40	80	80
4F9W[a]	383	*Homo sapiens*	98	80	22	80	67	40	80	80
2GTM[a]	348	*Mus musculus*	98	80	24	80	68	42	80	80
4TYH[a]	348	*Mus musculus*	98	81	23	80	68	43	81	81
3FI4[a]	372	*Homo sapiens*	98	80	22	80	66	41	80	80
4F9W[a]	383	*Homo sapiens*	98	80	22	80	67	40	80	80
3DT1[a]	383	*Homo sapiens*	98	80	22	80	66	40	80	80
6QYX[a]	366	*Homo sapiens*	98	81	22	81	67	42	81	81
4TYH[a]	366	*Homo sapiens*	98	81	22	81	67	42	81	81
2GTM[a]	348	*Mus muscus*	98	80	24	80	68	42	80	80
3TG1[a]	380	*Mus musculus*	98	80	22	80	67	40	80	80
3P4K[a]	370	*Mus musculus*	98	80	22	80	67	41	80	80
6SOI[a]	380	*Mus musculus*	98	80	22	80	67	40	80	80
3TG1[a]	380	*Mus musculus*	98	80	22	80	67	40	80	80
4TYH[a]	348	*Mus musculus*	98	81	23	80	68	43	81	81
3TG1[a]	380	*Mus musculus*	98	80	22	80	67	40	80	80
6SO1[a]	381	*Mus musculus*	98	80	22	80	67	40	80	80
4TYH[a]	348	*Mus musculus*	98	81	23	80	68	43	81	81
3TG1[a]	380	*Mus musculus*	98	80	22	80	67	40	80	80
3TG1[a]	380	*Mus musculus*	98	80	22	80	67	40	80	80
4ZZM[a]	350	*Homo sapiens*	83	90	23	90	68	42	90	90
4ZZM[b]	350	*Homo sapiens*	83	90	23	90	68	42	90	90
5WP1[b]	357	*Homo sapiens*	83	90	23	90	68	42	90	90
4XOZ[b]	351	*Rattus norvegicus*	83	90	23	90	68	42	90	90

Protein code	Amino acid residues	Producing organism	3IW7[a] (*Homo sapiens*)	ABI96897.1[b] (*Meloidogyne incognita*)	KAF7633967.1[j] (*Meloidogyne graminicola*)	KAF7638919.1[j] (*Meloidogyne graminicola*)	KAF7635334.1[j] (*Meloidogyne graminicola*)	KAF7633235.1[j] (*Meloidogyne graminicola*)	CAD56894.1[b] (*Meloidogyne artiellia*)	AMA07359.1[b] (*Meloidogyne enterolobii*)
4XNE[b]	346	*Rattus norvegicus*	83	90	23	90	68	42	90	90
7W5C[a]	355	*Arabidopsis thaliana*	83	81	24	81	69	42	81	81
3ZS5[a]	355	*Arabidopsis thaliana*	83	81	24	81	69	42	81	81
4IZ7[b]	356	*Homo sapiens*	83	91	23	90	68	42	90	91
5WP1[b]	357	*Homo sapiens*	83	90	23	90	68	42	90	90
5K4I[b]	352	*Homo sapiens*	83	90	23	90	68	42	90	90
4IZ7[b]	356	*Homo sapiens*	83	91	23	90	68	42	90	91
6DMG[b]	347	*Homo sapiens*	83	90	23	90	68	42	90	90
4IZ7[b]	356	*Homo sapiens*	83	91	23	90	68	42	90	91
4ZZM[b]	350	*Homo sapiens*	83	90	23	90	68	42	90	90
5K4I[b]	352	*Homo sapiens*	83	90	23	90	68	42	90	90
6DMG[b]	347	*Homo sapiens*	83	90	23	90	68	42	90	90
5K4I[b]	352	*Homo sapiens*	83	90	23	90	68	42	90	90
4IZ7[b]	356	*Homo sapiens*	83	91	23	90	68	42	90	91
5WP1[b]	357	*Homo sapiens*	83	90	23	90	68	42	90	90
5K4I[b]	352	*Homo sapiens*	83	90	23	90	68	42	90	90
4IZ7[b]	356	*Homo sapiens*	83	91	23	90	68	42	90	91
6DMG[b]	347	*Homo sapiens*	83	90	23	90	68	42	90	90
5K4I[b]	352	*Homo sapiens*	83	90	23	90	68	42	90	90
4ZZM[b]	350	*Homo sapiens*	83	90	23	90	68	42	90	90
3C9W[b]	357	*Rattus norvegicus*	83	90	23	90	68	42	90	90
4XP2[b]	351	*Rattus norvegicus*	83	90	23	90	68	42	90	90
4XOY[b]	351	*Rattus norvegicus*	83	90	23	90	68	42	90	90
3C9W[b]	357	*Rattus norvegicus*	83	90	23	90	68	42	90	90
3C9W[b]	357	*Rattus norvegicus*	83	90	23	90	68	42	90	90
4XP2[b]	351	*Rattus norvegicus*	83	90	23	90	68	42	90	90
4XOY[b]	351	*Rattus norvegicus*	83	90	23	90	68	42	90	90
3C9W[b]	357	*Rattus norvegicus*	83	90	23	90	68	42	90	90

Protein code	Amino acid residues	Producing organism	3IW7[a] (*Homo sapiens*)	ABI96897.1[b] (*Meloidogyne incognita*)	KAF7633967.1[j] (*Meloidogyne graminicola*)	KAF7638919.1[j] (*Meloidogyne graminicola*)	KAF7635334.1[j] (*Meloidogyne graminicola*)	KAF7633235.1[j] (*Meloidogyne graminicola*)	CAD56894.1[b] (*Meloidogyne artiellia*)	AMA07359.1[b] (*Meloidogyne enterolobii*)
4XOZ[b]	351	*Rattus norvegicus*	83	90	23	90	68	42	90	90
4XNE[b]	346	*Rattus norvegicus*	83	90	23	90	68	42	90	90
3OEF[a]	351	*Rattus norvegicus*	83	90	23	90	68	42	90	90
3C9W[b]	357	*Rattus norvegicus*	83	90	23	90	68	42	90	90
4XOZ[b]	351	*Rattus norvegicus*	83	90	23	90	68	42	90	90
2OZA[a]	372	*Rattus norvegicus*	82	89	22	89	67	40	90	89
6DTL[d]	364	*Arabidopsis thaliana*	82	81	24	81	69	41	81	81
7E75[b]	363	*Homo sapiens*	82	90	22	90	67	41	91	90
4QTA[b]	361	*Homo sapiens*	82	91	23	90	67	41	91	90
7E73[b]	363	*Homo sapiens*	82	90	22	90	67	41	91	90
5LCK[b]	360	*Homo sapiens*	82	90	23	90	67	41	90	90
5BYY[e]	346	*Homo sapiens*	82	81	24	81	69	42	81	81
6G9K[b]	368	*Homo sapiens*	82	90	22	90	67	41	91	90
4QTA[b]	361	*Homo sapiens*	82	91	23	90	67	41	91	90
7E75[b]	363	*Homo sapiens*	82	90	22	90	67	41	91	90
3SA0[b]	360	*Homo sapiens*	82	90	22	90	67	41	90	90
5V62[b]	351	*Homo sapiens*	82	90	23	90	68	42	90	90
7OPM[b]	364	*Homo sapiens*	82	90	22	90	67	41	90	90
5V62[b]	351	*Homo sapiens*	82	90	23	90	68	42	90	90
4IZA[b]	356	*Homo sapiens*	82	90	23	90	68	42	90	90
5LCK[b]	360	*Homo sapiens*	82	90	23	90	67	41	90	90
3SA0[b]	360	*Homo sapiens*	82	90	22	90	67	41	90	90
4ZSGe	347	*Homo sapiens*	82	81	24	81	69	42	81	81
5BYYe	346	*Homo sapiens*	82	81	24	81	69	42	81	81
2Y9Q[b]	362	*Homo sapiens*	82	91	23	90	67	41	91	90
1WZY[b]	368	*Homo sapiens*	82	90	22	90	67	41	91	90
6OPG[b]	354	*Homo sapiens*	82	90	23	90	68	42	90	90
4IZA[b]	356	*Homo sapiens*	82	90	23	90	68	42	90	90
5LCK[b]	360	*Homo sapiens*	82	90	23	90	67	41	90	90
2LGC[a]	346	*Homo sapiens*	82	81	24	81	69	42	81	81
4ZSJ[e]	344	*Homo sapiens*	82	81	24	81	69	42	81	81
4GSB[b]	364	*Rattus norvegicu*	82	90	22	90	67	41	90	90

Protein code	Amino acid residues	Producing organism	3IW7[a] (*Homo sapiens*)	ABI96897.1[b] (*Meloidogyne incognita*)	KAF7633967.1[j] (*Meloidogyne graminicola*)	KAF7638919.1[j] (*Meloidogyne graminicola*)	KAF7635334.1[j] (*Meloidogyne graminicola*)	KAF7633235.1[j] (*Meloidogyne graminicola*)	CAD56894.1[b] (*Meloidogyne artiellia*)	AMA07359.1[b] (*Meloidogyne enterolobii*)
6NBS[b]	367	*Rattus norvegicus*	82	91	23	90	67	41	91	91
2FYS[b]	364	*Rattus norvegicus*	82	90	23	90	67	41	90	90
3O71[b]	358	*Rattus norvegicus*	82	90	23	90	68	42	90	90
5HD7[b]	365	*Rattus norvegicus*	82	90	22	90	67	41	90	90
3QYW[b]	364	*Rattus norvegicus*	82	90	22	90	67	41	90	90
3R63[b]	358	*Rattus norvegicus*	82	90	23	90	68	42	90	90
6OT6[b]	358	*Rattus norvegicus*	82	90	23	90	68	42	90	90
3ZU7[b]	365	*Rattus norvegicus*	82	90	23	90	67	41	90	90
3O71[b]	358	*Rattus norvegicus*	82	90	23	90	68	42	90	90
6NBS[b]	367	*Rattus norvegicus*	82	91	23	90	67	41	91	91
4S30[b]	358	*Rattus norvegicus*	82	90	23	90	68	42	90	90
5HD7[b]	365	*Rattus norvegicus*	82	90	22	90	67	41	90	90
2Z7L[b]	366	*Rattus norvegicus*	82	90	23	90	67	41	90	90
6OT6[b]	358	*Rattus norvegicus*	82	90	23	90	68	42	90	90
4I5H[b]	359	*Rattus norvegicus*	82	90	23	90	67	42	90	90
4QYY[b]	365	*Rattus norvegicus*	82	90	23	90	67	41	90	90
6FXV[b]	364	*Rattus norvegicus*	82	90	22	90	67	41	90	90
3ZU7[b]	365	*Rattus norvegicus*	82	90	23	90	67	41	90	90
3R63[b]	358	*Rattus norvegicus*	82	90	23	90	68	42	90	90
2Z7L[b]	366	*Rattus norvegicus*	82	90	23	90	67	41	90	90

Protein code	Amino acid residues	Producing organism	3IW7[a] (*Homo sapiens*)	ABI96897.1[b] (*Meloidogyne incognita*)	KAF7633967.1[j] (*Meloidogyne graminicola*)	KAF7638919.1[j] (*Meloidogyne graminicola*)	KAF7635334.1[j] (*Meloidogyne graminicola*)	KAF7633235.1[j] (*Meloidogyne graminicola*)	CAD56894.1[b] (*Meloidogyne artiellia*)	AMA07359.1[b] (*Meloidogyne enterolobii*)
3ZU7[b]	365	*Rattus norvegicus*	82	90	23	90	67	41	90	90
3QYW[b]	364	*Rattus norvegicus*	82	90	22	90	67	41	90	90
4I5H[b]	359	*Rattus norvegicus*	82	90	23	90	67	42	90	90
6DTL[e]	364	*Arabidopsis thaliana*	82	81	24	81	69	41	81	81
1WZY[b]	368	*Homo sapiens*	82	90	22	90	67	41	91	90
1TVO[b]	368	*Homo sapiens*	82	91	22	90	67	41	91	91
2Z7L[b]	366	*Homo sapiens*	82	90	23	90	67	41	90	90
4IZ5[b]	356	*Homo sapiens*	82	90	23	90	68	42	90	90
4XJ0[b]	349	*Homo sapiens*	82	90	23	90	68	42	90	90
6D5Y[b]	348	*Homo sapiens*	82	90	23	90	68	42	90	90
4FUX[b]	360	*Homo sapiens*	82	91	23	90	67	41	91	90
8AOC[b]	368	*Homo sapiens*	82	90	22	90	67	41	91	90
5LCK[b]	360	*Homo sapiens*	82	90	23	90	67	41	90	90
4H3Q[b]	368	*Homo sapiens*	82	90	22	90	67	41	90	90
4ZSG[e]	347	*Homo sapiens*	82	81	24	81	69	42	81	81
5BYZ[e]	348	*Homo sapiens*	82	81	24	81	69	42	81	81
5BYY[e]	346	*Homo sapiens*	82	81	24	81	69	42	81	81
6HKM[e]	347	*Homo sapiens*	82	81	24	81	69	42	81	81
4ZSJ[e]	344	*Homo sapiens*	82	81	24	81	69	42	81	81
5BYZ[e]	348	*Homo sapiens*	82	81	24	81	69	42	81	81
4ZSJ[e]	344	*Homo sapiens*	82	81	24	81	69	42	81	81
2Y9Q[b]	362	*Homo sapiens*	82	91	23	90	67	41	91	90
4QTA[b]	361	*Homo sapiens*	82	91	23	90	67	41	91	90
1TVO[b]	368	*Homo sapiens*	82	91	22	90	67	41	91	91
2Z7L[b]	368	*Homo sapiens*	82	90	23	90	67	41	90	90
5V62[b]	351	*Homo sapiens*	82	90	23	90	68	42	90	90
3TEI[b]	362	*Homo sapiens*	82	90	23	90	67	41	90	90
6OPG[b]	354	*Homo sapiens*	82	90	23	90	68	42	90	90
5BUE[b]	361	*Homo sapiens*	82	91	23	90	67	41	91	90
4FV6[b]	360	*Homo sapiens*	82	91	23	90	67	41	91	91
2Y9Q[b]	362	*Homo sapiens*	82	91	23	90	67	41	91	90
1WZY[b]	368	*Homo sapiens*	82	90	22	90	67	41	91	90
1TVO[b]	368	*Homo sapiens*	82	91	22	90	67	41	91	91
6D5Y[b]	348	*Homo sapiens*	82	90	23	90	68	42	90	90
4FUX[b]	360	*Homo sapiens*	82	91	23	90	67	41	91	90
3TEI[b]	362	*Homo sapiens*	82	90	23	90	67	41	90	90

Protein code	Amino acid residues	Producing organism	3IW7[a] (*Homo sapiens*)	ABI96897.1[b] (*Meloidogyne incognita*)	KAF7633967.1[j] (*Meloidogyne graminicola*)	KAF7638919.1[j] (*Meloidogyne graminicola*)	KAF7635334.1[j] (*Meloidogyne graminicola*)	KAF7633235.1[j] (*Meloidogyne graminicola*)	CAD56894.1[b] (*Meloidogyne artiellia*)	AMA07359.1[b] (*Meloidogyne enterolobii*)
7OPM[b]	364	*Homo sapiens*	82	90	22	90	67	41	90	90
6OPG[b]	354	*Homo sapiens*	82	90	23	90	68	42	90	90
4IZA[b]	356	*Homo sapiens*	82	90	23	90	68	42	90	90
5V62[b]	351	*Homo sapiens*	82	90	23	90	68	42	90	90
6G9K[b]	368	*Homo sapiens*	82	90	22	90	67	41	91	90
3SA0[b]	360	*Homo sapiens*	82	90	22	90	67	41	90	90
6G9J[b]	368	*Homo sapiens*	82	90	22	90	67	41	90	90
4N0S[b]	360	*Homo sapiens*	82	90	22	90	67	41	90	90
6GDM[b]	368	*Homo sapiens*	82	90	22	90	66	41	90	90
4ZSG[e]	347	*Homo sapiens*	82	81	24	81	69	42	81	81
6HKM[e]	347	*Homo sapiens*	82	81	24	81	69	42	81	81
6D5Y[b]	348	*Homo sapiens*	82	90	23	90	68	42	90	90
4N0S[b]	360	*Homo sapiens*	82	90	22	90	67	41	90	90
5BYZ[e]	348	*Homo sapiens*	82	81	24	81	69	42	81	81
6G9K[b]	368	*Homo sapiens*	82	90	22	90	67	41	91	90
4ZSG[b]	347	*Homo sapiens*	82	81	24	81	69	42	81	81
5BYY[e]	346	*Homo sapiens*	82	81	24	81	69	42	81	81
4FV6[b]	360	*Homo sapiens*	82	91	23	90	67	41	91	91
4IZ5[b]	356	*Homo sapiens*	82	90	23	90	68	42	90	90
6GDM[b]	368	*Homo sapiens*	82	90	22	90	66	41	90	90
4N0S[b]	360	*Homo sapiens*	82	90	22	90	67	41	90	90
4ZSJ[e]	344	*Homo sapiens*	82	81	24	81	69	42	81	81
4H3Q[b]	362	*Homo sapiens*	82	90	22	90	67	41	90	90
4E5A[a]	368	*Homo sapiens*	82	90	22	90	66	41	90	90
3TG1[a]	347	*Homo sapiens*	82	81	24	81	69	42	81	81
2Y9Q[b]	362	*Homo sapiens*	82	91	23	90	67	41	91	90
4FV6[b]	360	*Homo sapiens*	82	91	23	90	67	41	91	91
7E73[b]	363	*Homo sapiens*	82	90	22	90	67	41	91	90
5LCJ[b]	368	*Homo sapiens*	82	90	22	90	67	41	91	90
3TEI[b]	362	*Homo sapiens*	82	90	23	90	67	41	90	90
6OPG[b]	354	*Homo sapiens*	82	90	23	90	68	42	90	90
4IZA[b]	356	*Homo sapiens*	82	90	23	90	68	42	90	90
6G9J[b]	382	*Homo sapiens*	82	90	22	90	67	41	90	90
4N0S[b]	368	*Homo sapiens*	82	90	22	90	67	41	90	90
6HKM[e]	347	*Homo sapiens*	82	81	24	81	69	42	81	81
4XJ0[b]	349	*Homo sapiens*	82	90	23	90	68	42	90	90
5LCJ[b]	368	*Homo sapiens*	82	90	22	90	67	41	91	90
7E75[b]	363	*Homo sapiens*	82	90	22	90	67	41	91	90
4H3Q[b]	362	*Homo sapiens*	82	90	22	90	67	41	90	90
5BYZ[e]	348	*Homo sapiens*	82	81	24	81	69	42	81	81

Protein code	Amino acid residues	Producing organism	3IW7[a] (*Homo sapiens*)	ABI96897.1[b] (*Meloidogyne incognita*)	KAF7633967.1[j] (*Meloidogyne graminicola*)	KAF7638919.1[j] (*Meloidogyne graminicola*)	KAF7635334.1[j] (*Meloidogyne graminicola*)	KAF7633235.1[j] (*Meloidogyne graminicola*)	CAD56894.1[b] (*Meloidogyne artiellia*)	AMA07359.1[b] (*Meloidogyne enterolobii*)
4QYY[b]	365	*Rattus norvegicus*	82	90	23	90	67	41	90	90
6OTS[b]	358	*Rattus norvegicus*	82	90	23	90	68	42	90	90
1GOL[b]	364	*Rattus norvegicus*	82	90	22	90	67	41	90	90
3R63[b]	358	*Rattus norvegicus*	82	90	23	90	68	42	90	90
4S30[b]	358	*Rattus norvegicus*	82	90	23	90	68	42	90	90
4S2Z[b]	358	*Rattus norvegicus*	82	90	23	90	68	42	90	90
2GPH[b]	364	*Rattus norvegicus*	82	90	23	90	67	41	90	90
2ERK[b]	365	*Rattus norvegicus*	82	90	22	90	67	41	90	90
ZUV[b]	364	*Rattus norvegicus*	82	90	22	90	67	41	90	90
6OPK[b]	352	*Rattus norvegicus*	82	90	23	90	68	42	90	90
4I5H[b]	359	*Rattus norvegicus*	82	90	23	90	67	42	90	90
6FXV[b]	364	*Rattus norvegicus*	82	90	22	90	67	41	90	90
6FI6[b]	364	*Rattus norvegicus*	82	90	22	90	67	41	90	90
4GSB[b]	364	*Rattus norvegicus*	82	90	22	90	67	41	90	90
4XRL[b]	345	*Rattus norvegicus*	82	90	23	90	68	42	90	90
6GDM[b]	351	*Rattus norvegicus*	82	90	22	90	66	41	90	90
6RFO[ab]	372	*Rattus norvegicus*	82	89	22	89	67	40	90	89
6OTS[b]	358	*Rattus norvegicus*	82	90	23	90	68	42	90	90
3O71[b]	358	*Rattus norvegicus*	82	90	23	90	68	42	90	90
2GPH[b]	364	*Rattus norvegicus*	82	90	23	90	67	41	90	90

Protein code	Amino acid residues	Producing organism	3IW7[a] (*Homo sapiens*)	ABI96897.1[b] (*Meloidogyne incognita*)	KAF7633967.1[j] (*Meloidogyne graminicola*)	KAF7638919.1[j] (*Meloidogyne graminicola*)	KAF7635334.1[j] (*Meloidogyne graminicola*)	KAF7633235.1[j] (*Meloidogyne graminicola*)	CAD56894.1[b] (*Meloidogyne artiellia*)	AMA07359.1[b] (*Meloidogyne enterolobii*)
2FYS[b]	364	*Rattus norvegicus*	82	90	23	90	67	41	90	90
4QYY[b]	365	*Rattus norvegicus*	82	90	23	90	67	41	90	90
4S30[b]	358	*Rattus norvegicus*	82	90	23	90	68	42	90	90
1GOL[f]	364	*Rattus norvegicus*	82	90	22	90	67	41	90	90
6OPK[b]	352	*Rattus norvegicus*	82	90	23	90	68	42	90	90
3ZUV[b]	364	*Rattus norvegicus*	82	90	22	90	67	41	90	90
2Z7L[b]	366	*Rattus norvegicus*	82	90	23	90	67	41	90	90
6QYX[a]	358	*Rattus norvegicus*	82	90	23	90	68	42	90	90
4S2Z[b]	358	*Rattus norvegicus*	82	90	23	90	68	42	90	90
3QYW[b]	364	*Rattus norvegicus*	82	90	22	90	67	41	90	90
2ERK[f]	365	*Rattus norvegicus*	82	90	22	90	67	41	90	90
4I5H[b]	359	*Rattus norvegicus*	82	90	23	90	67	42	90	90
6FXV[b]	364	*Rattus norvegicus*	82	90	22	90	67	41	90	90
4GSB[b]	364	*Rattus norvegicus*	82	90	22	90	67	41	90	90
6RFO[ab]	372	*Rattus norvegicus*	82	89	22	89	67	40	90	89
6OT6[b]	358	*Rattus norvegicus*	82	90	23	90	68	42	90	90
6NBS[b]	367	*Rattus norvegicus*	82	91	23	90	67	41	91	91
6FI6[b]	364	*Rattus norvegicus*	82	90	22	90	67	41	90	90
4XRL[b]	345	*Rattus norvegicus*	82	90	23	90	68	42	90	90
4O6E[b]	368	*Homo sapiens*	81	90	23	90	67	41	90	90
4QTB[g]	380	*Homo sapiens*	81	90	22	90	67	40	90	90

Protein code	Amino acid residues	Producing organism	3IW7[a] (*Homo sapiens*)	ABI96897.1[b] (*Meloidogyne incognita*)	KAF7633967.1[j] (*Meloidogyne graminicola*)	KAF7638919.1[j] (*Meloidogyne graminicola*)	KAF7635334.1[j] (*Meloidogyne graminicola*)	KAF7633235.1[j] (*Meloidogyne graminicola*)	CAD56894.1[b] (*Meloidogyne artiellia*)	AMA07359.1[b] (*Meloidogyne enterolobii*)
5NHH[b]	381	*Homo sapiens*	81	90	22	91	66	40	91	90
5CI6[d]	370	*Arabidopsis thaliana*	81	80	24	80	69	40	80	80
4QP4[b]	369	*Homo sapiens*	81	90	22	90	67	41	91	90
2OJG[b]	380	*Homo sapiens*	81	90	22	90	67	40	91	90
5NHH[b]	381	*Homo sapiens*	81	90	22	91	66	40	91	90
4QP1[b]	369	*Homo sapiens*	81	90	22	90	67	41	91	90
2ZOQ[g]	380	*Homo sapiens*	81	90	22	89	67	39	90	90
5O7I[e]	358	*Homo sapiens*	81	81	23	81	68	42	81	81
4ZSL[e]	341	*Homo sapiens*	81	81	24	81	69	42	81	81
6HKN[e]	340	*Homo sapiens*	81	81	24	81	69	42	81	81
4ZSL[e]	341	*Homo sapiens*	81	81	24	81	69	42	81	81
5O7I[e]	358	*Homo sapiens*	81	81	23	81	68	42	81	81
2OJG[e]	380	*Homo sapiens*	81	90	22	90	67	40	91	90
7W5O[b]	368	*Homo sapiens*	81	90	22	90	67	41	90	90
5NGU[b]	381	*Homo sapiens*	81	90	22	90	66	40	91	90
1PME[f]	380	*Homo sapiens*	81	90	22	90	67	40	90	90
2ZOQ[d]	382	*Homo sapiens*	81	90	22	89	67	39	90	90
7W5O[b]	368	*Homo sapiens*	81	90	22	90	67	41	90	90
5NGU[b]	381	*Homo sapiens*	81	90	22	90	66	40	91	90
6HKN[e]	340	*Homo sapiens*	81	81	24	81	69	42	81	81
4O6E[b]	368	*Homo sapiens*	81	90	23	90	67	41	90	90
4QP4[b]	369	*Homo sapiens*	81	90	22	90	67	41	91	90
4QP1[b]	369	*Homo sapiens*	81	90	22	90	67	41	91	90
4QTB[g]	380	*Homo sapiens*	81	90	22	90	67	40	90	90
6HKN[e]	340	*Homo sapiens*	81	81	24	81	69	42	81	81
4ZSL[e]	341	*Homo sapiens*	81	81	24	81	69	42	81	81
6RFP[b]	378	*Rattus norvegicus*	81	90	22	90	67	40	90	90
2B9F[c]	364	*Arabidopsis thaliana*	80	80	23	80	68	42	80	80
2B9H[c]	360	*Homo sapiens*	80	80	23	79	68	42	79	80
CAD56894.1[b]	394	*Meloidogyne artiellia*	80	96	21	96	66	40	100	96
AMA07359.1[b]	394	*Meloidogyne enterolobii*	80	99	21	98	66	40	96	100
KAF7638919.1[b]	395	*Meloidogyne graminicola*	80	97	21	100	66	40	96	98
ABI96897.1[b]	394	*Meloidogyne incognita]*	80	100	21	97	66	40	96	99

Protein code	Amino acid residues	Producing organism	3IW7[a] (*Homo sapiens*)	ABI96897.1[b] (*Meloidogyne incognita*)	KAF7633967.1[j] (*Meloidogyne graminicola*)	KAF7638919.1[j] (*Meloidogyne graminicola*)	KAF7635334.1[j] (*Meloidogyne graminicola*)	KAF7633235.1[j] (*Meloidogyne graminicola*)	CAD56894.1[b] (*Meloidogyne artiellia*)	AMA07359.1[b] (*Meloidogyne enterolobii*)
2F9G[c]	353	*Saccharomyces cerevisiae*	80	80	23	80	68	42	80	80
2B9F[c]	353	*Saccharomyces cerevisiae*	80	80	23	80	68	42	80	80
2B9H[c]	353	*Saccharomyces cerevisiae*	80	80	23	79	68	42	79	80
3D7Z[a]	398	*Homo sapiens (human)*	79	79	23	79	68	38	79	79
4B99e	398	*Homo sapiens*	79	79	23	79	68	38	79	79
4IC7e	442	*Homo sapiens*	75	76	21	76	65	38	76	76
7M0K[b]	289	*Homo sapiens*	73	71	25	71	69	53	71	71
6CQD[b]	297	*Homo sapiens (human)*	73	71	25	71	69	53	71	71
7L24[b]	288	*Homo sapiens (human)*	73	71	25	70	69	53	71	71
7L26[b]	287	*Homo sapiens*	73	71	25	70	69	53	71	71
6NFY[b]	300	*Homo sapiens*	73	71	24	70	68	53	71	71
6CQE[b]	295	*Homo sapiens (human)*	73	71	25	71	69	53	71	71
6CQF[b]	297	*Homo sapiens (human)*	73	71	25	71	69	53	71	71
7M0L[b]	290	*Homo sapiens (human)*	73	71	25	71	69	53	71	71
7L25[b]	289	*Homo sapiens (human)*	73	71	25	70	69	53	71	71
7M0M[b]	293	*Homo sapiens (human)*	73	71	25	71	69	53	71	71

[a]Mitogen activated protein kinase 14
[b]Mitogen activated protein kinase 1
[c]Mitogen activated protein kinase FUS3
[d]Mitogen activated protein kinase 6
[e]Mitogen activated protein kinase 7
[f]Extracellular regulated kinase 2
[g]Mitogen activated protein kinase 3

[h]Mitogen activated protein kinases p38
[i]Mitogen activated protein kinase p38 alpha
[j]Mitogen activated protein kinases

TABLE S4 | Similarity (%) of amino acid sequences to the protein kinase 2 2DS1, calculated by Ugene 1.32.0[23], which considered the gaps. The calculation was made after alignment with Clustal Omega 1.2.4, through 4 iterations[24].

Protein code	Amino acid residue	Producing organism	2DS1 (*Homo sapiens)*	KAF7636171.1[t] (*Meloidogyne graminicola*)	KAF7634908.1[t] (*Meloidogyne graminicola*)
2DS1[a]	298	*Homo sapiens*	100	65	45
1AQ1[b]	298	*Homo sapiens*	100	65	45
1GII[a]	298	*Homo sapiens*	100	65	45
1OIT[a]	299	*Homo sapiens*	99	65	45
5K4J[b]	299	*Homo sapiens*	99	65	45
7E34[b]	298	*Homo sapiens*	99	65	45
1B38[a]	299	*Homo sapiens*	99	65	45
1PF8[a]	298	*Homo sapiens*	99	65	45
6OQI[a]	299	*Homo sapiens*	99	65	45
6INL[b]	299	*Homo sapiens*	99	65	45
7NVQ[b]	300	*Homo sapiens*	99	65	45
5UQ1[b]	301	*Homo sapiens*	99	65	45
3EZR[a]	300	*Homo sapiens*	99	65	45
3PJ8[a]	299	*Homo sapiens*	99	65	45
5OO0[b]	303	*Homo sapiens*	99	65	44
1GZ8[a]	299	*Homo sapiens*	99	65	45
4EON[b]	300	*Homo sapiens*	99	65	45
4EOI[b]	258	*Homo sapiens*	99	65	45
4I3Z[b]	296	*Homo sapiens*	99	65	45
1GY3[a]	299	*Homo sapiens*	99	65	45
1W98[a]	298	*Homo sapiens*	99	65	45
1E9H[a]	261	*Homo sapiens*	99	65	45
1FQ1[b]	212	*Homo sapiens*	99	65	45
1H01[b]	298	*Homo sapiens*	99	65	45
1OIR[a]	299	*Homo sapiens*	99	65	45
3BHT[a]	300	*Homo sapiens*	99	65	45
4CFU[b]	303	*Homo sapiens*	99	65	44
4EOS[b]	300	*Homo sapiens*	99	65	45

Protein code	Amino acid residue	Producing organism	2DS1 (*Homo sapiens)*	KAF7636171.1[t] (*Meloidogyne graminicola*)	KAF7634908.1[t] (*Meloidogyne graminicola*)
4EOP[b]	300	*Homo sapiens*	99	65	45
4BCM[b]	262	*Homo sapiens*	99	65	45
4EOQ[b]	301	*Homo sapiens*	99	65	44
7VDU[b]	300	*Homo sapiens*	99	65	45
2IW6[a]	260	*Homo sapiens*	99	65	44
4EOO[b]	299	*Homo sapiens*	99	65	45
3QHR[a]	261	*Mus musculus*	99	65	45
2IW8[a]	302	*Homo sapiens*	99	65	44
1H1P[a]	258	*Homo sapiens*	99	65	44
6GUE[b]	302	*Homo sapiens*	99	65	44
2CJM[a]	298	*Homo sapiens*	99	65	45
6Q4G[b]	306	*Homo sapiens*	98	65	44
1VYW[a]	309	*Homo sapiens*	98	65	44
3PXF[a]	306	*Homo sapiens*	98	65	44
4ERW[a]	306	*Homo sapiens*	98	65	44
4EOK[b]	300	*Homo sapiens*	98	65	45
4EOJ[b]	302	*Homo sapiens*	98	65	44
4EOM[b]	301	*Homo sapiens*	98	65	44
5OO1[b]	303	*Homo sapiens*	98	65	44
2JGZ[a]	289	*Homo sapiens*	98	65	45
5MHQ[b]	306	*Homo sapiens*	98	65	44
6Q4I[b]	306	*Homo sapiens*	98	65	44
4YC6[b]	297	*Homo sapiens*	81	64	44
4Y72[b]	302	*Homo sapiens*	81	64	44
1V0B[c]	288	*Plasmodium falciparum*	80	64	44
1V0O[c]	288	*Plasmodium falciparum*	80	64	44
1OB3[c]	288	*Plasmodium falciparu*m	80	64	44
1H4L[d]	292	*Homo sapiens*	79	64	43
7VDP[d]	292	*Homo sapiens*	*78*	64	43

Protein code	Amino acid residue	Producing organism	2DS1 (*Homo sapiens)*	KAF7636171.1[t] (*Meloidogyne graminicola*)	KAF7634908.1[t] (*Meloidogyne graminicola*)
4AU8[d]	296	*Homo sapiens*	78	64	43
1UNG[d]	292	*Homo sapiens*	78	64	43
7NJ0[b]	2,233	*Homo sapiens*	78	63	44
2QKR[e]	313	*Cryptosporidium parvum*	77	64	64
2PK9[f]	293	*Saccharomyces cerevisiae*	75	62	42
3MTL[g]	324	*Homo sapiens*	72	62	43
7UKZ[h]	319	*Homo sapiens*	69	60	43
6B3E[i]	320	*Homo sapiens*	68	61	40
4AGU[j]	321	*Saccharomyces cerevisiae*	68	61	40
4UN0[k]	259	*Homo sapiens*	67	60	40
6GZH[l]	326	*Homo sapiens*	65	60	40
5L1Z[l]	330	*Homo sapiens*	65	60	40
3BLH[l]	331	*Homo sapiens*	65	60	40
4BCF[l]	331	*Homo sapiens*	65	60	40
6Z45[l]	330	*Homo sapiens*	65	60	41
4OR5[l]	326	*Homo sapiens*	65	61	41
6W9E[l]	330	*Homo sapiens*	65	60	40
6XD3[m]	93	*Homo sapiens*	64	75	43
1UA2[n]	346	*Homo sapiens*	64	76	43
5EFQ[o]	347	*Homo sapiens*	64	60	41
4IMY[l]	332	*Homo sapiens*	64	60	40
4NST[i]	268	*Homo sapiens*	63	60	41
3MI9[l]	351	*Homo sapiens*	61	59	41
7JV7[p]	355	*Saccharomyces cerevisiae*	60	59	42
4EC8[l]	373	*Homo sapiens*	58	59	41
5FGK[q]	364	*Homo sapiens*	56	52	66

Protein code	Amino acid residue	Producing organism	2DS1 (*Homo sapiens)*	KAF7636171.1[t] (*Meloidogyne graminicola*)	KAF7634908.1[t] (*Meloidogyne graminicola*)
5HNB[q]	370	*Homo sapiens*	55	51	66
5IDN[q]	370	*Homo sapiens*	55	51	66
6TPA[q]	405	*Homo sapiens*	50	50	66
3RGF[q]	405	*Homo sapiens*	50	50	66
6QTG[q]	405	*Homo sapiens*	50	50	66
6T41[q]	407	*Homo sapiens*	50	50	66
4CRL[q]	406	*Homo sapiens*	50	50	66
6Z3U[r]	425	*Thermochaetoides thermophila*	48	49	31
7KPV[s]	555	*Saccharomyces cerevisiae*	28	25	28

[a] Cel division protein kinase 2
[b]Cyclin-dependent protein kinase 2
[c]Cell division control protein 2 homolog
[d] Cell division protein kinase 5
[e] Cdc2-like cdk2/cdc28 like protein kinase
[f]Cyclin-dependent protein kinase pho85
[g] Cell division protein kinase 16
[h] Cyclin-dependent kinase 11b
[i]Cyclin-dependent kinase 12
[j]Cyclin-dependent kinase-like 1
[k]Cyclin-k
[l]Cyclin-dependent kinase 9
[m]Cdk-activating kinase assembly factor mat1
[n]Cell division protein kinase 7
[o]Cyclin-dependent kinase 13
[p]Ctd kinase subunit alpha
[q]Cyclin-dependent kinase 8
[r]Cyclin domain-containing protein

[s]Meiotic mrna stability protein kinase ssn3
[t]Protein kinase domain-containing protein

TABLE S5 | Codes of the biological units of mitogen-activated protein kinase 14, which were obtained from the RCSB Protein Data Bank.

Protein code	Number of amino acid residues	Producing organism	Refer-ence
1BMK	379	*Homo sapiens*	[25]
1DI9	360	*Homo sapiens*	[26]
1IAN	366	*Homo sapiens*	[27]
1LEW	360	*Mus musculus*	[1]
1M7Q	366	*Homo sapiens*	[2]
1OZ1	372	*Homo sapiens*	[28]
1PME	380	*Homo sapiens*	[29]
1TVO	368	*Homo sapiens*	[3]
1WZY	368	*Homo sapiens*	[30]
1ZZL	351	*Homo sapiens*	[4]
2B9F	353	*Saccharomyces cerevisiae*	[5]
2B9H	353	*Saccharomyces cerevisiae*	[5]
1WZY	368	*Homo sapiens*	[30]
2BAJ	365	*Homo sapiens*	[31]
2ERK	365	*Rattus norvegicus*	[32]
2F9G	353	*Saccharomyces cerevisiae*	[33]
2FSL	367	*Homo sapiens*	[34]
2FST	367	*Homo sapiens*	[35]
2FSO	367	*Homo sapiens*	[35]
2FYS	364	*Rattus norvegicus*	[6]
2GFS	372	*Homo sapiens*	[36]
2GPH	364	*Rattus norvegicus*	[37]
2GTM	348	*Mus musculus*	[7]
2LGC	359	*Homo sapiens*	[38]
2NPQ	367	*Homo sapiens*	[35]
2OJG	380	*Homo sapiens*	[39]
2YIS	359	*Homo sapiens*	[8]
2Z7L	366	*Rattus norvegicus*	[40]
2ZOQ	382	*Homo sapiens*	[9]
3C9W	357	*Rattus norvegicus*	[41]
3D7Z	357	*Rattus norvegicus*	[10]
3DT1	383	*Homo sapiens*	[42]
3HEC	348	*Homo sapiens*	[43]
3HVC	362	*Homo sapiens*	[44]
3IW7	360	*Homo sapiens*	[45]
3K3I	350	*Homo sapiens*	[46]
3K3J	362	*Homo sapiens*	[46]
3NNU	354	*Homo sapiens*	[47]
3NNX	354	*Homo sapiens*	[47]
3O71	358	*Rattus norvegicus*	[48]
3OD6	360	*Homo sapiens*	[49]
3ODZ	360	*Homo sapiens*	[49]
3OEF	360	*Homo sapiens*	[49]
3P4K	370	*Mus musculus*	[50]
3QYW	364	*Rattus norvegicus*	[51]

Protein code	Number of amino acid residues	Producing organism	Refer-ence
3R63	364	*Rattus norvegicus*	[52]
3S3I	349	*Homo sapiens*	[11]
3SA0	360	*Homo sapiens*	[53]
3TEI	362	*Homo sapiens*	[54]
3ZS5	362	*Homo sapiens*	[55]
4E5A	360	*Homo sapiens*	[56]
4F9W	383	*Homo sapiens*	[12]
4H3Q	362	*Homo sapiens*	[57]
4I5H	359	*Rattus norvegicus*	[58]
4LOO	361	*Mus musculus*	[13]
4N0S	360	*Homo sapiens*	[59]
4O6E	368	*Homo sapiens*	[14]
4QP1	369	*Homo sapiens*	[60]
4QP4	369	*Homo sapiens*	[60]
4QTB	380	*Homo sapiens*	[61]
4QYY	365	*Rattus norvegicus*	[62]
4XJ0	349	*Homo sapiens*	[63]
4XOY	351	*Rattus norvegicus*	[64]
4XOZ	351	*Rattus norvegicus*	[64]
4XP2	351	*Rattus norvegicus*	[64]
4XRL	345	*Rattus norvegicus*	[64]
4ZSG	347	*Homo sapiens*	[17]
4ZSJ	344	*Homo sapiens*	[17]
4ZSL	341	*Homo sapiens*	[17]
5BYZ	348	*Homo sapiens*	[17]
4ZZM	350	*Homo sapiens*	[16]
5CI6	370	*Arabidopsis thaliana*	[65]
5HD7	365	*Rattus norvegicus*	[66]
5K4I	352	*Homo sapiens*	[67]
5LCJ	368	*Homo sapiens*	[68]
5LCK	360	*Homo sapiens*	[68]
5NGU	381	*Homo sapiens*	[18]
5O7I	358	*Homo sapiens*	[69]
5O8V	360	*Homo sapiens*	[70]
5V62	351	*Homo sapiens*	[19]
6D5Y	348	*Homo sapiens*	[71]
6DMG	347	*Homo sapiens*	[72]
6DTL	364	*Arabidopsis thaliana*	[20]
6G9J	368	*Homo sapiens*	[73]
6G9K	368	*Homo sapiens*	[73]
6GDM	368	*Homo sapiens*	[74]
6HKM	347	*Homo sapiens*	[75]
6HKN	340	*Homo sapiens*	[75]
6NBS	367	*Rattus norvegicus*	[76]
6OPG	354	*Homo sapiens*	[77]
6OPK	352	*Rattus norvegicus*	[77]
6OT6	358	*Rattus norvegicus*	[78]
6OTS	358	*Rattus norvegicus*	[78]

Protein code	Number of amino acid residues	Producing organism	Reference
6QYX	366	*Homo sapiens, Crassostrea ariakensis*	[79]
6RFO	372	*Rattus norvegicus, Homo sapiens*	[79]
6RFP	378	*Rattus norvegicus*	[79]
6SO1	381	*Mus musculus*	[80]
6SOI	381	*Mus musculus*	[81]
7E73	363	*Homo sapiens*	[81]
7E75	363	*Homo sapiens*	[82]
7OPM	363	*Homo sapiens*	[83]
7W5C	355	*Arabidopsis thaliana*	[84]
7W5O	368	*Homo sapiens*	[85]
8AOC	368	*Homo sapiens*	

s

TABLE S6 | Codes and names of three-dimensional structures of inhibitors of mitogen-activated protein kinases 14 that are experimentally complexed to such enzymes.

Protein code	Inhibitor code	Inhibitor name	References
1M7Q	DQO	1-(2,6-dichlorophenyl)-5-(2,4-difluorophenyl)-7-piperazin-1-yl-3,4-dihydroquinazolin-2(1*H*)-one	[2]
1TVO	FRZ	5-(2-phenylpyrazol[1,5-a]pyridine-3-mil)-1*H*-pyrazolo[3,4-c]pyridazine-3-amine	[3]
1WZY	F29	1-allyl-5-(2-phenylpyrazol[1,5-a]pyridine-3-yl)-1*H*-pyrazolo[3,4-c]pyridazine-3-amine	[30]
1ZZL	TZY	6-[4-(4-fluorophenyl)-1,3-oxazol-5-mil]-3-isopropyl[1,2,4]triazolo[4,3-a]pyridine	[4]
2ZOQ	5ID	(2*R*,3*R*,4*S*,5*R*)-2-(4-amino-5-iodo-7*H*-pyrrolo[2,3-d]pyrimidin-7-yl)-5-(hydroxymethyl)tetrahydrofuran-3,4-diol	[9]
2GFS	PBQ	5-amino-1-(4-fluoro-phenyl)-1*H*-pyrazol-4-yl](3-{[(2r)-2,3-dihydroxy-propyl]-oxy}-phenyl)-methanone	[36]
2GTM	LID	8-(2-chlorophenyl amino)-2-(2,6-difluorophenyl amino)-9-ethyl-9*H*-purine-1,7-diium	[7]
2OJG	19A	*N,N*-dimethyl-4-(4-phenyl-1*H*-pyrazol-3-yl)-1*H*-pyrrole-2-carboxamide	[39]
3D7Z	GK5	*N*-3-cyclopropyl-*N*-4-(cyclopropyl methyl)-6-methylbiphenyl-3,4'-dicarboxamide	[10]
3IW7	IPK	2-({4-[(4-benzyl piperidin-1-yl)carbonyl]benzyl}sulfonyl)-3*H*-imidazo[4,5-c]pyridine	[45]
3S3I	CQ0	3-(3-tert-butyl[1,2,4]triazolo[4,3-a]pyridin-7-yl)-*N*-cyclopropyl-4-methylbenzamide	[11]
4F9W	LM4	*N,N*-dimethyl-6-(naphthalen-2-yl)-5-(pyridin-4-yl)pyridazin-3-amine	[12]
4FUX	E75	*Trans*-4-{[4-(5-methyl-3-phenyl-1,2-oxazol-4-yl)pyrimidin-2-yl]amino}cyclohexanol	https://www.rcsb.org/structure/4FUX
4LOO	SB4	4-(4-fluorophenyl)-1-(4-piperidinyl)-5-(2-amino-4-pyrimidinyl)-imidazole	[13]
4O6E	2SH	*N*-[(1*S*)-1-(3-chloro-4-fluorophenyl)-2-hydroxyethyl]-2-(tetrahydro-2*H*-pyran-4-ylamino)-5,8-dihydropyrido[3,4- d] pyrimidine-7(6*H*)-carboxamide	[14]
4XJ0	41B	N-[(1*S*)-1-(3-chloro-4-fluorophenyl)-2-hydroxyethyl]-2-(tetrahydro-2*H*-pyran-4-ylamino)-5,8-dihydropyrido[3,4- d] pyrimidine-7(6*H*)-carboxamid	[63]
4ZZM	CQ6	*N*-[(1*S*)-1-(3-chloro-4-fluorophenyl)-2-hydroxyethyl]-2-(tetrahydro-2*H*-pyran-4-ylamino)-5,8-dihydropyrido[3,4- d] pyrimidine-7(6*H*)-carboxamid	[16]

Protein code	Inhibitor code	Inhibitor name	References
5BYY	4WG	2-{[2-ethyl-4-(4-hydroxy piperidin-1-yl)phenyl]amino}-5,11-dimethyl-5,11-dihydro-6*H*-pyrimido[4,5-b][1,4]benzodiazepine-6-one	[17]
5NHH	8XH	5-(2-methyl ethyl)-2-[2-(hexan-4-amino)pyrimidine-4-yl]-6,7-dihydro-1-{*H*}-pyrrolo[3,2-c] pyridin-4-one	[18]
5V62	FRZ	5-(2-phenylpyrazol[1,5-a]pyridine-3-mil)-1*H*-pyrazolo[3,4-c]pyridazine-3-amine	[19]
5NGU	8X2	2-[2-[[4-(4-dimethyl piperazin-1-yl)phenyl]amino]pyrimidine-4-yl]-1,5,6,7-tetrahydropyrrolo[3,2-c]pyridin- 4-one	[18]

TABLE S7 | Results of the search in the Ligand Expo[88] for protein ligands three-dimensionally similar to the conformations of benzotriazine A6.

Tanimoto Score	Protein code	Ligand code	Protein type	Organism of origin of the protein	Reference
0.49	2Y57	V37	Acetylcholine receptor	*Aplysia californica*	[86]
0.48	2NSD	4PI	Enoyl-[acyl-carrier-protein] reductase	*Mycobacterium tuberculosis* H37Rv	[87]
0.48	2VYA	PF7	Hydrolase 1	*Rattus norvegicus*	[88]
0.47	2Y56	V11	Acetylcholine receptor	*Aplysia californica*	[86]
0.45	1UK0	FRM	Poly [ADP-ribose] polymerase-1	*Homo sapiens*	[89]
0.45	2BYS	LOB	Acetylcholine binding protein	*Aplysia californica*	[90]
0.45	3QEM	QEM	NMDA glutamate receptor subunit	*Xenopus laevis*	[91]
0.44	3B3P	JI7	Nitric oxide synthase	*rattus norvegicus*	[92]
0.43	1IF8	SBS	Carbonic anhydrase II	*Homo sapiens*	[93]
0.43	3IW7	IPK	Mitogen-activated protein kinase 14	*Homo sapiens*	[45]
0.43	2WPC	WP7	Tripanotiona redutase	*Trypanosoma brucei brucei*	[94]
0.43	3EIO	AJH	Soluble form of dipeptidyl peptidase 4	*Homo sapiens*	[95]
0.43	2Y58	V38	Soluble acetylcholine receptor	*Aplysia californica*	[86]
0.42	3H0J	B36	Soluble acetylcholine receptor	*Saccharomyces cerevisiae*	[96]
0.42	3E68	AT6	Nitric oxide synthase, inducible	*Mus musculus*	[97]
0.41	1UK0	FRM	Poly[ADP-ribose] polymerase-1	*Homo sapiens*	[89]
0.41	3H0S	B38	Acetyl-CoA carboxylase	*Saccharomyces cerevisiae*	[96]
0.41	3SFF	0DI	Histone deacetylase 8	*Homo sapiens*	[98]
0.41	1IA4	TQ6	Dihydrofolate reductase	*Candida albicans*	[99]
0.41	3EAI	328	Nitric oxide synthase, inducible	*Mus musculus*	[97]
0.40	3EKR	PY9	Heat shock protein HSP 90-alpha	*Homo sapiens*	[100]
0.40	1UK1	FRQ	Poly [ADP-ribose] polymerase-1	*Homo sapiens*	[101]
0.40	3B3P	JI7	Nitric-oxide synthase	*Rattus norvegicus*	[92]
0.40	1ZZ1	SHH	Histone deacetylase	*Alcaligenaceae bacterium*	[102]
0.40	1RPW	DID	Transcriptional regulator qacR	*Staphylococcus aureus*	[103]
0.40	3DQT	JI7	Nitric oxide synthase, endothelial	*Rattus norvegicus*	[92]
0.40	3DQS	JI3	Nitric oxide synthase, endothelia	*Bos taurus*	[92]

Tanimoto Score	Protein code	Ligand code	Protein type	Organism of origin of the protein	Reference
0.40	1IF7	SBR	Carbonic anhydrase ii	*Homo sapiens*	[93]

TABLE S8 | Results of the search in the Ligand Expo[88] for protein ligands three-dimensionally similar to the conformations of benzotriazine A8.

Tanimoto score	Protein code	Ligand code	Protein type	Organism of origin of the protein	Reference
0.5	2DS1	1CD	Protein kinase 2	*Homo sapiens*	[104]
0.48	2NSD	4PI	Enoyl-[acyl-carrier-protein] reductase	*Mycobacterium tuberculosis*	[105]
0.48	2VYA	PF7	Hydrolase 1	*Rattus norvegicus*	[88]
0.47	1IF8	SBS	Carbonic anhydrase II	*Homo sapiens*	[93]
0.45	2Y57	V37	Soluble acetylcholine receptor	*Aplysia californica*	[86]
0.44	2NSD	4PI	Enoyl-[acyl-carrier-protein] reductase	*Mycobacterium tuberculosis*	[87]
0.44	2VYA	PF7	Hydrolase 1	*Rattus norvegicus*	[88]
0.43	2Y56	V11	Soluble acetylcholine receptor	*Aplysia californica*	[86]
0.43	3ZK3 [1]	LCM	Enterochelin uptake periplasmic binding protein	*Campylobacter jejuni*	[106]
0.43	1IF7	SBR	Carbonic anhydrase II	*Homo sapiens*	[93]
0.43	3IW7	IPK	Mitogen-activated protein kinase 14	*Homo sapiens*	[45]
0.43	3EIO	AJH	Soluble form of dipeptidyl peptidase 4	*Homo sapiens*	[95]
0.43	2Y58	V38	Soluble acetylcholine receptor	*Aplysia californica*	[86]
0.41	1UK0	FRM	Poly[ADP-ribose] polymerase-1	*Homo sapiens*	[89]
0.41	3SFF	0DI	Histone deacetylase 8	*Homo sapiens*	[98]
0.41	3EAI	328	Nitric oxide synthase, inducible	*Mus musculus*	[97]
0.41	2BYS	LOB	Acetylcholine binding protein	*Aplysia californica*	[90]

TABLE S9 | Proteins whose amino acid sequences were similar (scores greater than 200) to amino acid sequences extracted from the genomes of *Meloidogyne* spp., according to calculations made with the Blastp +2.13.0 programme (https://blast.ncbi.nlm.nih.gov/Blast.cgi).

1 Entry at https://www.rcsb.org/ of code 3ZK3 is replaced by 5A1J

Code of the selected protein	**Name of selected protein**	**Organism of origin of the selected protein**	**Biological unit of the selected protein**	**Number of residues per chain**	**Name of the protein found in the genome of Meloidogyne spp., with a score above 200**	**Number of amino acid residues of the protein found in the genome of *Meloidogyne* spp.**	**Protein score**	**Coverage**	**Nematode species**
2DS1	Cell division protein kinase 2	*Homo sapiens*	Monomeric	298aa	Protein kinase domain	597aa	323	95%	*Meloidogyne graminicola*
3IW7	Mitogen-activated protein kinase 14	*Homo sapiens*	Monomeric	360aa	Protein Kinase 1	394aa	363	95%	*Meloidogyne incognita*

TABLE S10 | Mitogen-activated protein kinases 14, whose three-dimensional structures were employed in the molecular docking study.

Protein code	Amino acid residue	Producing organism	References
1LEW	360	*Mus musculus*	[1]
1M7Q	366	*Homo sapiens*	[2]
1TVO	368	*Homo sapiens*	[3]
1ZZL	351	*Homo sapiens*	[4]
2B9F	351	*Homo sapiens*	[5]
2FYS	364	*Rattus norvegicus*	[6]
2GTM	348	*Mus musculus*	[7]
2LGC	359	*Homo sapiens*	[38]
2YIS	359	*Homo sapiens*	[8]
2ZOQ	382	*Homo sapiens*	[9]
3D7Z	360	*Homo sapiens*	[10]
3S3I	349	*Homo sapiens*	[11]
4F9W	383	*Homo sapiens*	[12]
4FUX	360	*Homo sapiens*	https://www.rcsb.org/structure/4FUX
4LOO	361	*Mus musculus*	[13]
4O6E	368	*Homo sapiens*	[14]
4XJO	457	*Mycobacterium tuberculosis*	[15]
4ZZM	350	*Homo sapiens*	[16]
5BYY	346	*Homo sapiens*	[17]
5NGU	381	*Homo sapiens*	[18]
5NHH	381	*Homo sapiens*	[18]
5V62	351	*Homo sapiens*	[19]
6DTL	364	*Arabidopsis thaliana*	[20]

TABLE S11| Mitogen-activated protein kinases 14 aligned to 3IW7[46], using Lovoalign version 17.027[21]. Root mean square deviation of the atomic positions (RMSD) were calculated in relation to 3IW7.

Proteins codes	Amino acid residues	RMSD(Å)
1DI9	360	1.75
1LEW	360	1.70
1M7Q	366	1.54
1OZ1	372	1.52
1WZY	368	2.77
1ZZL	351	1.48
2B9F	353	2.94
2BAJ	365	1.32
2FYS	364	2.93
2LGC	359	1.54
2OJG	380	2.92
2ZOQ	382	3.26
3C9W	357	2.99
3D7Z	360	1.61
3DT1	383	1.59
3IW7	360	0.00
3NNU	354	1.43
3NNX	354	1.65
3S3I	349	1.45
4FUX	360	2.63
4FV6	360	3.12
4FV7	360	2.91
4IZ7	356	2.93
4LOO	361	1.58
4QP4	369	2.74
4QYY	365	2.55
4XJ0	349	3.09
4XOZ	351	2.47
4ZSG	347	2.81
4ZSJ	344	2.65
4ZSL	341	2.66
5BYY	346	2.56
5BYZ	348	2.88
5K4I	352	3.57
507I	358	2.59
6DMG	347	2.87
6DTL	364	3.28
6NBS	367	2.68
60PK	352	2.76
7W5C	352	3.80

References

[1] C.-I. Chang, B. Xu, R. Akella, M. H. Cobb, and E. J. Goldsmith, "Crystal Structures of MAP Kinase p38 Complexed to the Docking Sites on Its Nuclear Substrate MEF2A and Activator MKK3b," *Molecular cell*, vol. 9, no. 6, pp. 1241–1249, Jun. 2002, doi: 10.1016/S1097-2765(02)00525-7.

[2] J. E. Stelmach *et al.*, "Design and synthesis of potent, orally bioavailable dihydroquinazolinone inhibitors of p38 MAP kinase," *Bioorganic & Medicinal Chemistry Letters*, vol. 13, no. 2, pp. 277–280, 2003, doi: 10.1016/S0960-894X(02)00752-7.

[3] M. Ohori *et al.*, "Identification of a selective ERK inhibitor and structural determination of the inhibitor-ERK2 complex," *Biochemical and Biophysical Research Communications*, vol. 336, no. 1, pp. 357–363, Oct. 2005, doi: 10.1016/j.bbrc.2005.08.082.

[4] K. F. McClure *et al.*, "Theoretical and experimental design of atypical kinase inhibitors: Application to p38 MAP kinase," *Journal of Medicinal Chemistry*, vol. 48, no. 18, pp. 5728–5737, Sep. 2005, doi: 10.1021/jm050346q.

[5] A. Reményi, M. C. Good, R. P. Bhattacharyya, and W. A. Lim, "The role of docking interactions in mediating signaling input, output, and discrimination in the yeast MAPK network," *Molecular cell*, vol. 20, no. 6, pp. 951–962, Dec. 2005, doi: 10.1016/j.molcel.2005.10.030.

[6] S. Liu, J.-P. Sun, B. Zhou, and Z.-Y. Zhang, "Structural basis of docking interactions between ERK2 and MAP kinase phosphatase 3," 2006. [Online]. Available: www.pnas.orgcgi-doi10.1073pnas.0510506103

[7] M. Sabat *et al.*, "The development of novel C-2, C-8, and N-9 trisubstituted purines as inhibitors of TNF-α production," *Bioorganic & Medicinal Chemistry Letters*, vol. 16, no. 16, pp. 4360–4365, Aug. 2006, doi: 10.1016/j.bmcl.2006.05.050.

[8] D. S. Millan *et al.*, "Design and Synthesis of Inhaled p38 Inhibitors for the Treatment of Chronic Obstructive Pulmonary Disease," *Journal of Medicinal Chemistry*, vol. 54, no. 22, pp. 7797–7814, Nov. 2011, doi: 10.1021/jm200677b.

[9] T. Kinoshita *et al.*, "Crystal structure of human mono-phosphorylated ERK1 at Tyr204," *Biochemical and Biophysical Research Communications*, vol. 377, no. 4, pp. 1123–1127, Dec. 2008, doi: 10.1016/j.bbrc.2008.10.127.

[10] R. Angell *et al.*, "Biphenyl amide p38 kinase inhibitors 3: Improvement of cellular and in vivo activity," *Bioorganic & Medicinal Chemistry Letters*, vol. 18, no. 15, pp. 4428–4432, Aug. 2008, doi: 10.1016/j.bmcl.2008.06.048.

[11] J. Aiguadé *et al.*, "Novel triazolopyridylbenzamides as potent and selective p38α inhibitors," *Bioorganic & Medicinal Chemistry Letters*, vol. 22, no. 10, pp. 3431–3436, May 2012, doi: 10.1016/j.bmcl.2012.03.099.

[12] D. M. Watterson *et al.*, "Development of Novel *In Vivo* Chemical Probes to Address CNS Protein Kinase Involvement in Synaptic Dysfunction," *PLoS One*, vol. 8, no. 6, Jun. 2013, doi: 10.1371/journal.pone.0066226.

[13] G. F. De Nicola *et al.*, "Mechanism and consequence of the autoactivation of p38α mitogen-activated protein kinase promoted by TAB1," *Nature Structural & Molecular biology*, vol. 20, no. 10, pp. 1182–1192, Oct. 2013, doi: 10.1038/nsmb.2668.

[14] J. F. Blake *et al.*, "Discovery of 5,6,7,8-tetrahydropyrido[3,4-d]pyrimidine inhibitors of Erk2," *Bioorganic & Medicinal Chemistry Letters*, vol. 24, no. 12, pp. 2635–2639, Jun. 2014, doi: 10.1016/j.bmcl.2014.04.068.

[15] F. Liu *et al.*, "Structure-Based Optimization of Pyridoxal 5′-Phosphate-Dependent Transaminase Enzyme (BioA) Inhibitors that Target Biotin Biosynthesis in Mycobacterium tuberculosis," *Journal of Medicinal Chemistry*, vol. 60, no. 13, pp. 5507–5520, Jul. 2017, doi: 10.1021/acs.jmedchem.7b00189.

[16] R. A. Ward *et al.*, "Structure-Guided Design of Highly Selective and Potent Covalent Inhibitors of ERK1/2," *Journal of Medicinal Chemistry*, vol. 58, no. 11, pp. 4790–4801, Jun. 2015, doi: 10.1021/acs.jmedchem.5b00466.

[17] H. Chen *et al.*, "Discovery of a novel allosteric inhibitor-binding site in ERK5: Comparison with the canonical kinase hinge ATP-binding site," *Biological Crystallography*, vol. 72, no. 5, pp. 682–693, 2016, doi: 10.1107/S2059798316004502.

[18] R. A. Ward *et al.*, "Structure-Guided Discovery of Potent and Selective Inhibitors of ERK1/2 from a Modestly Active and Promiscuous Chemical Start Point," *Journal of Medicinal Chemistry*, vol. 60, no. 8, pp. 3438–3450, Apr. 2017, doi: 10.1021/acs.jmedchem.7b00267.

[19] B. C. Lechtenberg *et al.*, "Structure-Guided Strategy for the Development of Potent Bivalent ERK Inhibitors," *ACS Medicinal Chemistry Letters*, vol. 8, no. 7, pp. 726–731, Jul. 2017, doi: 10.1021/acsmedchemlett.7b00127.

[20] A. Putarjunan *et al.*, "Bipartite anchoring of SCREAM enforces stomatal initiation by coupling MAP kinases to SPEECHLESS," *Nature plants*, vol. 5, no. 7, pp. 742–754, Jul. 2019, doi: 10.1038/s41477-019-0440-x.

[21] L. Martínez, R. Andreani, and J. M. Martínez, "Convergent algorithms for protein structural alignment," *BMC Bioinformatics*, vol. 8, Aug. 2007, doi: 10.1186/1471-2105-8-306.

[22] E. F. Pettersen *et al.*, "UCSF Chimera - A visualization system for exploratory research and analysis," *Journal of Computational Chemistry*, vol. 25, no. 13, pp. 1605–1612, Oct. 2004, doi: 10.1002/jcc.20084.

[23] K. Okonechnikov *et al.*, "Unipro UGENE: A unified bioinformatics toolkit," Apr. 2012. doi: 10.1093/bioinformatics/bts091.

[24] F. Sievers and D. G. Higgins, "Clustal Omega for making accurate alignments of many protein sequences," *Protein Science*, vol. 27, no. 1, pp. 135–145, Jan. 2018, doi: 10.1002/pro.3290.

[25] Z. Wang *et al.*, "Structural basis of inhibitor selectivity in MAP kinases," *Structure*, vol. 6, no. 9, pp. 1117–1128, Sep. 1998, doi: 10.1016/S0969-2126(98)00113-0.

[26] L. Shewchuk *et al.*, "Binding mode of the 4-anilinoquinazoline class of protein kinase inhibitor: X-ray crystallographic studies of 4-anilinoquinazolines bound to cyclin-dependent kinase 2 and p38 kinase," *Journal of Medicinal Chemistry*, vol. 43, no. 1, pp. 133–138, Jan. 2000, doi: 10.1021/jm990401t.

[27] L. Tong *et al.*, "A highly specific inhibitor of human p38 MAP kinase binds in the ATP pocket," 1997. [Online]. Available: http://www.nature.com/nsmb

[28] A. Trejo *et al.*, "Design and Synthesis of 4-Azaindoles as Inhibitors of p38 MAP Kinase," *Journal of Medicinal Chemistry*, vol. 46, no. 22, pp. 4702–4713, Oct. 2003, doi: 10.1021/jm0301787.

[29] T. Fox *et al.*, "A single amino acid substitution makes ERK2 susceptible to pyridinyl imidazole inhibitors of p38 MAP kinase," *Protein Science*, vol. 7, no. 11, pp. 2249–2255, 1998, doi: 10.1002/pro.5560071102.

[30] T. Kinoshita, M. Warizaya, M. Ohori, K. Sato, M. Neya, and T. Fujii, "Crystal structure of human ERK2 complexed with a pyrazolo[3,4-c]pyridazine derivative," *Bioorganic & Medicinal Chemistry Letters*, vol. 16, no. 1, pp. 55–58, Jan. 2006, doi: 10.1016/j.bmcl.2005.09.055.

[31] J. E. Sullivan *et al.*, "Prevention of MKK6-dependent activation by binding to p38α MAP kinase," *Biochemistry*, vol. 44, no. 50, pp. 16475–16490, Dec. 2005, doi: 10.1021/bi051714v.

[32] B. J. Canagarajah, A. Khokhlatchev, M. H. Cobb, and E. J. Goldsmith, "Activation Mechanism of the MAP Kinase ERK2 by Dual Phosphorylation," *Cell*, vol. 90, no. 5, pp. 859–869, Sep. 1997, doi: 10.1016/S0092-8674(00)80351-7.

[33] R. P. Bhattacharyya, A. Reményi, M. C. Good, C. J. Bashor, A. M. Falick, and W. A. Lim, "The Ste5 scaffold allosterically modulates signaling output of the yeast mating pathway," *Science (1979)*, vol. 311, no. 5762, pp. 822–826, Feb. 2006, doi: 10.1126/science.1120941.

[34] R. Diskin, M. Lebendiker, D. Engelberg, and O. Livnah, “Structures of p38α Active Mutants Reveal Conformational Changes in L16 Loop that Induce Autophosphorylation and Activation,” *Journal of Molecular Biology*, vol. 365, no. 1, pp. 66–76, Jan. 2007, doi: 10.1016/j.jmb.2006.08.043.

[35] R. Diskin, D. Engelberg, and O. Livnah, “A Novel Lipid Binding Site Formed by the MAP Kinase Insert in p38α,” *Journal of Molecular Biology*, vol. 375, no. 1, pp. 70–79, Jan. 2008, doi: 10.1016/j.jmb.2007.09.002.

[36] D. M. Goldstein *et al.*, “Discovery of *S*-[5-amino-1-(4-fluorophenyl)-1*H*-pyrazol-4-yl]-[3-(2,3-dihydroxypropoxy)phenyl]-methanone (RO3201195), an orally bioavailable and highly selective inhibitor of p38 Map kinase,” *Journal of Medicinal Chemistry*, vol. 49, no. 5, pp. 1562–1575, Mar. 2006, doi: 10.1021/jm050736c.

[37] T. Zhou, L. Sun, J. Humphreys, and E. J. Goldsmith, “Docking Interactions Induce Exposure of Activation Loop in the MAP Kinase ERK2,” *Structure*, vol. 14, no. 6, pp. 1011–1019, Jun. 2006, doi: 10.1016/j.str.2006.04.006.

[38] V. S. Honndorf, N. Coudevylle, S. Laufer, S. Becker, C. Griesinger, and M. Habeck, “Inferential NMR/X-ray-based structure determination of a dibenzo[a,d]cycloheptenone inhibitor-p38α MAP kinase complex in solution,” *Angewandte Chemie International Edition*, vol. 51, no. 10, pp. 2359–2362, 2012, doi: 10.1002/anie.201105241.

[39] A. M. Aronov *et al.*, “Flipped out: Structure-guided design of selective pyrazolylpyrrole ERK inhibitors,” *Journal of Medicinal Chemistry*, vol. 50, no. 6, pp. 1280–1287, Mar. 2007, doi: 10.1021/jm061381f.

[40] N. Katayama *et al.*, “Identification of a key element for hydrogen-bonding patterns between protein kinases and their inhibitors,” *Proteins: Structure, Function and Genetics*, vol. 73, no. 4, pp. 795–801, Dec. 2008, doi: 10.1002/prot.22207.

[41] G. Rastelli, R. Rosenfeld, R. Reid, and D. V. Santi, "Molecular modeling and crystal structure of ERK2-hypothemycin complexes," *Journal of Structural Biology*, vol. 164, no. 1, pp. 18–23, Oct. 2008, doi: 10.1016/j.jsb.2008.05.002.

[42] B. Herberich *et al.*, "Discovery of highly selective and potent p38 inhibitors based on a phthalazine scaffold," *Journal of Medicinal Chemistry,* vol. 51, no. 20, pp. 6271–6279, Oct. 2008, doi: 10.1021/jm8005417.

[43] H. V. Namboodiri, M. Bukhtiyarova, J. Ramcharan, M. Karpusas, Y. Lee, and E. B. Springman, "Analysis of imatinib and sorafenib binding to p38α Compared with c-Abl and b-Raf provides structural insights for understanding the selectivity of inhibitors targeting the DFG-out form of protein kinases," *Biochemistry*, vol. 49, no. 17, pp. 3611–3618, May 2010, doi: 10.1021/bi100070r.

[44] J. J. P. Perry, R. M. Harris, D. Moiani, A. J. Olson, and J. A. Tainer, "p38α MAP Kinase C-Terminal Domain Binding Pocket Characterized by Crystallographic and Computational Analyses," *Journal of Molecular Biology*, vol. 391, no. 1, pp. 1–11, Aug. 2009, doi: 10.1016/j.jmb.2009.06.005.

[45] J. R. Simard *et al.*, "High-throughput screening to identify inhibitors which stabilize inactive kinase conformations in p38α," *Journal of the American Chemical Society*, vol. 131, no. 51, pp. 18478–18488, Dec. 2009, doi: 10.1021/ja907795q.

[46] H. Tecle *et al.*, "The Design, Synthesis and Potential Utility of Fluorescence Probes that Target DFG-out Conformation of p38α for High Throughput Screening Binding Assay," *Chemical Biology & Drug Design*, vol. 74, no. 6, pp. 547–559, Dec. 2009, doi: 10.1111/j.1747-0285.2009.00884.x.

[47] Y. M. Ahn *et al.*, "Switch control pocket inhibitors of p38-MAP kinase. Durable type II inhibitors that do not require binding into the canonical ATP hinge region," *Bioorganic & Medicinal Chemistry Letters*, vol. 20, no. 19, pp. 5793–5798, Oct. 2010, doi: 10.1016/j.bmcl.2010.07.134.

[48] W. Ma, Y. Shang, Z. Wei, W. Wen, W. Wang, and M. Zhang, "Phosphorylation of DCC by ERK2 Is Facilitated by Direct Docking of the Receptor P1 Domain to the Kinase," *Structure*, vol. 18, no. 11, pp. 1502–1511, Nov. 2010, doi: 10.1016/j.str.2010.08.011.

[49] N. Tzarum, R. Diskin, D. Engelberg, and O. Livnah, "Active mutants of the TCR-mediated p38α alternative activation site show changes in the phosphorylation lip and DEF site formation," *Journal of Molecular Biology*, vol. 405, no. 5, pp. 1154–1169, Feb. 2011, doi: 10.1016/j.jmb.2010.11.023.

[50] R. Akella, X. Min, Q. Wu, K. H. Gardner, and E. J. Goldsmith, "The third conformation of p38α MAP kinase observed in phosphorylated p38α and in solution," *Structure*, vol. 18, no. 12, pp. 1571–1578, Dec. 2010, doi: 10.1016/j.str.2010.09.015.

[51] A. Le Maire *et al.*, "In-plate protein crystallization, in situ ligand soaking and X-ray diffraction," *Biological Crystallography*, vol. 67, no. 9, pp. 747–755, Sep. 2011, doi: 10.1107/S0907444911023249.

[52] A. Plotnikov, D. Chuderland, Y. Karamansha, O. Livnah, and R. Seger, "Nuclear Extracellular Signal-Regulated Kinase 1 and 2 Translocation Is Mediated by Casein Kinase 2 and Accelerated by Autophosphorylation," *Molecular and Cellular Biology*, vol. 31, no. 17, pp. 3515–3530, Sep. 2011, doi: 10.1128/MCB.05424-11.

[53] J. Li *et al.*, "Norathyriol suppresses skin cancers induced by solar ultraviolet radiation by targeting ERK kinases," *Cancer Research*, vol. 72, no. 1, pp. 260–270, Jan. 2012, doi: 10.1158/0008-5472.CAN-11-2596.

[54] Á. Garai *et al.*, "Specificity of Linear Motifs That Bind to a Common Mitogen-Activated Protein Kinase Docking Groove," *Science Signaling*, vol. 5, no. 245, pp. ra74–ra74, Oct. 2012, doi: 10.1126/scisignal.2003004.

[55] R. Azevedo, M. Van Zeeland, H. Raaijmakers, B. Kazemier, J. De Vlieg, and A. Oubrie, "X-ray structure of p38 bound to TAK-715: Comparison with three classic inhibitors," *Biological Crystallography*, vol. 68, no. 8, pp. 1041–1050, Aug. 2012, doi: 10.1107/S090744491201997X.

[56] N. Tzarum, Y. Eisenberg-Domovich, J. J. Gills, P. A. Dennis, and O. Livnah, "Lipid Molecules Induce p38α Activation via a Novel Molecular Switch," *Journal of Molecular Biology*, vol. 424, no. 5, pp. 339–353, 2012, doi: https://doi.org/10.1016/j.jmb.2012.10.007.

[57] G. Gógl, I. Töro, and A. Reményi, "Protein-peptide complex crystallization: A case study on the ERK2 mitogen-activated protein kinase," *Biological Crystallography*, vol. 69, no. 3, pp. 486–489, Mar. 2013, doi: 10.1107/S0907444912051062.

[58] S. B. Hari, E. A. Merritt, and D. J. Maly, "Sequence Determinants of a Specific Inactive Protein Kinase Conformation*," Chemistry & Biology*, vol. 20, no. 6, pp. 806–815, 2013, doi: https://doi.org/10.1016/j.chembiol.2013.05.005.

[59] G. Yang *et al.*, "Caffeic acid directly targets ERK1/2 to attenuate solar UV-induced skin carcinogenesis," *Cancer Prevention Research*, vol. 7, no. 10, pp. 1056–1066, Oct. 2014, doi: 10.1158/1940-6207.CAPR-14-0141.

[60] D. J. Burdick *et al.*, "Fragment-based discovery of potent ERK2 pyrrolopyrazine inhibitors," *Bioorganic & Medicinal Chemistry Letters*, vol. 25, no. 21, pp. 4728–4732, Nov. 2015, doi: 10.1016/j.bmcl.2015.08.048.

[61] A. Chaikuad *et al.*, "A unique inhibitor binding site in ERK1/2 is associated with slow binding kinetics," *Nature Chemical Biology*, vol. 10, no. 10, pp. 853–860, Oct. 2014, doi: 10.1038/nchembio.1629.

[62] Y. Deng *et al.*, "Discovery of novel, dual mechanism ERK inhibitors by affinity selection screening of an inactive kinase," *Journal of Medicinal Chemistry*, vol. 57, no. 21, pp. 8817–8826, Nov. 2014, doi: 10.1021/jm500847m.

[63] L. Ren *et al.*, "Discovery of highly potent, selective, and efficacious small molecule inhibitors of ERK1/2," *Journal of Medicinal Chemistry*, vol. 58, no. 4, pp. 1976–1991, Feb. 2015, doi: 10.1021/jm501921k.

[64] M. Gelin *et al.*, "Combining 'dry' co-crystallization and in situ diffraction to facilitate ligand screening by X-ray crystallography," *Biological Crystallography*, vol. 71, pp. 1777–1787, Aug. 2015, doi: 10.1107/S1399004715010342.

[65] B. Wang *et al.*, "Analysis of crystal structure of Arabidopsis MPK6 and generation of its mutants with higher activity," *Scientific Reports*, vol. 6, May 2016, doi: 10.1038/srep25646.

[66] S. Jha *et al.*, "Dissecting therapeutic resistance to ERK inhibition," *Molecular Cancer Therapeutics*, vol. 15, no. 4, pp. 548–559, Apr. 2016, doi: 10.1158/1535-7163.MCT-15-0172.

[67] J. F. Blake *et al.*, "Discovery of (*S*)-1-(1-(4-Chloro-3-fluorophenyl)-2-hydroxyethyl)-4-(2-((1-methyl-1*H*-pyrazol-5-yl)amino)pyrimidin-4-yl)pyridin-2(1*H*)-one (GDC-0994), an Extracellular Signal-Regulated Kinase 1/2 (ERK1/2) Inhibitor in Early Clinical Development," *Journal of Medicinal Chemistry*, vol. 59, no. 12, pp. 5650–5660, Jun. 2016, doi: 10.1021/acs.jmedchem.6b00389.

[68] H. Lebraud, D. J. Wright, C. E. East, F. P. Holding, M. O'Reilly, and T. D. Heightman, "In-gel activity-based protein profiling of a clickable covalent ERK1/2 inhibitor," *Molecular BioSystems*, vol. 12, no. 9, pp. 2867–2874, Sep. 2016, doi: 10.1039/c6mb00367b.

[69] S. M. Myers *et al.*, "Identification of a novel orally bioavailable ERK5 inhibitor with selectivity over p38α and BRD4," *European Journal of Medicinal Chemistry*, vol. 178, pp. 530–543, Sep. 2019, doi: 10.1016/j.ejmech.2019.05.057.

[70] M. Bührmann, J. Hardick, J. Weisner, L. Quambusch, and D. Rauh, " Kovalente Liganden zur Adressierung einer lipophilen Bindetasche in der MAPK p38 α ," *Angewandte Chemie*, vol. 129, no. 43, pp. 13415–13419, Oct. 2017, doi: 10.1002/ange.201706345.

[71] B. S. Jaiswal *et al.*, "ERK Mutations and amplification confer resistance to ERK-inhibitor therapy," *Clinical Cancer Research*, vol. 24, no. 16, pp. 4044–4055, Aug. 2018, doi: 10.1158/1078-0432.CCR-17-3674.

[72] G. C. P. Van Zundert *et al.*, "QFit-ligand Reveals Widespread Conformational Heterogeneity of Drug-Like Molecules in X-Ray Electron Density Maps," *Journal of Medicinal Chemistry*, vol. 61, no. 24, pp. 11183–11198, Dec. 2018, doi: 10.1021/acs.jmedchem.8b01292.

[73] T. D. Heightman *et al.*, "Fragment-Based Discovery of a Potent, Orally Bioavailable Inhibitor That Modulates the Phosphorylation and Catalytic Activity of ERK1/2," *Journal of Medicinal Chemistry.*, vol. 61, no. 11, p. 4978, 2018, doi: 10.1021/acs.jmedchem.8b00421.

[74] T. D. Heightman *et al.*, "Fragment-Based Discovery of a Potent, Orally Bioavailable Inhibitor That Modulates the Phosphorylation and Catalytic Activity of ERK1/2," *Journal of Medicinal Chemistry*, vol. 61, no. 11, pp. 4978–4992, Jun. 2018, doi: 10.1021/acs.jmedchem.8b00421.

[75] D. Nguyen *et al.*, "Discovery and Characterization of the Potent and Highly Selective (Piperidin-4-yl) pyrido [3, 2-d] pyrimidine Based *in Vitro* Probe BAY-885 for the Kinase ERK5," *Journal of Medicinal Chemistry*, vol. 62, no. 2, pp. 928–940, 2018, doi :10.1021/acs.jmedchem.8b01606

[76] R. M. Sammons *et al.*, "A Novel Class of Common Docking Domain Inhibitors That Prevent ERK2 Activation and Substrate Phosphorylation," *ACS chemical Biology*, vol. 14, no. 6, pp. 1183–1194, Jun. 2019, doi: 10.1021/acschembio.9b00093.

[77] L. M. Pegram *et al.*, "Activation loop dynamics are controlled by conformation-selective inhibitors of ERK2," *Proceedings of the National Academy of Sciences*, vol. 116, no. 31, pp. 15463–15468, Jul. 2019, doi: 10.1073/pnas.1906824116.

[78] C. A. Taylor *et al.*, "Functional divergence caused by mutations in an energetic hotspot in ERK2," *Proceedings of the National Academy of Sciences*, vol. 116, no. 31, pp. 15514–15523, Jul. 2019, doi: 10.1073/pnas.1905015116.

[79] L. Gur-Arie, M. Eitan-Wexler, N. Weinberger, I. Rosenshine, and O. Livnah, "The bacterial metalloprotease NleD selectively cleaves mitogen-activated protein kinases that have high flexibility in their activation loop," *Journal of Biological Chemistry*, vol. 295, no. 28, pp. 9409–9420, Jul. 2020, doi: 10.1074/jbc.ra120.013590.

[80] C. Nichols *et al.*, "Mining the PDB for Tractable Cases Where X-ray Crystallography Combined with Fragment Screens Can Be Used to Systematically Design Protein-Protein Inhibitors: Two Test Cases Illustrated by IL1β-IL1R and p38α-TAB1 Complexes," *Journal of Medicinal Chemistry*, vol. 63, no. 14, pp. 7559–7568, Jul. 2020, doi: 10.1021/acs.jmedchem.0c00403.

[81] Y. S. Park, M. Kim, and S. E. Ryu, "Structural mechanism of inhibitor-resistance by ERK2 mutations," *Biodesign*, vol. 9, no. 1, pp. 14–18, Mar. 2021, doi: 10.34184/kssb.2021.9.1.14.

[82] A. Alexa *et al.*, "A non-catalytic herpesviral protein reconfigures ERK-RSK signaling by targeting kinase docking systems in the host," *Nature Communications*, vol. 13, no. 1, Dec. 2022, doi: 10.1038/s41467-022-28109-x.

[83] A. Siodmak *et al.*, "Essential role of the CD docking motif of MPK4 in plant immunity, growth, and development," *New Phytologist*, vol. 239, no. 3, pp. 1112–1126, Aug. 2023, doi: 10.1111/nph.18989.

[84] M. Yoshida, H. Nagao, H. Sugiyama, M. Sawa, and T. Kinoshita, "Identification of a novel target site for ATP-independent ERK2 inhibitors," *Biochemical and Biophysical Research Communications*, vol. 593, pp. 73–78, Feb. 2022, doi: 10.1016/j.bbrc.2022.01.035.

[85] J. D. St. Denis *et al.*, "X-ray Screening of an Electrophilic Fragment Library and Application toward the Development of a Novel ERK 1/2 Covalent Inhibitor," *Journal of Medicinal Chemistry*, vol. 65, no. 18, pp. 12319–12333, Sep. 2022, doi: 10.1021/acs.jmedchem.2c01044.

[86] E. Edink *et al.*, "Fragment growing induces conformational changes in acetylcholine-binding protein: A structural and thermodynamic analysis," *Journal of Medicinal Chemistry*, vol. 133, no. 14, pp. 5363–5371, Apr. 2011, doi: 10.1021/ja110571r.

[87] X. He, A. Alian, and P. R. Ortiz de Montellano, “Inhibition of the Mycobacterium tuberculosis enoyl acyl carrier protein reductase InhA by arylamides,” *Bioorganic & Medicinal Chemistry*, vol. 15, no. 21, pp. 6649–6658, 2007, doi: 10.1016/j.bmc.2007.08.013.

[88] M. Mileni *et al.*, “Structure-guided inhibitor design for human FAAH by interspecies active site conversion,” *Proceedings of the National Academy of Sciences*, vol. 105, no. 35, pp. 12820–12824, Sep. 2008, doi: 10.1073/pnas.0806121105.

[89] T. Kinoshita *et al.*, “Inhibitor-induced structural change of the active site of human poly(ADP-ribose) polymerase,” *FEBS Letters*, vol. 556, no. 1–3, pp. 43–46, Jan. 2004, doi: 10.1016/S0014-5793(03)01362-0.

[90] S. B. Hansen, G. Sulzenbacher, T. Huxford, P. Marchot, P. Taylor, and Y. Bourne, “Structures of Aplysia AChBP complexes with nicotinic agonists and antagonists reveal distinctive binding interfaces and conformations,” *EMBO Journal*, vol. 24, no. 20, pp. 3635–3646, Oct. 2005, doi: 10.1038/sj.emboj.7600828.

[91] E. Karakas, N. Simorowski, and H. Furukawa, “Subunit arrangement and phenylethanolamine binding in GluN1/GluN2B NMDA receptors,” *Nature*, vol. 475, no. 7355, pp. 249–253, Jul. 2011, doi: 10.1038/nature10180.

[92] J. Igarashi *et al.*, “Crystal structures of constitutive Nitric Oxide synthases in complex with de novo designed inhibitors,” *Journal of Medicinal Chemistry*, vol. 52, no. 7, pp. 2060–2066, Apr. 2009, doi: 10.1021/jm900007a.

[93] B. A. Grzybowski *et al.*, “Combinatorial computational method gives new picomolar ligands for a known enzyme,” *Proceedings of the National Academy of Sciences*, vol. 99, no. 3, pp. 1270–1273, Feb. 2002, doi: 10.1073/pnas.032673399.

[94] S. Patterson *et al.*, "Dihydroquinazolines as a novel class of Trypanosoma brucei trypanothione reductase inhibitors: Discovery, synthesis, and characterization of their binding mode by protein crystallography," *Journal of Medicinal Chemistry*, vol. 54, no. 19, pp. 6514–6530, Oct. 2011, doi: 10.1021/jm200312v.

[95] J. H. Ahn *et al.*, "Synthesis and biological evaluation of homopiperazine derivatives with β-aminoacyl group as dipeptidyl peptidase IV inhibitors," *Bioorganic & Medicinal Chemistry Letters*, vol. 18, no. 24, pp. 6525–6529, Dec. 2008, doi: 10.1016/j.bmcl.2008.10.076.

[96] J. W. Corbett *et al.*, "Discovery of small molecule isozyme non-specific inhibitors of mammalian acetyl-CoA carboxylase 1 and 2," *Bioorganic & Medicinal Chemistry Letters*, vol. 20, no. 7, pp. 2383–2388, Apr. 2010, doi: 10.1016/j.bmcl.2009.04.091.

[97] E. D. Garcin *et al.*, "Anchored plasticity opens doors for selective inhibitor design in nitric oxide synthase," *Nature Chemical Biology*, vol. 4, no. 11, pp. 700–707, 2008, doi: 10.1038/nchembio.115.

[98] L. Whitehead *et al.*, "Human HDAC isoform selectivity achieved via exploitation of the acetate release channel with structurally unique small molecule inhibitors," *Bioorganic & Medicinal Chemistry,* vol. 19, no. 15, pp. 4626–4634, Aug. 2011, doi: 10.1016/j.bmc.2011.06.030.

[99] M. Whitlow *et al.*, "X-ray crystal structures of Candida albicans dihydrofolate reductase: High resolution ternary complexes in which the dihydronicotinamide moiety of NADPH is displaced by an inhibitor," *Journal of Medicinal Chemistry*, vol. 44, no. 18, pp. 2928–2932, Aug. 2001, doi: 10.1021/jm0101444.

[100] P. P. Kung *et al.*, "Dihydroxylphenyl amides as inhibitors of the Hsp90 molecular chaperone," *Bioorganic & Medicinal Chemistry Letters*, vol. 18, no. 23, pp. 6273–6278, Dec. 2008, doi: 10.1016/j.bmcl.2008.09.081.

[101] K. Hattori *et al.*, "Rational approaches to discovery of orally active and brain-penetrable quinazolinone inhibitors of poly(ADP-ribose)polymerase," *Bioorganic & Medicinal Chemistry Letters*, vol. 47, no. 17, pp. 4151–4154, Aug. 2004, doi: 10.1021/jm0499256.

[102] T. K. Nielsen, C. Hildmann, A. Dickmanns, A. Schwienhorst, and R. Ficner, "Crystal Structure of a Bacterial Class 2 Histone Deacetylase Homologue," *Journal of Molecular Biology*, vol. 354, no. 1, pp. 107–120, 2005, doi: https://doi.org/10.1016/j.jmb.2005.09.065.

[103] D. S. Murray, M. A. Schumacher, and R. G. Brennan, "Crystal Structures of QacR-Diamidine Complexes Reveal Additional Multidrug-binding Modes and A Novel Mechanism of Drug Charge Neutralization," *Journal of Biological Chemistry*, vol. 279, no. 14, pp. 14365–14371, Apr. 2004, doi: 10.1074/jbc.M313870200.

[104] N. Kawanishi *et al.*, "Structure-based drug design of a highly potent CDK1,2,4,6 inhibitor with novel macrocyclic quinoxalin-2-one structure," *Bioorganic & Medicinal Chemistry Letters*, vol. 16, no. 19, pp. 5122–5126, Oct. 2006, doi: 10.1016/j.bmcl.2006.07.026.

[105] X. He, A. Alian, and P. R. Ortiz de Montellano, "Inhibition of the Mycobacterium tuberculosis enoyl acyl carrier protein reductase InhA by arylamides," *Bioorganic & Medicinal Chemistry,* vol. 15, no. 21, pp. 6649–6658, Nov. 2007, doi: 10.1016/j.bmc.2007.08.013.

[106] D. J. Raines, O. V. Moroz, K. S. Wilson, and A. Duhme-Klair, "Interactions of a Periplasmic Binding Protein with a Tetradentate Siderophore Mimic," *Angewandte Chemie*, vol. 125, no. 17, pp. 4693–4696, Apr. 2013, doi: 10.1002/ange.201300751.

molecular informatics

ARTICLE 2

A Simple Procedure Involving Virtual Screening, Docking, and Comparisons of Amino Acid Sequences to Select Inhibitors of Sodium-Dependent Serotonin Transporter Protein as Potential New Nematicides

Article Submitted to Molecular Informatics

DOI: 10.1002/minf.200((full DOI will be filled in by the editorial staff))

Geraldo Jamisse Hodela,[a] Vitor Pereira de Sousa,[b] Mariana Castro de Melo,[a] Rodrigo Martins Fráguas,[a] Willian César Terra[b] and Denilson Ferreira de Oliveira[a]

[a]Department of Chemistry, Federal University of Lavras, P.O. BOX 3037, Lavras-37203-202, MG-Brazil
[b]Department of Phytopathology, Federal University of Lavras, P.O. Box 3037, Lavras-37203-202, MG-Brazil

Correspondence: Denilson Ferreira de Oliveira (denilson@ufla.br)

Abstract: Nematodes of the genus *Meloidogyne* cause major losses in agricultural production worldwide. To identify potentially useful chemical structures for developing new nematicides, this study initially aimed to determine, *in silico* – using computationally efficient techniques – the protein target of chaetoglobosins A and B in these nematodes. This process led to the selection of the sodium-dependent serotonin transporter protein (SERT). The activities of SERT inhibitors were subsequently evaluated *in vitro*. The best result was obtained with paroxetine, which caused 50% mortality in second-stage juveniles (J2) of *Meloidogyne incognita* at an LC_{50} concentration of 351.26 μg/mL. Under the same conditions, the commercial nematicide fluensulfone showed an LC_{50} of 39.31 μg/mL. In plant trials, paroxetine reduced the pathogenicity of *M. incognita* J2. Therefore, further investigation of SERT inhibitors holds promise for the development of new nematicides.

Keywords: Molecular docking, paroxetine, *Meloidogyne*, nematicide, sodium-dependent serotonin transporter.

1 Introduction

Plant-parasitic nematodes (PPNs) significantly reduce agricultural production worldwide [1]. Among these soil-borne pathogens, root-knot nematodes (*Meloidogyne* spp.) cause damage across various regions of the world [2]. Currently, chemical nematicides remain one of the primary methods for controlling PPNs; however, they pose risks to both the environment and human health [3]. As a result, many chemical nematicides have been gradually withdrawn from the market [2,4], increasing the demand for new products for PPN control. Consequently, new compounds – particularly those of natural origin – have been tested against PPNs [5]. One such example is chaetoglobosins A and B (Figure 1).

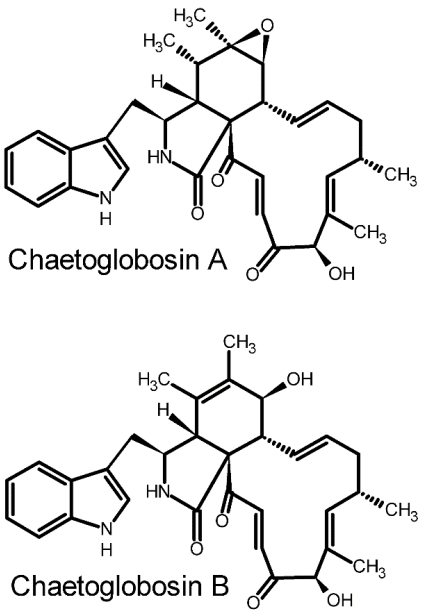

Figure 1. Chemical structures of chaetoglobosins.

According to the literature [6], the lethal concentration (LC_{50}) required to affect 50% of second-stage juveniles (J2) of *Meloidogyne javanica* (Treub) Chitwood was 88.4 *µ*g/mL for chaetoglobosin A and 107.07 *µ*g/mL for chaetoglobosin B. In a plant inoculation experiment using the same nematode species, researchers found that chaetoglobosin A reduced the number of galls (nematode pathogenicity) by 59.0%, the number of egg masses by 71.1%, and the number of eggs by 30.1%. Chaetoglobosin B demonstrated similar effectiveness, reducing the number of galls by 61.5%, the number of egg masses by 72.4%, and the number of nematode eggs by 35.4%.

Although chaetoglobosins have shown promising results, their structural complexity makes large-scale production for commercial PPN control economically unfeasible at present. To address this challenge, understanding how chaetoglobosins interact with PPNs could facilitate the development of simpler, effective compounds. With this goal in mind, the primary objective of this study was to identify *in silico* the protein target of chaetoglobosins in *Meloidogyne* spp. using computationally efficient techniques. The specific objectives were as follows: i) select protein ligands structurally similar to chaetoglobosins A and B; ii) identify, among the proteins whose ligands were selected, those with the greatest similarity in amino acid sequences to those of *Meloidogyne* spp.; iii) conduct molecular docking of the chaetoglobosins and inhibitors of the selected proteins to determine which protein sites could be inhibited by chaetoglobosins; and iv) perform biological tests with *M. incognita* and inhibitors of the selected proteins to validate the results obtained *in silico*.

2 Experimental Section

2.1 Preparation of Three-Dimensional Structures of Chaetoglobosins

Using the Open3Dalign 2.3 computer program [7], the three-dimensional structures of chaetoglobosins A and B (Figure 1) underwent conformational searches through molecular dynamics simulations, utilizing the Merck Molecular Force Field 94 (MMFF94). For each substance, 1,000 molecular dynamics simulations were conducted, with 1,000 steps of 1 fs per simulation. The most stable conformations, along with all those within 10 kcal/mol of the most stable, were then optimized using the Mopac 2016 program (http://openmopac.net/background.html).

For this optimization, the PM7 Hamiltonian was applied, with the solvent (water) implicitly considered through the Conductor-Like Screening Model (COSMO). Using the same program, the optimized structures underwent thermodynamic calculations to determine Gibbs free energy values. The Boltzmann distributions were then calculated for each chaetoglobosin conformation. Finally, using the computer program VMD 1.9.3 [8,9], the root mean square deviation (RMSD) of atomic positions between each pair of conformations was calculated.

2.2 Virtual Screening

Only conformations representing 7.0% or more of the populations of chaetoglobosins A and B were used (Supporting Information, Figure S1). The initial database utilized was Ligand Expo (http://ligand-expo.rcsb.org/ld-download.html) [10]. The search was conducted using the Lisica 1.0.1 computer program (http://insilab.org/lisica) [11]. Since all results had Tanimoto scores < 0.4, the search was expanded to the ChEMBL database (https://www.ebi.ac.uk) [12]. In this case, compounds with Tanimoto scores ≥ 0.4 were selected (Supporting Information, Table S1).

2.3 Amino Acid Sequence Analysis

The amino acid sequences of the proteins inhibited by the compounds selected in Section 2.2 were used to conduct a search in the NCBI database (https://www.ncbi.nlm.nih.gov) [13] using the Blastp +2.13.0 computer program [14]. This search aimed to identify similar sequences within the genomes of *Meloidogyne* spp. (taxid:18290). Only proteins with a score above 200 were selected (Supporting Information, Table S2).

2.4 Sodium-Dependent Serotonin Transporter (SERT)

The three-dimensional structures and amino acid sequences of the following SERTs (UniProtKB accession: P31645) were obtained from the RCSB Protein Data Bank (https://www.rcsb.org) [15]: 6VRH [16], 6VRK [16], 6VRL [16], 5I6X [17], 5I6Z [17], 5I66 [17], 5I73 [17], 5I74 [17], 5I75 [17]; 6AWN [18], 6AWP [18], 6AWQ [18]; 6DZV [19], 6DZW [19], 6DZY [19], 6DZZ [19]; 6W2C [16], 6W2B [16]; 7LI7 [20], 7LI8 [20], 7LI9 [20], 7LIA [20] , 7MGW [20], and 7LWD[21].

Using UGENE version 1.32.0 [22], with the Clustal Omega 1.2.1 algorithm [23], the amino acid sequences of all the SERTs were aligned in four iterations. Hamming dissimilarities (%) were calculated, accounting for all the gaps. Sequences with similarities (100 - Hamming dissimilarity) of a least 86% compared to 6VRH [16] (Supporting Information, Table S3) were selected.

Antibodies not chemically bound to the SERTs were removed before performing the three-dimensional alignment provided by Lovoalign 21.027 [24]. This program was also used to calculate the root mean square deviation (RMSD) of atomic positions (Supporting Information, Table S4) for each pair of three-dimensional structures. Finally, mutant SERTs were discarded.

2.5 Molecular Docking

SDF files containing the three-dimensional structures of SERT inhibitors were obtained from the RCSB Protein Data Bank (https://www.rcsb.org/) [15] (Supporting Information, Table S5). Using the MarvinSketch 22.11 program (https://chemaxon.com/), the protonation states of these inhibitors were calculated at pH 7. The structures of these inhibitors, the conformations of chaetoglobosins A and B (Supporting Information, Figure S1), and the three-dimensional structures of the biological units of the SERTs (Supporting Information, Table S4), after alignment with the 6VRH [16] protein, were converted to PDBQT format using MGLTools Version 1.5.7rc1 [25].

The docking grid was centered at 133.85, 123.71, and 123.68 Å (x, y and z), with dimensions of 24.31, 21.41, and 28.75 Å (x, y and z), ensuring full coverage of the region where inhibitors were experimentally complexed to the SERTs. Using the QuickVina 2.1 program [26], the SERT inhibitors (Supporting Information Table S5) and the conformations of chaetoglobosins A and B (Supporting Information, Figure S1) were docked to the SERTs (Supporting Information, Table S6). Except for the exhaustiveness parameter, which was increased to 256, all other parameters remained at their default values.

Overlaps between docked inhibitors and the same inhibitors experimentally complexed to SERTs were analyzed using the UCSF Chimera 1.17.3 program (https://www.cgl.ucsf.edu/chimera/download.html) [27]. The affinity values obtained from the docking procedure were subjected to analysis of variance (ANOVA), and the means were compared using the Scott-Knott [28] grouping test at 5% significance, conducted with the R program version 4.4.0 [29,30].

2.6 Obtaining Eggs and Second Stage Juveniles (J2) of *M. incognita*

Roots of tomato plants (*Solanum lycopersicum* L. 'Santa Clara'), grown in a greenhouse and infested with *M. incognita*, were thoroughly washed and cut into approximately 1 cm pieces. The roots were then ground in a blender for 30 seconds in a 0.5% (g/mL) sodium hypochlorite solution.

The resulting suspension was filtered through two sieves with 200- and 500-mesh pores. The eggs were washed thoroughly with water to remove any remaining sodium hypochlorite. Eggs retained on the 500-mesh sieve were collected and placed in a hatching chamber at a fixed temperature of 28 ºC to obtain second-stage juveniles (J2). Any J2 hatched within the first 24 hours were discarded. Only those hatched within a maximum of 48 h before the experiment setup were used in the tests.

2.7 *M. incognita* J2 Mobility and Mortality Test

In 96-well microplates, 20 µL of an aqueous suspension containing approximately 20 J2 of *M. incognita* and 100 µL of each SERT inhibitor solution (Figure 2) were added. These solutions were prepared by dissolving the inhibitors in an aqueous Tween 80® (Sigma-Aldrich, MO, USA) solution at 0.02 g/mL, up to a concentration of 600 µg/mL. The microplates were kept in a BOD at 28 ºC.

The experiment was conducted in five replicates, using fluensulfone (Nimitz®, ADAMA) at 34 µg/mL (final concentration after adding the J2 suspension) as a positive control. A Tween 80® solution containing 0.02 g/mL served as the negative control. After 48 h, mobile and immobile J2 were counted under a microscope. A freshly prepared 1.0 mol/L NaOH solution (5 µL) was then added to each cavity, and J2 were counted again for up to 1 min after NaOH addition. J2 that did

not respond to the NaOH solution and remained straight and immobile were classified as dead, while those that exhibited movement and twisting were considered alive, following the method described by Chen and Dickson [31], as adapted by Amaral et al. [32].

The data were converted into percentages and subjected to the Shapiro-Wilk [33] normality test and Barlett's [34] homoscedasticity test. Despite multiple transformations, normalization and homoscedasticity were not achieved. Consequently, a non-parametric Kruskal-Wallis [35] test was performed, revealing that at least one treatment differed significantly from the others. The Conover [36] test was then applied at a 5% significance level, using the Bonferoni [37] method to adjust *p-values*. This experiment was performed twice.

2.8 Lethal Concentrations for 50% (LC_{50}) of *M. incognita* J2

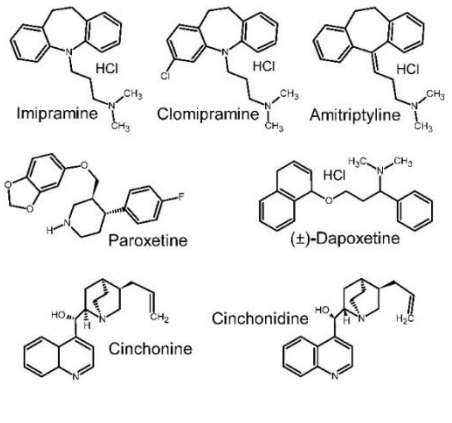

Figure 2. Chemical structures of SERT inhibitors: amitriptyline (purity ≥ 98%; origin: Cayman Chemical), imipramine (purity: ≥ 98%; origin: Cayman Chemical), (±)-dapoxetine (purity: ≥ 98%; origin: Cayman Chemical), clomipramine (purity: ≥ 98%; origin: Cayman Chemical), paroxetine (purity: ≥ 98%; origin: Sigma-Aldrich), cinchonine (purity: ≥ 98%; origin: Sigma-Aldrich), and cinchonidine (purity: ≥ 98%; origin: Sigma-Aldrich).

The procedure used was the same as described in Section 2.7 to determine J2 mortality. The final concentrations in the wells, after mixing with the J2 suspension, were 200, 250, 300, 350, and 400 *µ*g/mL for paroxetine (Figure 2, purity: ≥ 98%; Origin: Cayman Chemical) and 25, 30, 35, 40, and 45 *µ*g/mL for fluensulfone (Nimitz®, ADAMA, USA). The LC_{50} values were calculated through logit analyses [38], performed with the drc package [39] in the R statistical program, version 4.4.0 [29,30]. This experiment was conducted three times.

2.9 Effect of Paroxetine on the Pathogenicity of *M. incognita* in Tomato Plants

Based on the literature [40], tomato seeds (*Solanum lycopersicum* L. 'Santa Clara') susceptible to *M. incognita* were sown in commercial substrate (Tropstrato®, Vida Verde Indústria e Comércio de Insumos Orgânicos Ltda., Mogi Mirim, São Paulo, Brazil) contained in Styrofoam seed cells, with 72 cells of 121 mL each.

Paroxetine (Sigma-Aldrich, ≥ 98%) was dissolved in an aqueous Tween 80® solution (0.02 g/mL) to concentrations of 243.25 and 121.62 *µ*g/mL. An aqueous suspension (5.6 mL) containing approximately 500 J2 of *M. incognita* was applied to four holes (0.4 cm wide and 1.5 deep) around the stem of each 25-day-old tomato plant (1.4 mL per hole). Immediately afterwards, 2 mL of one of the solutions of paroxetine were applied separately to the same holes (0.5 mL per hole). Tween 80® at 0.02 g/mL and fluensulfone (Nimitz®, ADAMA, USA) at 108.89 *µ*g/mL, dissolved in water, were used as controls.

The seedlings were kept in a shaded room at approximately 28ºC for 48h before being transferred to a greenhouse, where they remained for approximately 45 days. After this period, the roots were removed, washed with water, dried with paper towels, and subjected to the nematode galls count.

The experiment was conducted twice. When combined for statistical analysis, the data did not

pass the Shapiro-Wilk [33] normality test or Barlett's [34] homoscedasticity test. Consequently, they were transformed using the Ordered Quantile [41] method, which enabled normalization and homoscedasticity. Two-way ANOVA revealed no interaction between the independent variables, experiment repetition, or additive effects. The Scott-Knott [28] test was then performed at a 5% significance level. All analyses were conducted using the R program, version 4.4.0 [29,30].

3 Results and Discussion

3.1 Preparation of Three-Dimensional Structures of Chaetoglobosins

Two conformations were observed to be the most stable for each of the two substances (Supporting Information, Figure S1). For chaetoglobosin A, an RMSD of 2.45 Å was observed between conformations 2 and 42, while chaetoglobosin B exhibited an RMSD of 1.96 Å between conformations 38 and 40. Therefore, both conformations for each chaetoglobosin were considered in subsequent steps.

3.2 Protein Ligands Three-Dimensionally Similar to Chaetoglobosins

The search for three-dimensional structures similar to chaetoglobosins identified ligands for the following proteins: sodium-dependent serotonin transporter [42], glutaminase [43], and AmpC *β*-lactamase [44] (Supporting Information, Table S1). These findings suggest that chaetoglobosins A and B may also inhibit these proteins.

3.3 Amino Acid Sequence Analysis

In the search for amino acid sequences similar to the three proteins selected in Section 3.2 contained within the genomes of *Meloidogyne* spp. (taxid:18290), the only protein with a score above 200 was the sodium-dependent serotonin transporter (SERT) [42]. Its score, identity, and coverage were 610, 81%, and 53.28%, respectively (Supporting Information, Table S2), suggesting that SERT may be a target of chaetoglobosins in *Meloidogyne* spp.

SERT is a protein encoded by the *SLC6* gene and functions as a neurotransmitter-related transporter, facilitating the movement of serotonin, sodium, and chloride from the synaptic spaces to the presynaptic neurons. In this process, SERT also transports potassium ions out of the cells. Located in cell membranes, it consists of approximately 630 amino acid residues [47,48].

In nematodes, serotonin plays an important role in host-plant invasion by inducing rhythmic stylet movement [45] and influencing egg-laying behavior [46]. One example is research involving reserpine, an alkaloid isolated from *Rauwolfia serpentina* L. [45], which inhibited serotonergic signaling, negatively affecting the nematode's ability to invade the host plant. Similarly, a study on the nematicidal activity of bilobalide against *Caenorhabditis elegans* Maupas demonstrated its inhibitory effect on nematode egg-laying [46]. These findings suggest that substances inhibiting SERT may serve as promising candidates for the development of new nematicides to control PPNs.

3.4 Molecular Docking

Both the active sites of the SERTs used (Figure 3) and their overall three-dimensional structures (Figure 4) showed strong overlap, indicating favorable conditions for obtaining data with normality and homoscedasticity during the molecular docking stage. These properties were confirmed by statistical calculations, which also demonstrated that the affinities of the chaetoglobosins for SERTs were statistically equivalent to the affinities calculated for SERT inhibitors (Figure 5). These findings support the hypothesis that SERT is the target of the chaetoglobosins in *Meloidogyne* spp.

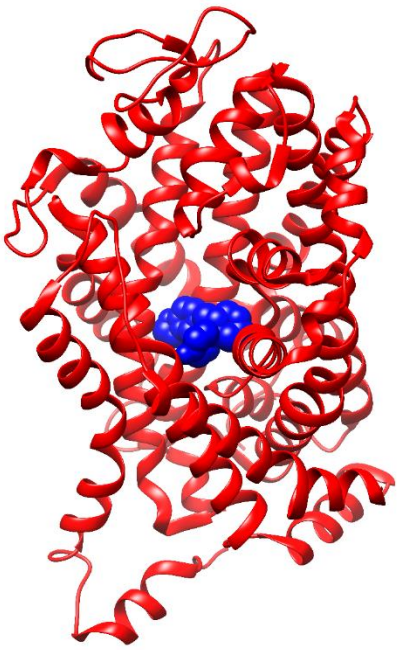

Figure 3. Three-dimensional structure of the sodium-dependent serotonin transporter (SERT) 6VRH [16], with the ligands experimentally complexed to various SERTs in blue.

When analyzing the interactions of chaetoglobosins with the active site of SERTs, hydrogen bonds were formed from the hydroxyl group and the nitrogen atom of the amide group (Figure 6). The amino acid residues Tyr (35), Glu (493), Asp (98), and Phe (335) were responsible for the interaction with chaetoglobosin A (Figure 6A), while chaetoglobosin B formed a hydrogen bond with the Try (35) residue (Figure 6B).

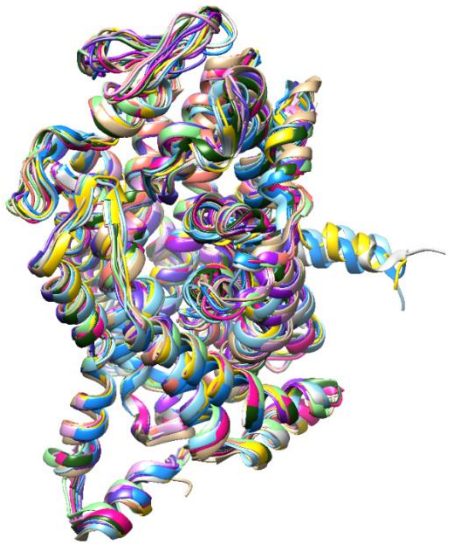

Figure 4. Three-dimensional structures of sodium-dependent serotonin transporters 7MGW [20], 7LI7 [20], 7LWD [21], 7LIA [20], 7LI9 [20], 7LI8 [20], 7LI6 [20], 6DZZ [19], 6VRH [16], 6VRL [16], 6VRK [16], and 6DZV [16] aligned by the Lovoalign 18.320 program [24]. Image generated by UCSF Chimera 1.13.1 [27].

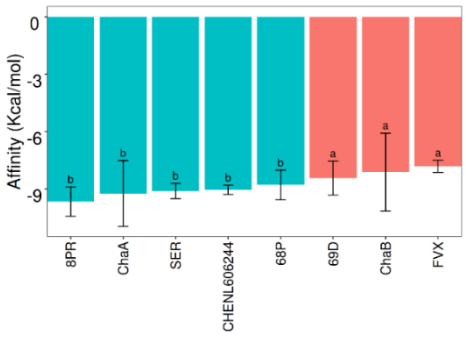

Figure 5. Affinities of chaetoglobosins A (ChaA) and B (ChaB), and of the following inhibitors of sodium-dependent serotonin transporters (SERTs): 68P [17], 69D [17], 8PR (Paroxetine) [16] CHEMBL606244 [42], FVX [18], and SER [18]. The affinities for the SERTs active site were calculated using the QuickVina 2.1 [26] computer program. Columns with the same letter are statistically equal to each other according to the Scott-Knott test [28] ($p < 0.05$). Error bars correspond to the standard deviation.

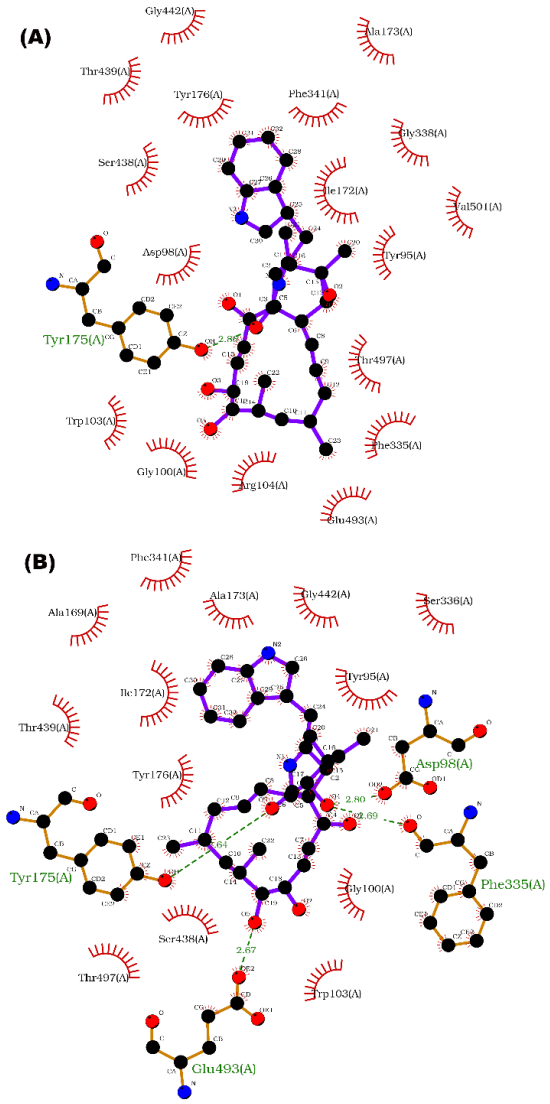

Figure 6. (A) Two-dimensional representation of the interactions of chaetoglobosin A with the active site of the sodium-dependent serotonin transporter 6VRL [16], to which the compound was docked with the computer program QuickVina 2.1 [26]. **(B)** The same representation for chaetoglobosin B. This figure was generated with the program LigPlot 2.2.8 [47].

3.5 Immobility and Mortality of *M. incognita* J2 After Exposure to SERT Inhibitors

All tested inhibitors reduced the mobility of *M. incognita*, with paroxetine causing the highest nematode mortality. Although imipramine, clomipramine, (±)-dapoxetine, cinchonine, and cichonidine increased J2 mortality compared to the negative control, the percentages of dead J2 were no higher than 28% (Figure 7).

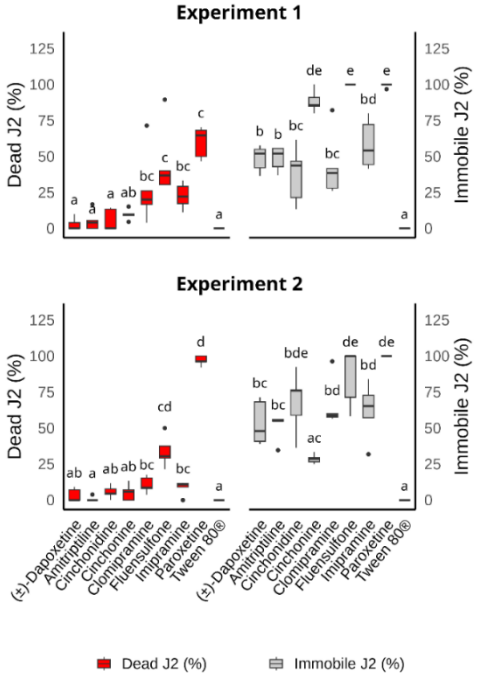

Figure 7. Dead and immobile J2 of *Meloidogyne incognita* after 48 h exposure to different SERT inhibitors (amitriptyline, imipramine, (±)-dapoxetine, clomipramine, paroxetine, cinchonine, and cichonidine). Columns of the same color, with at least one letter in common, in each graphic/experiment, are statistically equal to each other according to the Conover [36] test ($p < 0.05$), with p-value correction using the Bonferoni [37] method.

When different concentrations of paroxetine were tested, its LC_{50} was determined to be 351.2 μg/mL. Under the same conditions, fluensulfone had an LC_{50} of 39.31 μg/mL, a value closely aligned with those reported in the literature for this commercial nematicide [48,49].

Paroxetine is a selective serotonin reuptake inhibitor (SSRI), used to treat depression, panic disorder, anxiety, post-traumatic stress disorder, and social phobia, among other conditions [50,51]. However, no information is currently available regarding its nematicidal activity against *M. incognita*. The only existing data on nematicidal

activity involve its *in vitro* effects on the free-living nematode *C. elegans* [52].

Although the LC_{50} calculated for paroxetine is approximately 8.9 times higher than that of fluensulfone, it is important to note that fluensulfone is a commercial product that has undergone extensive optimization in order to maximize its efficacy against nematodes. In contrast, paroxetine has not yet been structurally optimized for nematode activity. Given this context, an LC_{50} only 8.9 times higher than that of a well-established commercial nematicide is a highly promising result.

3.6 Effect of Paroxetine on The Pathogenicity of *M. incognita* J2 in Tomato Plants

At both tested concentrations, paroxetine treatment reduced the number of nematode galls per root mass compared to the negative control (Tween 80®). Notably, both concentrations of paroxetine produced statistically equivalent results (Figure 8).

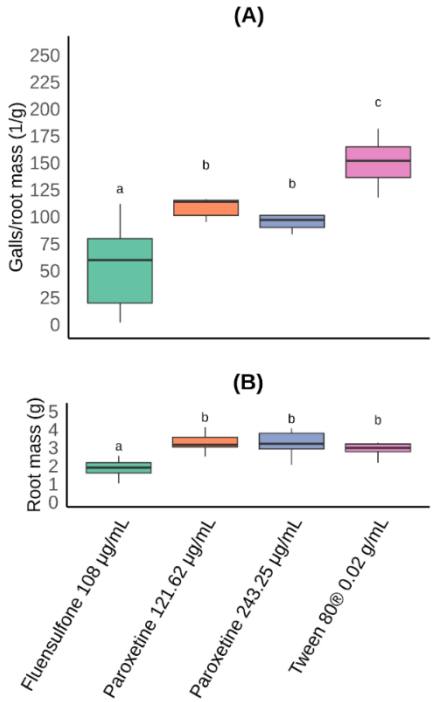

Figure 8. Galls per root mass (1/g) **(A)**, and root mass (g) **(B)** of tomato plants treated with paroxetine (two concentrations) and inoculated with *Meloidogyne incognita*. Fluensulfone (commercial nematicide) and Tween 80® were used as controls. Boxes with the same letter in each graphic are statistically equal to each other according to the Scott-Knott [28] test ($p < 0.05$), after ordered quantile transformation of data.

Although the positive control (fluensulfone at 108 µg/mL) was more effective in reducing nematode gall formation, it is important to consider that the root mass of plants treated with fluensulfone was statistically lower than that of the negative control. This significant root mass loss indicates the phytotoxic effects of this commercial nematicide on tomato plants.

Since no phytotoxic effects were observed for paroxetine (Figure 8), this substance presents significant potential for structural optimization aimed at maximizing its nematicidal activity.

4 Conclusions

Computational calculations suggest that chaetoglobosins A and B act against *Meloidogyne* spp. by inhibiting the SERT produced by the nematodes. Paroxetine, which is a SERT inhibitor, reduced the mobility and increased the mortality of J2 of *M. incognita* in *in vitro* experiments. Additionally, it decreased the pathogenicity of the nematode in experiments in tomato seedlings trials.

Therefore, studying SERT inhibitors – particularly compounds derived from paroxetine – holds significant potential for developing molecular structures aimed at controlling *M. incognita.*

Acknowledgements

Financial support and fellowships were provided by Fundação de Amparo à Pesquisa do Estado de Minas Gerais (FAPEMIG), Coordenação de Aperfeiçoamento de Pessoal de Nível Superior (CAPES), and Conselho Nacional de Desenvolvimento Científico e Tecnológico (CNPq).

Conflicts of Interest

The authors declare no conflicts of interest

Data Availability Statement

The data that supports the findings of this study are available in the Supporting Information of this article

References

[1] J. Chen, Q. X. Li, B. Song, "Chemical Nematicides: Recent Research Progress and Outlook," *Journal of Agricultural and Food Chemistry* 68 (2020): 12175–12188, https://doi.org/10.1021/acs.jafc.0c02871.

[2] X. Chen, H. Jia, Z. Li, X. Xu, "Synthesis and Nematicidal Evaluation of 1,2,3-Benzotriazin-4-one Derivatives Containing Piperazine as Linker Against Meloidogyne incognita," *Chinese Chemical Letters* 30 (2019): 1207–1213, https://doi.org/10.1016/j.cclet.2019.02.033.

[3] A. R. Burns, R. J. Baker, M. Kitner, et al., "Selective control of parasitic nematodes using bioactivated nematicides," *Nature* 618 (2023): 102–109, https://doi.org/10.1038/s41586-023-06105-5.

[4] N. Yadav, R. Kumar, S. Sangwan, et al., "Design, Synthesis, Nematicidal Evaluation, and Molecular Docking Study of Pyrano[3,2-c]pyridones against Meloidogyne incognita," *Journal of Agricultural and Food Chemistry* 72 (2024): 15512–15522, https://doi.org/10.1021/acs.jafc.4c00103.

[5] D. E. El-Habashy, M. A. Abdel Rasoul, S. A. M. Abdelgaleil, "Nematicidal Activity of Phytochemicals and their Potential Use for the Control of Meloidogyne javanica Infected Eggplant in the Greenhouse," *European Journal of Plant Pathology* 158 (2020): 381–390, https://doi.org/10.1007/s10658-020-02079-6.

[6] B. Khan, W. Yan, S. Wei, et al., "Nematicidal Metabolites from Endophytic Fungus Chaetomium globosum YSC5," *FEMS Microbiology Letters* 336 (2019): fnz169, https://doi.org/10.1093/femsle/fnz169.

[7] P. Tosco, T. Balle, F. Shiri, "Open3DALIGN: An Open-Source Software Aimed at Unsupervised Ligand Alignment," *Journal of Computer-Aided Molecular Design* 25 (2011): 777–783, https://doi.org/10.1007/s10822-011-9462-9.

[8] W. Humphrey, A. Dalke, K. Schulten, "VMD: Visual Molecular Dynamics," *Journal of Molecular Graphics* 14 (1996): 33–38, https://doi.org/10.1016/0263-7855(96)00018-5.

[9] J. Hénin, L. J. S. Lopes, G. Fiorin, "Human Learning for Molecular Simulations: The Collective Variables Dashboard in VMD," *Journal of Chemical Theory and Computation* 18 (2022): 1945–1956, https://doi.org/10.1021/acs.jctc.1c01081.

[10] Z. Feng, L. Chen, H. Maddula, et al., "Ligand Depot: A Data Warehouse for Ligands Bound to Macromolecules," *Bioinformatics* 20 (2004): 2153–2155, https://doi.org/10.1093/bioinformatics/bth214.

[11] S. Lešnik, T. Štular, B. Brus, et al., "LiSiCA: A Software for Ligand-Based Virtual Screening and Its Application for the Discovery of Butyrylcholinesterase Inhibitors," *Journal of Chemical Information and Modeling* 55 (2015): 1521–1528, https://doi.org/10.1021/acs.jcim.5b00136.

[12] D. Mendez, A. Gaulton, A. P. Bento, et al., "ChEMBL: Towards Direct Deposition of Bioassay Data," *Nucleic Acids Research* 47 (2019): D930–D940, https://doi.org/10.1093/nar/gky1075.

[13] E. W. Sayers, E. E. Bolton, J. R. Brister, et al., "Database Resources of the National Center for Biotechnology Information," *Nucleic Acids Research* 50 (2022): D20–D26, https://doi.org/10.1093/nar/gkab1112.

[14] S. F. Altschul, T. L. Madden, A. A. Schäffer, et al., "Gapped BLAST and PSI-BLAST: A New Generation of Protein Database Search Programs," *Nucleic Acids Research* 25 (1997): 3389–3402, https://doi.org/10.1093/nar/25.17.3389.

[15] H. Berman, K. Henrick, H. Nakamura, J. L. Markley, "The Worldwide Protein Data Bank

(wwPDB): Ensuring a Single, Uniform Archive of PDB Data," *Nucleic Acids Research* 35 (2007): D301–D303, https://doi.org/10.1093/nar/gkl971.

[16] J. A. Coleman, V. Navratna, D. Antermite, D. Yang, J. A. Bull, E. Gouaux, "Chemical and Structural Investigation of the Paroxetine-Human Serotonin Transporter Complex," *eLife* 9 (2020): e56427, https://doi.org/10.7554/eLife.56427.

[17] J. A. Coleman, E. M. Green, E. Gouaux, "X-ray Structures and Mechanism of the Human Serotonin Transporter," *Nature* 532 (2016): 334–339, https://doi.org/10.1038/nature17629.

[18] J. A. Coleman, E. Gouaux, "Structural Basis for Recognition of Diverse Antidepressants by the Human Serotonin Transporter," *Nature Structural & Molecular Biology* 25 (2018): 170–175, https://doi.org/10.1038/s41594-018-0026-8.

[19] J. A. Coleman, D. Yang, Z. Zhao, et al., "Serotonin Transporter–Ibogaine Complexes Illuminate Mechanisms of Inhibition and Transport," *Nature* 569 (2019): 141–145, https://doi.org/10.1038/s41586-019-1135-1.

[20] D. Yang, E. Gouaux, "Illumination of Serotonin Transporter Mechanism and Role of the Allosteric Site," *Science Advances* 7 (2021), *7*, eabl3857, https://doi.org/10.1126/sciadv.abl385.

[21] P. Plenge, D. Yang, K. Salomon, et al., "The Antidepressant Drug Vilazodone is an Allosteric Inhibitor of the Serotonin Transporter," *Nature Communications* 12 (2021): 5063, https://doi.org/10.1038/s41467-021-25363-3.

[22] K. Okonechnikov, O. Golosova, M. Fursov, et al., "Unipro UGENE: A Unified Bioinformatics Toolkit," *Bioinformatics* 28 (2012): 1166–1167, https://doi.org/10.1093/bioinformatics/bts091.

[23] F. Sievers, D. G. Higgins, "Clustal Omega for Making Accurate Alignments of Many Protein Sequences," *Protein Science* 27 (2018): 135–145, https://doi.org/10.1002/pro.3290.

[24] L. Martínez, R. Andreani, J. M. Martínez, "Convergent Algorithms for Protein Structural Alignment," *BMC Bioinformatics* 8 (2007): 306, https://doi.org/10.1186/1471-2105-8-306.

[25] G. M. Morris, H. Ruth, W. Lindstrom, et al., "AutoDock4 and AutoDockTools4: Automated Docking with Selective Receptor Flexibility," *Journal of Computational Chemistry* 30 (2009): 2785–2791, https://doi.org/10.1002/jcc.21256.

[26] S. D. Handoko, X. Ouyang, C. T. T. Su, C. K. Kwoh, Y. S. Ong, "QuickVina: Accelerating AutoDock Vina Using Gradient-Based Heuristics for Global Optimization," *IEEE/ACM Transactions on Computational Biology and Bioinformatics* 9 (2012): 1266–1272, https://doi.org/10.1109/TCBB.2012.82.

[27] E. F. Pettersen, T. D. Goddard, C. C. Huang, et al., "UCSF Chimera – A Visualization System for Exploratory Research and Analysis," *Journal of Computational Chemistry* 25 (2004): 1605–1612, https://doi.org/10.1002/jcc.20084.

[28] A. J. Scott, M. Knott, "A Cluster Analysis Method for Grouping Means in the Analysis of Variance," *Biometrics* 30 (1974): 507–512, https://doi.org/10.2307/2529204.

[29] C. Ismay, A. Y. Kim, "Statistical Inference via Data Science: A ModernDive into R and the Tidyverse", (2019), https://doi.org/10.1201/9780367409913.

[30] R Core Team, "R: A Language and Environment for Statistical Computing," R Foundation for Statistical, Vienna, Austria (2020), https://www.r-project.org/.

[31] S. Y. Chen, D. W. Dickson, "A Technique for Determining Live Second-stage Juveniles of *Heterodera glycines"*, *Journal of Nematology* 32(1):117–121. 2000.

[32] D. R. Amaral, F. E. da Rocha Oliveira, D. F. Oliveira, V. P. Campos, "Purification of Two Substances from Bulbs of Onion (Allium cepa L.) with Nematicidal Activity Against Meloidogyne exigua Goeldi," *Nematology* 5 (2003): 859–864, https://doi.org/10.1163/156854103773040763.

[33] S. S. Shapiro, M. B. Wilk, "An Analysis of Variance Test for Normality (Complete Samples)," *Biometrika* 52 (1965): 591–611, https://doi.org/10.1093/biomet/52.3-4.591.

[34] M. S. Bartlett, “Properties of Sufficiency and Statistical Tests,” *Proceedings of the Royal Society A* 160 (1937): 268–282, https://doi.org/10.1098/rspa.1937.0109.

[35] W. H. Kruskal, W. A. Wallis, “Use of Ranks in One-Criterion Variance Analysis,” *Journal of the American Statistical Association* 47 (1952): 583–621, https://doi.org/10.1080/01621459.1952.10483441.

[36] W. J. Conover and R. L. Iman, “Multiple-Comparisons Procedures. Informal Report,” U.S. Department of Energy, Los Alamos National Laboratory, University of California, Los Alamos, NM, (1979), https://doi.org/10.2172/6057803.

[37] C. Bonferroni, “Teoria Statistica Delle Classi e Calcolo Delle Probabilita,” Pubblicazioni del R Istituto Superiore di Scienze Economiche e Commericiali di Firenze (Libreria Internazionale Seeber, Florence, Italy), 8 (1936): 3–62, 1936.

[38] J. Tolles, W. J. Meurer, “Logistic Regression: Relating Patient Characteristics to Outcomes,” *JAMA* 316 (2016): 533–534, https://doi.org/10.1001/jama.2016.7653.

[39] C. Ritz, F. Baty, J. C. Streibig, D. Gerhard, “Dose-Response Analysis Using R,” *PLoS One* 10 (2015): e0146021, https://doi.org/10.1371/journal.pone.0146021.

[40] D. F. Oliveira, V. A. Costa, W. C. Terra, V. P. Campos, P. M. Paula, S. J. Martins, “Impact of Phenolic Compounds on Meloidogyne incognita in Vitro and in Tomato Plants,” *Experimental Parasitology* 199 (2019): 17–23, https://doi.org/10.1016/j.exppara.2019.02.009.

[41] R. A. Peterson, J. E. Cavanaugh, “Ordered Quantile Normalization: A Semiparametric Transformation Built for the Cross-Validation Era,” *Journal of Applied Statistics* 47 (2020): 2312–2327, https://doi.org/10.1080/02664763.2019.1630372.

[42] L. R. Marcin, R. J. Mattson, Q. Gao, et al., “Synthesis and hSERT Activity of Homotryptamine Analogs. Part 6: [3+2] Dipolar Cycloaddition of 3-Vinylindoles,” *Bioorganic & Medicinal Chemistry Letters* 20 (2010): 1027–1030, https://doi.org/10.1016/j.bmcl.2009.12.043.

[43] S. C. Zimmermann, E. F. Wolf, A. Luu, et al., “Allosteric Glutaminase Inhibitors Based on a 1,4-Di(5-amino-1,3,4-thiadiazol-2-yl)butane Scaffold,” *ACS Medicinal Chemistry Letters* 7 (2016): 520–524, https://doi.org/10.1021/acsmedchemlett.6b00060.

[44] V. Buzzoni, J. Blazquez, S. Ferrari, S. Calò, A. Venturelli, M. P. Costi, “Aza-boronic Acids as Non-β-lactam Inhibitors of AmpC-β-lactamase,” *Bioorganic & Medicinal Chemistry Letters* 14 (2004): 3979–3983, https://doi.org/10.1016/j.bmcl.2004.05.054.

[45] A. Crisford, F. Calahorro, E. Ludlow, et al., “Identification and Characterisation of Serotonin Signalling in the Potato Cyst Nematode Globodera pallida Reveals New Targets for Crop Protection,” *PLoS Pathogens* 16 (2020): e1008884, https://doi.org/10.1371/journal.ppat.1008884.

[46] M. K. Brown, Y. Luo, “Bilobalide Modulates Serotonin-Controlled Behaviors in the Nematode Caenorhabditis elegans,” *BMC Neuroscience* 10 (2009): 62, https://doi.org/10.1186/1471-2202-10-62.

[47] A. C. Wallace, R. A. Laskowski, J. M. Thornton, “LIGPLOT: a program to generate schematic diagrams of protein-ligand interactions,” *Protein Engineering* 8 (1995): 127–134, https://doi.org/10.1093/protein/8.2.127.

[48] H. B. Pacule, J. A. G. Vanegas, W. C. Terra, V. P. Campos, D. F. Oliveira, “(R)-Carvone is a Potential Soil Fumigant Against Meloidogyne incognita whose likely Enzymatic Target in the Nematode is Acetylcholinesterase,” *Experimental Parasitology* 241 (2022): 108359, https://doi.org/10.1016/j.exppara.2022.108359.

[49] J. A. G. Vanegas, H. B. Pacule, R. M. Capitão, et al., “Methyl Esters of (E)-Cinnamic Acid: Activity against the Plant-Parasitic Nematode Meloidogyne incognita and In Silico Interaction

with Histone Deacetylase," *Journal of Agricultural and Food Chemistry* 70 (2022): 6624–6633, https://doi.org/10.1021/acs.jafc.1c08142.

[50] M. Bourin, P. Chue, Y. Guillon, "Paroxetine: A Review," *CNS Drug Reviews* 7 (2001): 25–47, https://doi.org/10.1111/j.1527-3458.2001.tb00189.x.

[51] S. Gibiino, A. Serretti, "Paroxetine for the Treatment of Depression: A Critical Update," *Expert Opinion on Pharmacotherapy* 13 (2012): 421–431, https://doi.org/10.1517/14656566.2012.652085.

[52] J. C. Weeks, W. M. Roberts, C. Leasure, et al., "Sertraline, Paroxetine, and Chlorpromazine Are Rapidly Acting Anthelmintic Drugs Capable of Clinical Repurposing," *Scientific Reports* 8 (2018): 975, https://doi.org/10.1038/s41598-017-18457-w.

SUPPORTING INFORMATION

A Simple Procedure Involving Virtual Screening, Docking, and Comparisons of Amino Acid Sequences to Select Inhibitors of Sodium -Dependent Serotonin Transporter Protein as Potential New Nematicides

Geraldo Jamisse Hodela, [a] **Vitor Pereira de Sousa**, [b] **Mariana Castro de Melo**, [a] **Rodrigo Martins Fráguas**, [a] **Willian César Terra** [b] **and Denilson Ferreira de Oliveira**[a]

[a] Department of Chemistry, Federal University of Lavras, P.O. BOX 3037, Lavras-37203-202, MG-Brazil
[b] Department of Phytopathology, Federal University of Lavras, P.O. Box 3037, Lavras-37.203-202, MG-Brazil

Correspondence: Denilson Ferreira de Oliveira (denilson@ufla.br)

Figure S1 Most stable conformations for chaetoglobosins A (conformation 2 and 42) and B (conformation 38 and 40).

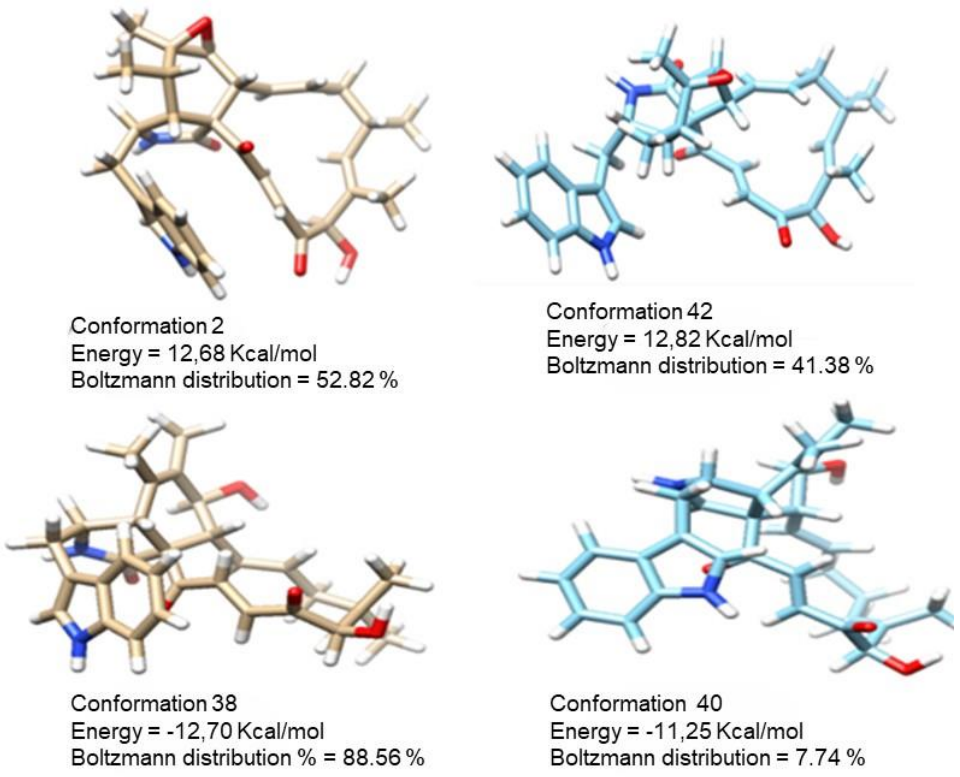

Table S1 Codes of substances selected in the three-dimensional search in the ChEMBL[1] database for chemical structures similar to chaetoglobosins A and B.

Substance code	Tanimoto Score	Protein on which the substance acts	Protein producing organism	Reference
CHEMBL606244	0.40	Sodium-dependent serotonin transporter (SERT)	*Homo sapiens*	[2]
CHEMBL2138465	0.40	Glutaminase	*Homo sapiens*	[3]
CHEMBL2138465	0.40	*Ampc-β*-lactamase	*Escherichia coli*	[4]

Table S2 Substance and protein code according to the search carried out in the ChEMBL database. Protein name of the amino acid sequence detected in the genome of *Meloidogyne graminicola*, followed by score, coverage and identity with respect to the amino acid sequence of the protein code.

Substance code	Protein code	Protein name	Score	Coverage	Identity
CHEMBL606244	P31645	Sodium-dependent serotonin transporter (SERT)	610	81%	53.28%

Table S3 Amino acid sequence similarity (%) of sodium-dependent serotonin transporters (SERTs), calculated by Ugene 1.32.0[5], after alignment with Clustal Omega 1.2.4 through four iterations[6] .

Protein codes	**Producing organism**	**Amino acid residues**	**P31645[a] (*Homo sapiens*)**	**6VRH[a] (*Homo sapiens*)**	**6VRK[a] (*Homo sapiens*)**	**6VRL[a] (*Homo sapiens*)**
P31645[a]	*Homo sapiens*	630	100	100	100	100
5I6X[a]	*Homo sapiens*	549	87	87	87	87
5I6Z[a]	*Homo sapiens*	549	87	87	87	87
5I71[a]	*Homo sapiens*	549	87	87	87	87
5I73[a]	*Homo sapiens*	549	87	87	87	87
5I74[a]	*Homo sapiens*	549	87	87	87	87
5I75[a]	*Homo sapiens*	549	87	87	87	87
6AWN[a]	*Homo sapiens*	549	87	87	87	87
6AWO[a]	*Homo sapiens*	549	87	87	87	87
6AWP[a]	*Homo sapiens*	549	87	87	87	87
6AWQ[a]	*Homo sapiens*	549	87	87	87	87
6DZV[a]	*Homo sapiens*	537	86	86	86	86
6DZW[a]	*Homo sapiens*	537	86	86	86	86
6DZY[a]	*Homo sapiens*	537	86	86	86	86
6DZZ[a]	*Homo sapiens*	540	87	87	87	87
6VRH[a]	*Homo sapiens*	630	100	100	100	100
6VRK[a]	*Homo sapiens*	630	100	100	100	100
6VRL[a]	*Homo sapiens*	630	100	100	100	100
6W2B[a]	*Homo sapiens*	549	87	87	87	87
6W2C[a]	*Homo sapiens*	549	87	87	87	87

7LI6[a]	*Homo sapiens*	539	87	87	87	87
7LI7[a]	*Homo sapiens*	537	86	86	86	86
7LI8[a]	*Homo sapiens*	539	87	87	87	87
7LI9[a]	*Homo sapiens*	539	87	87	87	87
7LIA[a]	*Homo sapiens*	539	87	87	87	87
7LWD[a]	*Homo sapiens*	541	87	87	87	87
7MGW[a]	*Homo sapiens*	537	86	86	86	86

[a] Sodium-dependent serotonin transporters (SERT).

Table S4 Codes for the three-dimensional structures of the biological units of SERTs, after alignment with the protein 6VRH[7], using the Lovoalign computer programme version 21.027[8], which was also used to calculate root mean square deviation of atomic positions (RMSD) in relation to 6VRH.

Protein codes	Amino acid residues	RMSD (Å)
5I6X	549	1.096
5I6Z	549	1.089
5I71	549	1.145
5I73	549	1.156
5I74	549	1.145
5I75	549	1.164
6AWN	549	1.113
6AWO	549	1.111
6AWP	549	1.116
6AWQ	549	1.111
6DZV	537	1.801
6DZW	537	1.275
6DZY	537	1.202
6DZZ	540	4.065
6VRH	630	0.000
6VRK	630	0.626
6VRL	630	0.589
6W2B	549	1.114
6W2C	549	1.114
7LI6	539	4.679
7LI7	537	1.740
7LI8	539	4.894
7LI9	539	4.160
7LIA	539	0.990
7LWD	541	1.028
7MGW	537	1.822

Table S5 Codes and names of sodium-dependent serotonin transporter (SERT) inhibitors.

Ligand codes	Ligand names	References
8PR	(3*S*,4*R*)-3-(1,3-benzodioxol-5-yloxymethyl)-4-(4-fluorophenyl)piperidine	[9]
68P	(1*S*)-1-[3-(dimethylamino)propyl]-1-(4-fluorophenyl)-1,3-dihydro-2-benzofuran-5-carbonitrile	[9]
69D	(1*S*)-1-(4-bromophenyl)-1-[3-(dimethylamino)propyl]-1,3-dihydro-2-benzofuran-5-carbonitrile	[9]
8PR	(3*S*,4*R*)-3-[(1,3-benzodioxol-5-yloxy) methyl]-4-(4-fluorophenyl) piperidine	[10]
FVX	2-[(*E*)-[5-methoxy-1-[4 (triflouromethyl)phenyl]pentylidene]amino]oxyethanamine	[10]
SRE	(1*S*,4*S*)-4-(3,4-dichlorophenyl)-*N*-methyl-1,2,3,4-tetrahydronaphthalen-1-amine	[10]

Table S6 Codes for the three-dimensional structures of sodium-dependent serotonin transporters (SERTs) that were selected for the molecular docking.

Protein codes	Producing species	Number of amino acid residues	References
7MGW	*Homo sapiens*	537	[11]
7LI7	*Homo sapiens*	537	[11]
7LWD	*Homo sapiens*	541	[12]
7LIA	*Homo sapiens*	539	[11]
7LI9	*Homo sapiens*	539	[11]
7LI8	*Homo sapiens*	539	[11]
6DZZ	*Homo sapiens*	540	[13]
7LI6	*Homo sapiens*	539	[13]
6VRL	*Homo sapiens*	630	[13]
6VRK	*Homo sapiens*	630	[13]
6VRH	*Homo sapiens*	630	[13]
6DZV	*Homo sapiens*	537	[13]

References

[1] D. Mendez, A. Gaulton, A. P. Bento, J. Chambers, M. De Veij, E. Félix, M. P. Magariños, J. F. Mosquera, P. Mutowo, M. Nowotka, *Nucleic Acids Research* **2019**, *47*, D930–D940.

[2] L. R. Marcin, R. J. Mattson, Q. Gao, D. Wu, T. F. Molski, G. K. Mattson, N. J. Lodge, *Bioorganic & Medicinal Chemistry Letters* **2010**, *20*, 1027–1030.

[3] S. C. Zimmermann, E. F. Wolf, A. Luu, A. G. Thomas, M. Stathis, B. Poore, C. Nguyen, A. Le, C. Rojas, B. S. Slusher, *ACS Medicinal Chemistry Letters*, *7*, 520–524.

[4] V. Buzzoni, J. Blazquez, S. Ferrari, S. Calo, A. Venturelli, M. P. Costi, *Bioorg Med Chem Lett* **2004**, *14*, 3979–3983.

[5] K. Okonechnikov, O. Golosova, M. Fursov, A. Varlamov, Y. Vaskin, I. Efremov, O. G. German Grehov, D. Kandrov, K. Rasputin, M. Syabro, T. Tleukenov, *Bioinformatics* **2012**, *28*, 1166–1167.

[6] F. Sievers, D. G. Higgins, *Protein Science* **2018**, *27*, 135–145.

[7] J. A. Coleman, V. Navratna, D. Antermite, D. Yang, J. A. Bull, E. Gouaux, *Elife* **2020**, *9*, e56427.

[8] L. Martínez, R. Andreani, J. M. Martínez, *BMC Bioinformatics* **2007**, *8*, DOI 10.1186/1471-2105-8-306.

[9] J. A. Coleman, E. M. Green, E. Gouaux, *Nature* **2016**, *532*, 334–339.

[10] J. A. Coleman, E. Gouaux, *Nature Structural & Molecular Biology* **2018**, *25*, 170–175.

[11] D. Yang, E. Gouaux, *Sci Adv* **2021**, *7*, eabl3857.

[12] P. Plenge, D. Yang, K. Salomon, L. Laursen, I. E. Kalenderoglou, A. H. Newman, E. Gouaux, J. A. Coleman, C. J. Loland, *Nature Communications* **2021**, *12*, 5063.

[13] J. A. Coleman, D. Yang, Z. Zhao, P.-C. Wen, C. Yoshioka, E. Tajkhorshid, E. Gouaux, *Nature* **2019**, *569*, 141–145.